In vitro evaluation of the toxicological properties of mineral oil hydrocarbons: focus on 1-2 ring and 3+ ring moah classes and correlation with the hydrocarbon composition of these mineral oils

Auteur : Pierret, Damien
Promoteur(s) : Purcaro, Giorgia
Faculté : Gembloux Agro-Bio Tech (GxABT)
Diplôme : Master en bioingénieur : chimie et bioindustries, à finalité spécialisée
Année académique : 2023-2024
URI/URL : http://hdl.handle.net/2268.2/21130

LIÈGE université
Gembloux
Agro-Bio Tech

IN VITRO EVALUATION OF THE TOXICOLOGICAL PROPERTIES OF MINERAL OIL HYDROCARBONS: FOCUS ON 1-2 RING AND 3+ RING MOAH CLASSES AND CORRELATION WITH THE HYDROCARBON COMPOSITION OF THESE MINERAL OILS

DAMIEN PIERRET

END-OF-STUDY THESIS SUBMITTED FOR OBTAINING THE MASTER'S DEGREE IN BIOENGINEERING IN CHEMISTRY AND BIO-INDUSTRIES

ACADEMIC YEAR 2023-2024

(CO)-PROMOTER(S): PROF. GIORGIA PURCARO, PROF. JEAN-MARIE COLET

LIÈGE université
Gembloux
Agro-Bio Tech

IN VITRO EVALUATION OF THE TOXICOLOGICAL PROPERTIES OF MINERAL OIL HYDROCARBONS: FOCUS ON 1-2 RING AND 3+ RING MOAH CLASSES AND CORRELATION WITH THE HYDROCARBON COMPOSITION OF THESE MINERAL OILS

DAMIEN PIERRET

END-OF-STUDY THESIS SUBMITTED FOR OBTAINING THE MASTER'S DEGREE IN BIOENGINEERING IN CHEMISTRY AND BIO-INDUSTRIES

ACADEMIC YEAR 2023-2024

(CO)-PROMOTER(S): PROF. GIORGIA PURCARO, PROF. JEAN-MARIE COLET

The master's thesis presented below was carried out in the *Analytical Chemistry and Food Technology* department of Gembloux Agro-Bio Tech (University of Liege, Belgium).

Acknowledgements

Firstly, I would like to extend my warmest thanks to my supervisor, Professor Giorgia Purcaro, who believed in me and enable me to grow and develop my full potential as a young scientist. Your availability and the countless meetings we have had the opportunity to have always brought me answers and serenity in times of doubts. I am already excited to continue my journey with you and learning more from your incredible knowledge in the world of chromatography.

Secondly, I would like then to heartly thank all the analytical chemistry laboratory team for their good spirit and their presence throughout my journey there. Donatella, Aleksandra, Paula, Damien, Steven, Sylvia, Pedro, Gregory, Francesca, Giovana, Irene, Giulia and Andrea, my time in the office and in the laboratory would not have been so enjoyable without you all and the pies would have not tasted the same way. I will always keep good memories of the time I spent with you all such as monthly perfume testing, trampoline, Friday (or any day of the week) beer, and of obviously the master's thesis student food contest. I can't wait to spend some more unforgettable moments with you.

Then, I would also give a special mention to Aleksandra who from the outset showed a great deal of concern for my success and development as a young researcher. You have been the support I needed to get started and believe in my abilities and for this, I will never be thankful enough. I also would like to thank you a countless number of times for the revisions you brought to this work and my lab meeting presentations. The quality of writing and the fluidity of the document would never have been the same without you. You are also the one that introduced me to the complex world of mineral oil, which would never have appealed to me so much without your sound advice and explanations.

Thirdly, I would like to mention our lab technician, Sophie, whose kindness and good spirit are unfailing. In the end you are a bit like a ray of sunshine, brightening our days with your smile. I would also have liked to highlight Virginie and Jean-Marie, from UMons, that shared this project with us, helping me generating data in the former case and analysing it in the latter one. Thank you for your time, your knowledge and your hospitality whenever I came to your lab.

Moving on, I would like to thank my parents and my brother which always believed in me and supported me through my university journey. Your invaluable support allowed me to pursue my dreams and made me the man I am today. You are the pillar that supports me in my everyday life and without who I would not be where I am today. Thank you for being the family you are, no one could ever hope for more than you.

Fourthly, I would like to give a special shout-out to the countless friends I have met here in Gembloux. I wish however to particularly highlight the indefectible core of friends I have now had for the last 2 years and with who I without any doubt spent the most incredible years of my life. Elise, Victor, Julien, Aubin, Emilie, Maëlle, Valentine, Hugo, Diego, Clément, Cyrille, Alice, Karelle, Naya, Neo, Pauline, Lisa, Pierre-Edouard, Lucien and Grégoire, I will always remember the moments we have shared together and the incredible life we had these last years together. I would just like to thank you for everything and for being who you are.

Finally, I would give an even more special mention to Maëlle and Diego, who have followed the same path as me and with whom I have forged lasting friendships.

RÉSUMÉ (FR)

Les hydrocarbures saturés d'huiles minérales (MOSH) et les hydrocarbures aromatiques d'huiles minérales (MOAH) sont des contaminants alimentaires omniprésents d'origine pétrolière. Les MOAH sont considérés comme une préoccupation toxicologique par l'Autorité européenne de sécurité des aliments (EFSA), en particulier pour les composés contenant trois anneaux aromatiques ou plus. Cependant, les données toxicologiques de tels composés sont peu nombreuses en raison des défis liés à leur obtention.

Ce projet vise à évaluer les propriétés toxicologiques (ex., mutagénicité, génotoxicité) des fractions MOSH et MOAH à l'aide de divers tests toxicologiques, comme le test d'Ames et celui des micronoyaux, tout en associant ces résultats à une caractérisation détaillée des substances étudiées. Les objectifs de ce travail de fin d'étude se sont concentrés sur l'optimisation des protocoles évaluant ces propriétés toxicologiques et le fractionnement d'huiles minérales en fraction MOSH, MOAH et les sous-fractions associées. Le travail à été divisé en trois parties :

La première partie est consacrée à l'élaboration d'un protocole de purification optimisé pour obtenir des fractions de MOAH pures à partir d'échantillons d'huiles minérales et également à la mise au point d'un autre protocole, optimisé pour fractionner MOAH en sous fractions relatives à leur nombre de noyaux aromatiques. La seconde partie consiste à exposer ces fractions purifiées à des cellules procaryotes et eucaryotes afin d'évaluer leurs propriétés toxicologiques. La troisième partie a examiné les méthodes industrielles officielles utilisées pour évaluer la conformité des huiles minérales à leur commercialisation (en termes de sécurité toxicologique), en cherchant à comprendre quelles compositions de MOAH étaient positives au test (donc, considérées comme toxiques) et s'ils étaient pertinents sur le plan toxicologique.

La purification des échantillons a produit une quantité importante de MOAH purifiés, mais a nécessité une optimisation des conditions d'élution selon la composition des échantillons. La solubilisation de ces fractions purifiées a été cruciale pour la réalisation des tests toxicologiques. La viabilité cellulaire a été évaluée, ainsi que la concentration maximale de MOAH ne compromettant pas cette viabilité. Le test d'Ames a évalué la mutagénicité des échantillons, le test étant positif pour l'échantillon Moltox (reference oil N°1). De plus, le test des micronoyaux sur des hépatocytes de la lignée cellulaire humaine HEPG2 a révélé un effet génotoxique de cet échantillon Moltox.

Enfin, la méthode industrielle utilisée pour évaluer la conformité des huiles minérales aux normes de sécurité a montré des résultats intéressants. Basée sur la mesure spectrophotométrique de MOAH extrait par du DMSO, elle a révélé une extraction et une concentration des composés toxiques, ouvrant des perspectives intéressantes pour de futures méthodes de screening (par exemple, dans l'alimentation).

ABSTRACT (EN)

Mineral oil saturated hydrocarbons (MOSH) and mineral oil aromatic hydrocarbons (MOAH) are ubiquitous petroleum-derived products that contaminate food products. The MOAH fraction has been considered a toxicological concern by the European Food Safety Authority (EFSA), in particular regarding the compounds having three aromatic rings or more. However, toxicological data on these specific compounds are relatively scarce due to the many challenges in obtaining such information.

The long-term goal of this project aims at evaluating the toxicological properties (e.g., mutagenicity, genotoxicity) of MOSH and MOAH fractions using various toxicological tests, such as the Ames test and the micronucleus test and associate them with a detailed characterization of the mixture tested. The objectives of this master thesis work were more focused on optimising the protocols necessary to assess these toxicological properties and to fractionate the minerals oils (MOs) to be evaluated into MOSH, MOAH and relative subfractions. The work was divided into three parts.

The first part focuses on developing an optimised purification protocol to obtain pure MOAH fractions from mineral oil samples and a further optimised protocol for fractionating these fractions based on the number of aromatic rings. The second part involves exposing these purified fractions to prokaryotic and eukaryotic cells to evaluate their toxicological properties. A third part investigated the official industry methods used to evaluate the suitability of MOs for commercialization (in terms of toxicological safety), trying to understand which MOAH compositions gave positive responses (i.e., considered toxic), and whether these MOAH were toxicologically relevant.

Sample purification produced a substantial amount of pure MOAH fractions but required optimization of the elution conditions based on the sample composition. Solubilization of these purified samples was crucial for toxicological testing. Cell viability was assessed and maximum MOAH concentration not compromising cell viability was determined. The Ames test evaluated the mutagenicity of the samples in both metabolized and unmetabolized forms, with Moltox reference oil No. 1 sample testing positive. Additionally, the mutagenicity assessment (micronucleus test) on human HEPG2 hepatocytes indicated that this same Moltox sample had a genotoxic effect on the cells.

Finally, the method used by the industry to evaluate the compliance of a MO with safety standards showed interesting results. This method, based on the spectrophotometric measure of a DMSO extract of MOAH, showed to extract and concentrate the toxic compounds, opening interesting perspective in future direction for screening methods (for instance, in food).

Table of contents

STATE OF THE ART

1. Introduction

Mineral oil hydrocarbons (MOH) are ubiquitous food contaminants deriving from petroleum usually not intentionally added to food [1]. They are commonly subdivided into two groups, which are mineral oil saturated hydrocarbons (MOSH) and mineral oil aromatic hydrocarbons (MOAH). Their presence in foodstuffs is of concern as MOAH have been associated with carcinogenic and mutagenic properties (particularly the 3-7 ring MOAH), while MOSH are known to accumulate in human tissues [2]. MOH also contains components that act as tumour promoters, as shown in mouse skin painting experiments. However, little is known about the formation and toxicity of MOSH biotransformation products, as well as the oral toxicity of MOAH, especially the 1-2 ring MOAH compounds [2]. Unfortunately, because of gaps in the toxicological data, few regulations regarding MOH content in food exists, while they would be necessary to protect the consumer [2,3].

The difficulty of evaluating the toxicological properties of MOSH and MOAH is primarily due to the complexity and variability of their composition. When analysing these two subfractions by gas chromatography (GC), they appear as unresolved complex mixtures (UCMs), with profiles that depend on the type of mineral oil (MO) from which these MOSH and MOAH originate [4]. Such UCMs are almost impossible to characterize in detail, as they comprise thousands of chemicals, including many structural isomers that cannot be chromatographically separated. This limited separation capability of one-dimensional chromatographic techniques, such as GC or high-performance liquid chromatography (HPLC), drives the shift toward two-dimensional chromatographic techniques. Comprehensive two-dimensional GC (GC×GC) improves sample separation, allowing for a better characterization and providing more structural information.

Hence, associating the toxicological properties of MOSH and MOAH with their composition is not straightforward, as it requires understanding how the different molecules (which are difficult to separate and identify) and their interactions influence toxicity. Filling these toxicological gaps would assure consumer protection and a more accurate risk assessment.

The following sections of this state-of-the-art review present detailed information on MO, its analysis methods, and known exposure and toxicology. Various toxicological tests for MO assessment and necessary sample pretreatments are also discussed. The final section outlines the research goals and identifies remaining gaps in the field of MO.

2. Mineral oil hydrocarbons (MOH) — a definition

2.1 General information

MOH are chemical compounds derived from MOs, which are distillation products of petroleum. They are used in various applications, including machinery lubrication, food packaging, printing inks, cosmetics, and pharmaceuticals formulation. Because of their ubiquitous nature, they easily find their way into the food chain and can therefore be ingested orally. Unfortunately, some MOH are suspected of possessing carcinogenic and genotoxic properties [5].

MOH are defined by the Joint Research Centre (JRC) guidance as "*a complex mixture of hydrocarbons, which originate from crude mineral oils or which are produced from coal, natural gas or biomass through Fischer-Tropsch synthesis*" [6]. The EFSA, for its part, is slightly more precise and defines MOH as "*hydrocarbons containing 10 to about 50 carbon atoms which have been divided into two main types: mineral oil saturated hydrocarbons (MOSH) and mineral oil aromatic hydrocarbons (MOAH). MOH are chemical compounds derived mainly from crude oil, but also produced synthetically from coal, natural gas and biomass*" [2].

Therefore, MOSH form a class of compounds composed of linear and branched paraffins, and alkyl-substituted naphthenes while MOAH gather alkyl-substituted aromatic hydrocarbons containing one or more fused aromatic rings (figure 1).

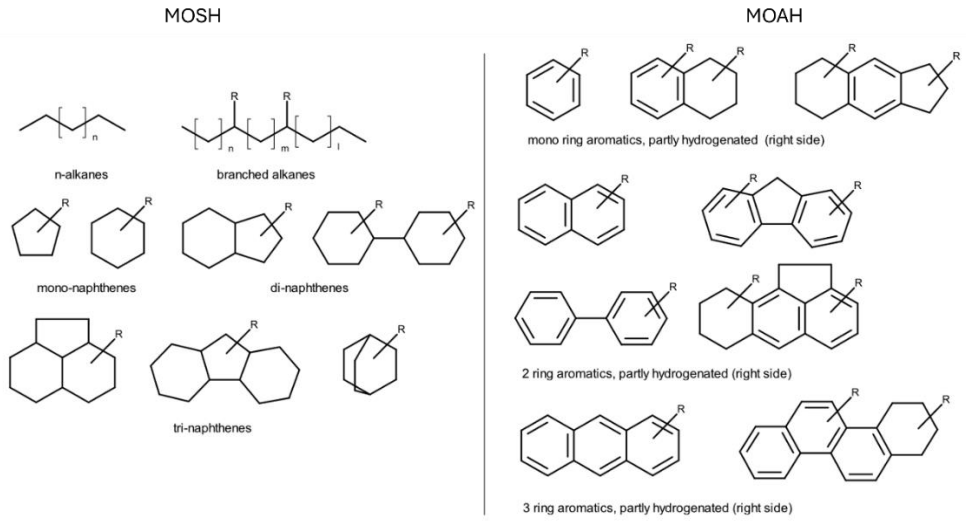

Figure 1: Example of MOSH and MOAH structures. MOSH are represented on the left side while MOAH are depicted on the right side. Reproduced from Hochegger et al. [7].

2.2 MOH Analysis

2.2.1. HPLC-GC-FID

The commonly utilized method for MOH analysis involves HPLC coupled online to GC with a Flame Ionization Detector (FID) (HPLC-GC-FID). The HPLC step aims at separating MOSH from MOAH but also separate these two fractions from some chemical species that are not of interest (e.g., other molecules from the analysed matrix). This separation is performed on a silica gel HPLC column (250mm × 2mm i.d., 5µm dp) using a gradient of *n*-hexane (C6) and dichloromethane (DCM) [4,8]. MOSH and MOAH fractions are then transferred (separately) to the GC system through an on-column interface. Detection is carried out using an FID, which virtually provides a mass-equivalent response for all hydrocarbons [9]. Alternatively, the analysis can also be performed off-line: MOSH and MOAH fractions can be collected into vials and then injected as a separate step into the GC system. In the latter case an on-column injector must be used to assure no discrimination based on the boiling point over the volatility range of interest (i.e., C10-C50). Moreover, ideally, a large volume injection is preferred to increase sensitivity and reduce sample manipulation, which may lead to cross-contamination [10].

Similarly to the online system, transferring a large volume of LC eluent into the GC is a critical step to ensure that the LC eluent does not enter the GC in its liquid form. This transfer is achieved using a retention gap (RG), which is an uncoated and non-retaining piece of capillary connected at the front of the analytical column. The role of the RG is to provide an evaporation surface for the solvent prior to the separation column protecting the latter from non-volatile material, as well as improving peak shape compared to directly injecting the sample into the separation column.

The solvent transfer into the GC through the on-column retention gap technique assures a consistent transfer regardless of the volatility (i.e., no discrimination in a broad range of volatility, not comparable to any other injection/transfer system). Indeed, the solvent evaporation is controlled by a series of processes, which allow for an optimal retention of the volatile compounds and refocusing the high boiling compounds before the chromatographic separation. For further details, interested reader are referred to already published references on the subject such as [10,11].

Only a few official methods are available for MOSH/MOAH analysis, such as the one for the determination of MO in vegetable oil (EN 16995:2017) [12]. The International Organization for Standardization (ISO) has introduced the ISO-ISO/CD 20122 method, which offers a lower limit of quantification for both MOSH and MOAH in vegetable fats and oils compared to the EN 16995:2017 method [13].

2.2.2. GC×GC

HPLC-GC-FID is effective for MOH analysis, but it has limitations that need to be addressed for better sample characterization. Indeed, the system's separation power is insufficient to provide detailed information such as the number of aromatic rings and the degree of alkylation, necessary for in-depth characterization of MOH needed in risk assessment studies [14]. Such additional information is obtained using a bidimensional chromatographic system. What's more, some co-eluting interferences non-separated from the MOAH hump in 1D GC might be separated in 2D. The comparison of GC and GC×GC chromatograms is depicted in figure 2.

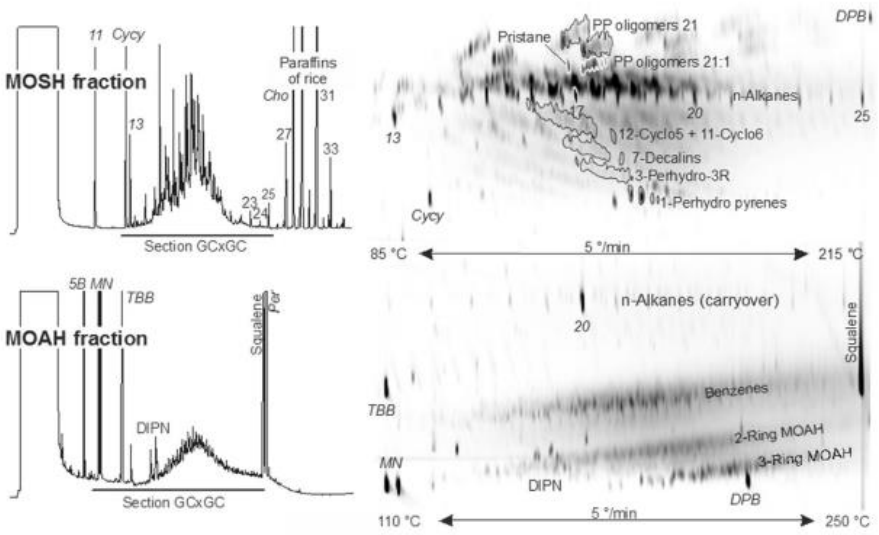

Figure 2 : Comparison of GC (left) and GCxGC (right) chromatograms of MOSH and MOAH fractions. Reproduced from Biedermann et al.[15].

GC×GC analysis for MOH analysis applied to food science, pioneered by Biederman and Grob in 2009, has enhanced the understanding of the various subclasses present in the unresolved hump of MOSH and MOAH obtained in 1D GC [16].

2.3. Variability of MOH composition

GC×GC analysis allows then to unravel the complexity of MO. Indeed, its MOH composition varies depending on the origin of the crude oil and the refining process it underwent to meet the industry and market requirements [3]. This crude oil must encounter a distillation process (depicted in figure 3) to yield different fractions, having each their own use.

Briefly, a first atmospheric distillation is carried out, generating different fractions representing various types of fuel commonly used today. The residual fraction from this distillation is distilled again, this time under vacuum and generates different vacuum distillates that can be further refined to MO [17]. The vacuum distillates, after being processed to remove most of the distillate aromatics, encounter a dewaxing process to achieve the desired techno-functional properties settled by the industry. The dewaxed fractions are then separated into two groups commonly named Lubricant Base Oils (LBOs) and Highly Refined Base Oils (HRBOs).

In LBOs the paraffin wax (here, wax is considered as >C20 n-alkanes) fractions are removed or transformed to avoid any crystallisation at lower temperatures which could reduce the oils functionalities [2,18]. HRBOs, also named white oils, derive from non-carcinogenic LBOs (*i.e.*, they pass the IP346 test, described in section 4.4.1) by undergoing a higher refining process to render them colourless, and more stable by removing the remaining aromatic fractions that naturally dyes oils. This high refining process consists of hydrogenation, sulfonation and/or acid treatment processes that target the elevated number of aromatic rings MOAH, the fraction of suspected carcinogenic potential [2,19].

HRBOs are then classified within two groups: technical white oil and pharmaceutical white oil. The difference of classification in the two group relies on the compliance with the European pharmacopeia monographs method based on a UV-Dimethyl Sulfoxide (DMSO) technique [20]. However, technical white oils intended for non-food contact meet the requirement settled by the united states food and drug agency (21CFR178.3620) relying on UV-absorbance limits and Saybolt color thresholds [18,21].

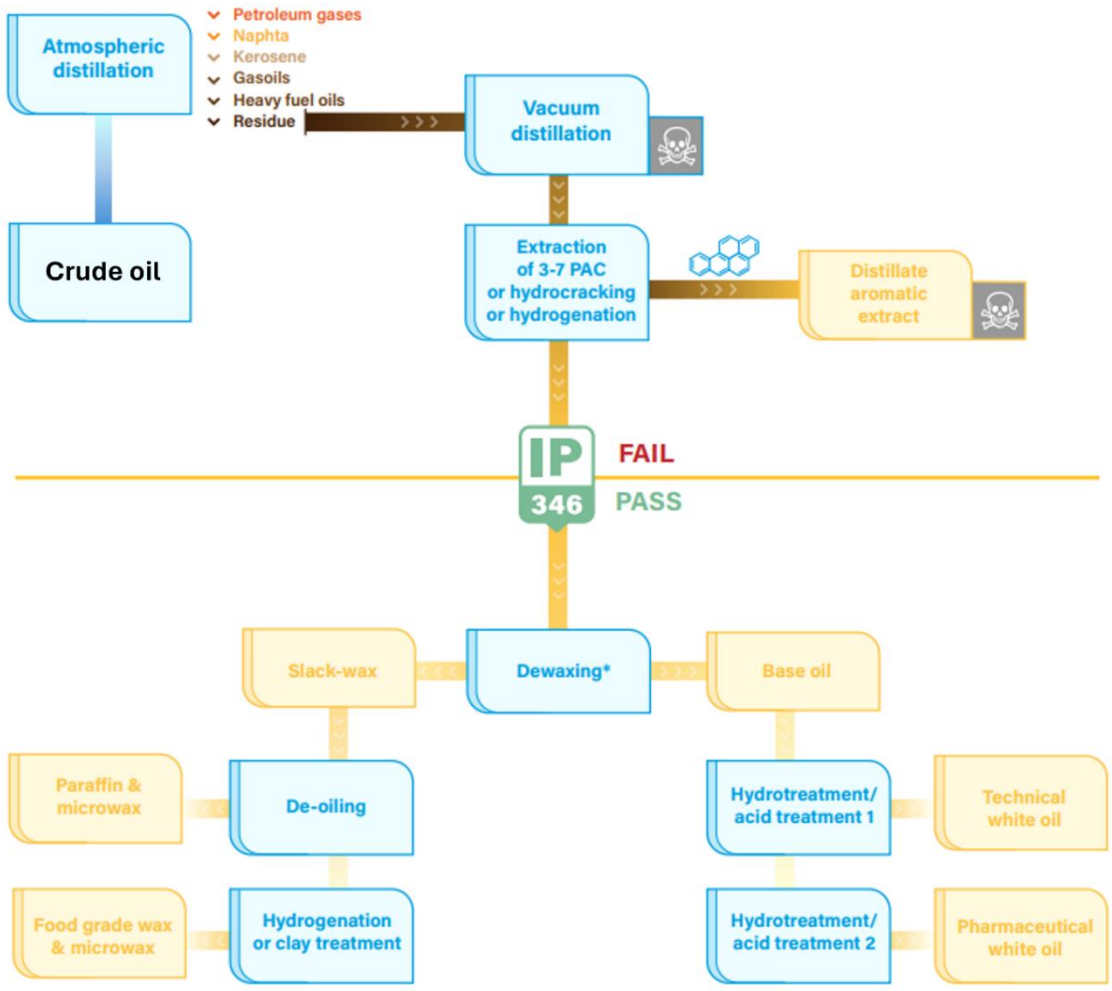

Figure 3: Refinery diagram of mineral oil and waxes manufacture. The IP346 limit allows establishment of refinement quality efficiency to separate carcinogenic fractions from non-ones. Adapted from Concawe [18].

3. Occurrence, human exposure and legislation

3.1. Historical background

Although MO have been used since the 19th century, their unintentional presence in food was only highlighted in 1989 by Biedermann and Grob. In early 1991, they published papers confirming that the contamination originated not only from the migration of food packaging materials but also from lubricating oils and release agents [22,23]. Additionally, a 1986 study on paraffinic waxes (classified as MOH in the most recent EFSA definition [2]) identified paraffinic residues on the skin of ducks after exposure during the defeathering process, leading to inevitable contamination [24].

However, it remained relatively understudied for the next 15 years until 2008, when it garnered significant attention following the discovery of high MOH contamination in a Ukrainian sunflower oil shipment reported by the Rapid Alert System for Food and Feed (RASFF) [3]. This event prompted the EFSA to publish an opinion on the presence of MOH in food products in 2012. The opinion underscored the scarcity of information on the subject, particularly regarding toxicological data. It also emphasized the challenges in analysis and the necessity for the development of analytical methods that allows for a better characterization of the contamination (e.g. aromatic rings' number identification present in the MOAH fraction) [3].

In 2019, the consumer rights organization FoodWatch identified the presence of MOAH in infant and follow-on formula products available on the European market. This discovery prompted the European Commission to request the EFSA to perform a rapid health risk assessment in the same year [25–27]. Later, the natural update of the previous risk assessment (2012) was released in early September 2023.

Since 2012, an increasing amount of data has been generated on various topics related to MOH, including toxicology, exposure assessment, and chemical characterization and identification. However, MOH remains under-studied, more especially regarding the toxicological aspects, as indicated by the latest EFSA report, which highlights data gaps and a lack of knowledge [2]. The latest EFSA recommendations notably underline the lack of data on the influence of aromatic ring alkylation in MOAH, particularly those with three aromatic rings or more, and the oral toxicity of MOAH with one or two aromatic rings. More information on the composition of MOAH contamination in food is also needed, for example regarding the number of aromatic rings of the compounds. Regarding MOSH, gaps exist in the analytical methods available for their characterisation and in understanding their structural features. Additionally, information on their accumulation, potential biotransformation and toxicity is lacking.

3.2. Human exposure

3.2.1. Food, cosmetics and environmental contaminations

MOH-containing (e.g., lipsticks and hand creams, where paraffin can be used as an ingredient) or MOH-contaminated (e.g., food) products are rather ubiquitous due to the wide range of applications of mineral oils. Human exposure can therefore occur through various pathways, with the most concerning being those leading to oral ingestion, such as through food, cosmetics, and medicine.

Cosmetics have been evaluated in the 2012 EFSA opinion [3] and in a more recent BfR (Bundesinstitut für Risikobewertung) opinion [28], both concluding that white oils and petrolatum used in the cosmetic industry do not pose health risks. Dermal contact and oral ingestion, resulting from the use of lipsticks, represent alternative pathways for the introduction of MO into the human body [29]. However, there is no clear evidence to suggest a significant contribution of these pathways to MO accumulation in the body [28].

Occurrence of MOSH and MOAH in food is large as many food products contain them in various concentrations. Table 1 depicts a non-exhaustive list of different foodstuffs and their respective MOSH and MOAH concentrations presented in the 2023 EFSA risk assessment [2].

Table 1: Non-exhaustive list of MO-contaminated food products. The values are taken from the EFSA "update of the risk assessment of mineral oil hydrocarbons in food" [2].

	Mean MOSH concentration (mg/kg)		**Mean MOAH concentration (mg/kg)**	
Food group	**Lower bound**	**Upper bound**	**Lower bound**	**Upper bound**
Olive pomace oil	108.67	108.71	13.54	13.56
Coconut oil/fat	25.91	26.85	3.69	5.17
Palm oil	11.49	12.94	1.02	2.75
Pasta and similar products	14.69	14.96	0.81	0.91
Canned/jarred fish	8.42	9.97	0.22	1.58
Milk chocolate	3.22	3.84	0.10	0.84

The origin of food contamination can stem from multiple sources, such as food contact materials (FCMs), environment and intentional use [2,3,30]. Examples of FCMs are sisal and jute bags, used for transporting products like cocoa beans, coffee beans, or rice. The treatment required to soften the fibres, necessary for manufacturing these bags, relies on MO, which later leads to significant release into foods in contact with the bags [31]. Other examples of FCMs are recycle paperboards, where not food grade but rather technical-grade MO are used (meaning with an aromatic compound content level between 15-25%) [32]. Moreover, it was shown that about 25% of the contamination derived from the printing ink [32,33]. The environment

undoubtedly hosts many sources of MO contaminants, but it remains an understudied subject that requires further investigation.

The use of LBOs in industries can lead to their contact with food and thus contaminate it, as for instance shown by Grob et al. in canned food in 1997 [34]. Finally, the intentional addition of MO to food (and therefore not considered contamination) occurs through its use in food additives, such as glazing agents, anti-dusting agents (USA only), release agents, and antifoaming agents [18,35].

3.3. Legislation

Legislation regarding MO content in food is limited, with no specific European regulation addressing acceptable levels of MOSH and MOAH in food products (although expected for the end of 2024). But, recently, the Standing Committee on Plants, Animals, Food, and Feed (SCoPAFF) has established *de-facto* a limit of 2 mg/kg of MOAH for fats and oils (> 50% fat/oil content), as well as 1 mg/kg for food with a fat/oil content between 4% and 50%, and 0.5 mg/kg for dry food with fat/oil levels equal to or lower than 4% fats [36]. These values are based on the limit of quantification (LOQ) specified in the JRC guidance document EUR29666 [6].

Additionally, certain regulations do impose restrictions on the use of MO. For instance, the use of MO as FCMs additives is laid down by regulation (EU) 10/2011 which sets a maximum migration limit (SML) of 60 mg/kg of food for "*waxes, paraffinic, refined, derived from petroleum based or synthetic hydrocarbon feedstocks, low viscosity*" as well as for "*white mineral oils, paraffinic, derived from petroleum-based hydrocarbon feedstock*". A more stringent specification applies to "*waxes, paraffinic, refined, derived from petroleum based or synthetic hydrocarbon feedstocks, low viscosity*" with a specified SML value of 0.05 mg/kg [37].

In the previous European regulation (EC) No 889/2008, MO and paraffin oils were permitted for use as pesticides or as co-formulants in plant protection products [38]. However, the latest European Commission document (EU) 2021/1165 allows the use of only paraffin oils for such applications [39]. In the cosmetic sector, specific European legislation (EC 1223/2009) prohibits the use of any MO that does not meet the IP 346 requirement [40]. The IP 346 requirement and method are explained in section 4.3.1.

4. Toxicology of mineral oil hydrocarbons

4.1. Definitions and parameters to assess

Toxicological evaluation is a complex process as it involves assessing multiple parameters to determine potential health risks. These parameters are studied through different *in vivo* (i.e., on animals) or *in vitro* methods, the latter being nowadays preferred due to ethical considerations. Nevertheless, *in vitro* approaches cannot consider all aspects of a living being, such as the immune system. Therefore, *in vivo* tests are sometimes still necessary to provide additional information that cannot be obtained using *in vitro* tests such as for instance further evaluating the genotoxic potential of a substance and confirming *in vitro* observations[41].

Various terms are used to define the toxicological characteristics of chemicals, but they can sometimes be misused and/or misunderstood. The definitions of the different terms used in the present work to assess the toxicological properties of MOSH and MOAH are presented here below to avoid any confusion.

- *Carcinogenicity*

The European commission, based on Adler et al. [42], defines "carcinogenicity" as such: "*Substances are defined as carcinogenic if after inhalation, ingestion, dermal application or injection they induce (malignant) tumours, increase their incidence or malignancy, or shorten the time of tumour occurrence*" [43].

- *Genotoxicity*

According to the Organisation for Economic Co-operation and Development (OECD) [44], genotoxicity is: "*a general term encompassing all types of DNA or chromosomal damage, including DNA strand breaks, adducts, rearrangements, mutations, structural chromosome aberrations, and aneuploidy. Not all types of genotoxic effects result in mutations or stable (transmissible) chromosomal damage".*

Distinction should be made between:

a. Direct-acting genotoxic carcinogen

Direct-acting genotoxic carcinogens lack a determinable safe threshold. The absence of a safe threshold means that even at the lowest possible exposure (theoretically, just one molecule), the substance can initiate cancer. With increased exposure, the risk correspondingly increases. Therefore, no matter how low the exposure, the risk of cancer development remains significant [45].

b. Indirect-acting genotoxic carcinogen

For indirect-acting genotoxic carcinogens, the determination of a safe limit can be established. These substances do not interact directly with DNA but ultimately cause damages to it. The mechanisms involved in such actions are inhibiting DNA repair, effects on the spindle apparatus and topoisomerase inhibition. Therefore, sufficient damages needs to accumulate for the effect to become evident, which establishes a threshold limit [45].

c. Non-genotoxic carcinogen

These substances promote cancer without directly or indirectly damaging DNA. A non-exhaustive list of such non-genotoxic mechanisms includes the regulation of gene expression (epigenetic mechanisms), disruption of hormonal balance, regulation of growth factors and steroid hormones, and immunosuppression. For such substances, a threshold can also be determined below which it is unlikely to observe carcinogenic effects [45].

❖ *Mutagenicity*

The OECD [44] defines "mutagenicity" as: "*a subset of genotoxicity. Mutagenicity results in events that alter the DNA and/or chromosomal number or structure that are irreversible and, therefore, capable of being passed to subsequent cell generations if they are not lethal to the cell in which they occur. Thus, mutations include the following:"*

1) "Changes in a single base pair; partial, single or multiple genes; or chromosome"

2) "Breaks in chromosomes that result in the stable (transmissible) deletion, duplication or rearrangement of chromosome segment"

3) "a change (gain or loss) in chromosome number (i.e. aneuploidy) resulting in cells that have not an exact multiple of the haploid number"

4) "DNA changes resulting from mitotic recombination"[44].

❖ *Mutagenic:*

The term mutagenic therefore refers to a chemical that "*produces a heritable change of DNA base- pair sequences(s) in genes or of the structure of chromosomes (chromosome aberrations)*" [46].

❖ *Clastogen*

Clastogen is said of "*a chemical that causes structural chromosomal aberrations in populations of cells or organisms*" [44].

4.2. Relevant toxicological test to study MOSH/MOAH

4.2.1. Mouse skin painting test

In the past, the mouse skin painting test was commonly used in toxicology to assess the carcinogenic potential of chemicals. Mice were often employed due to their suitability for evaluating the carcinogenicity of substances like MO, as the skin tumours developed in mice resemble those in humans, although mouse skin is more sensitive than human skin. However, this method is time-consuming, animals intensive, and raises ethical concerns [47–50].

Therefore, since 1990, the European legislation has adopted the DMSO-based IP 346 method (explained in section 4.3.1) as a faster screening method able to discriminate between carcinogenic and non-carcinogenic mineral oils [47]. This alternative method is, however, indirect and based on the correlation of its results with those of the mouse skin painting test. It does not involve a toxicological evaluation on a biological system.

4.2.2. Ames test

The Ames test, developed by Bruce Ames' laboratory in 1973, evaluates the mutagenicity of chemical compounds and their degradation products on prokaryotic cells.

This test involves exposing modified (auxotrophic) *Salmonella* strains to the chemicals under investigation [51]. Typically, these strains have mutations in amino acid-coding genes such as in the histidine operon (histidine auxotrophic), rendering them unable to form colonies if the culture media lack these specific amino acids. However, if the chemical to which the strains are exposed induces a reverse mutation in the genetically modified genes, it restores the bacteria's ability to produce the necessary amino acids, enabling them to grow and form colonies.

Chemicals can mutate genes through different pathways such as for instance base pair substitutions or frameshift mutations. Therefore, different Salmonella strains, such as TA98 (frameshift mutations) and TA100 (base pair substitution), have been generated by Bruces Ames' laboratory to assess the type of mutation caused by the studied substance.

In addition to using different strains, the Ames test can be conducted in two variations: with and without S9 mix. The S9 mix contains a metabolic activation system derived from rat liver (it can originate from other mammals), which mimics the metabolic processes that occur in mammals [52]. In fact, the *Salmonella* strains used in the Ames test do not express cytochrome P450 enzymes, which are responsible of xenobiotic metabolism in mammals. Hence, including an exogenous mammalian metabolic activation system S9 mix, allows for the assessment of mutagenic properties of metabolised compounds. Conversely, when performed without the S9 mix, the test evaluates the mutagenicity of the compounds in their non-metabolised form [51].

In terms of interpretation of the results, they depend on the intrinsic way in which the test operates. Indeed, the culture media contain a pH indicator, bromocresol purple, that shifts from purple to yellow when cells revert, as they produce organic acids that acidify the culture media [14,53]. Therefore, the number of positive wells in a 384-well plate is compared to the number of positive wells in the negative control to ensure that the observed mutations are due to the tested chemicals and not to hazard. Each well is then either positive or negative and if the ratio between the sum of positive wells of the tested substance with the sum of positive wells of the negative control is higher than 2, the studied substance can be considered mutagenic at the tested concentration.

To ensure consistency across experiments and procedures, the OECD has established international guidelines, such as *"Test No 471: Bacterial Reverse Mutation Test"* [54], that describes how to perform the test, the different reagents to use and how to interpret results [51]. The schematized procedure of the Ames test is shown in figure 4.

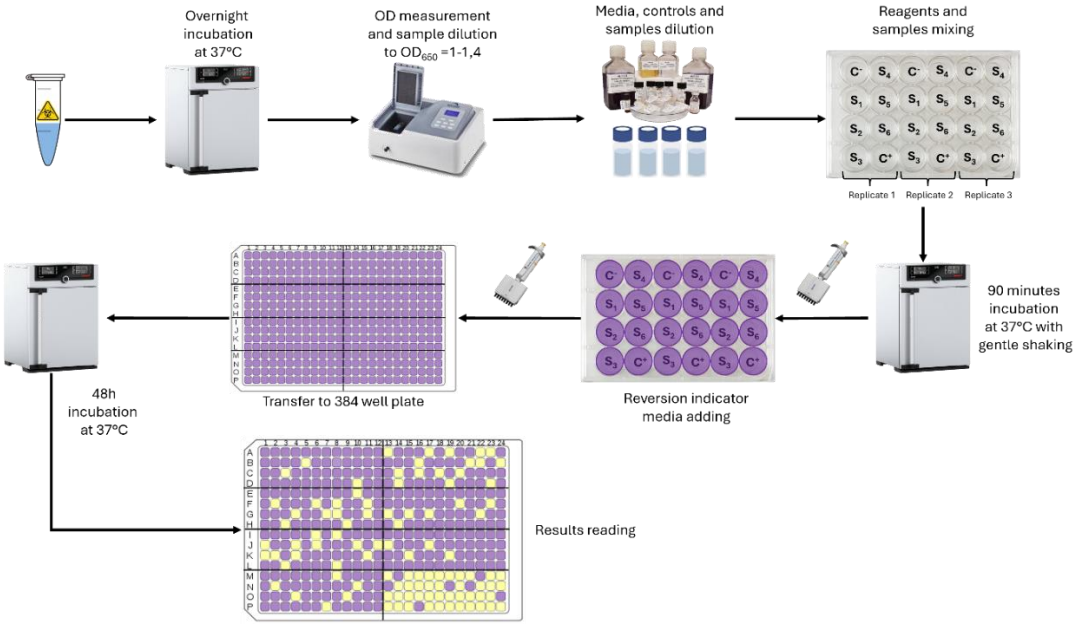

Figure 4: Schematic representation of the Ames test protocol. C- represent the negative control while C+ states for positive control. S1-6 stand for the different samples tested. In the last plate, yellow wells depict reverse mutation while purple wells show absence of mutations.

4.2.3. Micronucleus test

The micronucleus test assesses the genotoxic effects (clastogenic) of certain compounds on eukaryotic cells. Unlike the Ames test, it does not detect mutations in the genome but identifies chromosomal damage. The test involves observing the apparition of small DNA fragments (micronuclei) in the cytoplasm during interphase cell division, where they should not be found during this cell division stage), indicating chromosome damage caused by the tested compounds [46].

4.3. Indirect toxicological evaluation of mineral oils

4.3.1. MO carcinogenicity assessment: IP 346 method

The IP 346 method is a gravimetric technique developed by the industry to assess the carcinogenicity potential of MO, addressing the time-consuming nature of mouse skin painting experiments. The correlation between the carcinogenic hazard of a MO and the IP 346 has been established based on the outcomes of mouse skin painting studies.

The method is based on correlating the extracted mass to the carcinogenic potential of a MO using a DMSO extraction-based screening approach [47]. Specifically, if the substance yields less than 3% DMSO extract compared to the original MO weight as measured by the IP346 method, it is not considered carcinogenic [47,55]. Indeed, a strong correlation of DMSO extractable content above 3% in mass and skin cancer occurrence has been demonstrated. Figure 5 illustrates the schematic representation of the IP346 method.

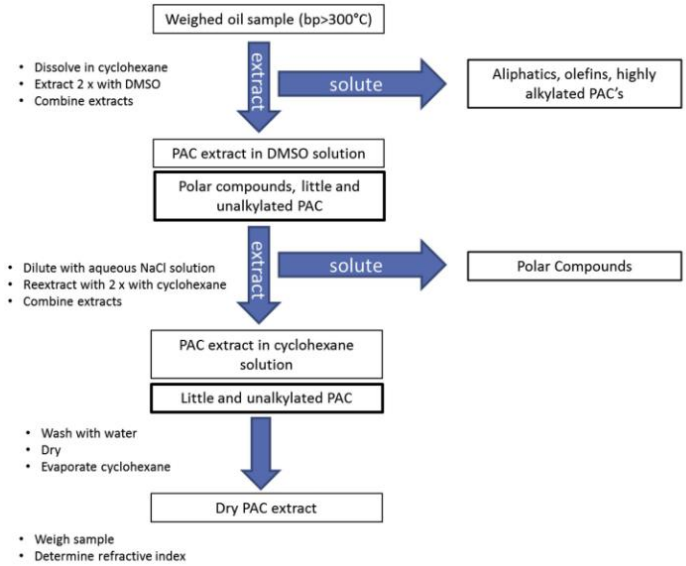

Figure 5: IP346 method scheme. The acronym "bp" in the first box stands for boiling point. Reproduced from Carrillo et al. (2019) [47].

DMSO has been chosen for this method as it is highly selective towards PAHs. Indeed, outer electrons belonging to the sulphur atom of DMSO are attracted by the π-electrons sites of the PAHs (figure 6).

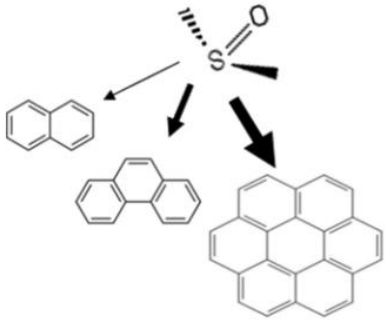

Figure 6: DMSO's sulfur atom attracted toward the π-electrons rich sites of the polyaromatics compounds. Reproduced from Carrillo et al. (2019) [47].

4.3.2. Pharmacopoeia and MO composition correlation

The European pharmacopoeia method (Ph. Eur) [20] is used to determine whether a MO can be considered as medicinal grade or not. However, this specific method has been developed to target PAHs and not PACs. Therefore, no correlation between the composition of tested MO, the DMSO extracted content, and the result of the test has ever been made. Meaning that no MOAH content has been settled below which the test would give a negative result.

Thus, the mouse skin painting assay and the IP 346 method is a notable example of correlation that has already been achieved, enabling conclusions to be drawn about the carcinogenic nature of a MO using a test that is easier to implement than the one carried out on mice. But despite the correlation that has been established for this carcinogenic character, there is no clear evidence of which compounds, composition or concentration cause the test to be positive. Moreover, the documentation related to the elaboration of this specific correlation has never been published [47]. Moreover, the IP346 method still present some drawbacks such as the solvent quantity required to perform the test which prompts industrials to avoid carrying out the test whenever it is possible.

4.4. MOSH/MOAH toxicity: Accumulation and metabolism

The toxicity of MOH depends on its composition, notably the MOSH and MOAH distribution. The MOSH fraction has not shown any evidence of carcinogenic or genotoxic properties so far. The MOAH fraction, which contains aromatic rings ranging between 1-7, is considered concerning for human health and more especially due to the 3-7 rings compounds. In fact, crude oils that undergo insufficient refinement and still contain aromatic compounds have been shown to induce carcinogenic effects in rat skin painting experiments [47]. Furthermore, there is sufficient scientific data to evaluate that unrefined or mildly refined MO are carcinogenic for humans and are therefore classified as group 1 carcinogens [56].

4.3.1. MOSH

4.3.1.1. Metabolism

MOSH are composed of many hydrocarbons that for some are difficult, if not impossible for the body to be metabolized. The structural characteristics of MOSH (especially alkylated naphthenes) impede its biotransformation and its excretion by the body, therefore leading to the accumulation of such absorbed compounds [2]. However, not all MOSH are non-metabolised as some alkanes can undergo omega oxidation in the small intestine or in the liver. Cycloalkanes can also be metabolised to form cyclanols if oxidation occurs on rings or on alkyl side chains (figure 7) [2,57]. Branched alkanes could also be oxidised to form tertiary alcohols but as stated

in the EFSA report [2], the reported branched alkanes studied did not go through any kind of biotransformation both in human and rat liver microsomes [2].

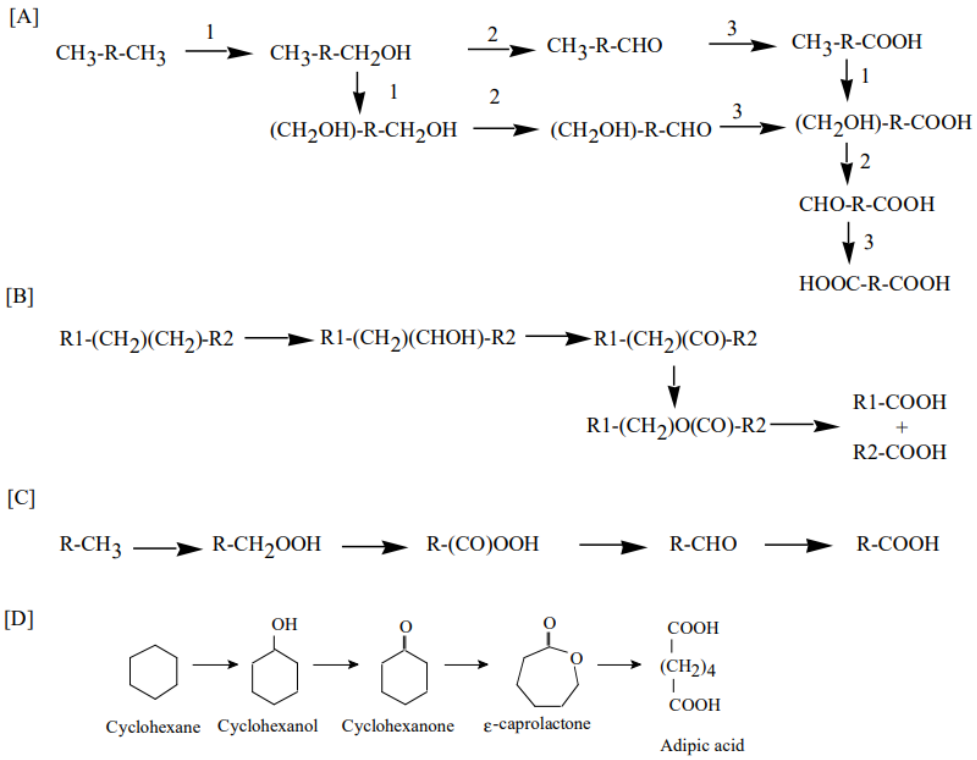

Figure 7: Representation of alkanes' degradation by different pathways. [A] Terminal oxidation of n-alkanes (α & ω hydroxylation). [B] n-alkane subterminal oxidation. [C] Alkyl hydroperoxide n-alkane degradation pathway. [D] Cyclohexane degradation. Reproduced from Harayama et al. [57].

4.3.1.2. Accumulation

❖ *Human accumulation*

The accumulation potential of MO through the body requires specific attention as for instance, the consequences on human health of long-term accumulation of MOSH have never been examined and are uncertain [2]. Although MOSH substances are not categorized as mutagenic, the accumulation of it into different body parts may lead to unknown health effects [2,58]. A study from Barp et al. [59] has been conducted on 37 individuals and MOSH concentrations found in different organs are reported in table 2.

Table 2 : MOSH concentration values found in human organs reported in Barp et al. [59].

Organ	Median concentration (mg/kg)	Highest detected quantities (mg/kg)
Spleen	28	1400
Mesenteric lymph node (MLN)	166	1390
Liver	71	900
Adipose tissue	87	\
Lung	7	\

The MOSH composition in the liver and spleen was quite similar and consisted of n-alkanes ranging between n-C18 and n-C45, with most MOSH centred on n-alkanes between C25-C27 [59]. But the most important point emerging from this table is the significant differential accumulation degree between the various organs.

Nevertheless, some studies have been conducted on animals, and more especially rats (Fischer 344 and Sprague Dawley) to assess the accumulation of MOSH through their body and thereafter try to extrapolate the results to humans and compare them to see similarities [3,35,59–61]. However, there is not always an agreement on the extrapolation of toxicological data to humans by using rat models [61]. The accumulation of MOSH in rats and humans is then differing in different aspects, such as the most MOSH-accumulating organ but also the range of carbon compounds preferentially stocked in the organ.

4.3.2. MOAH

4.3.2.1. Metabolism

The MOAH biotransformation is closely linked to the functioning of the cytochrome P450 later explained in this section. The metabolism of PAHs has been extensively studied and may be similar to that of MOAH. PAHs metabolism is the result of a cascade of reactions originating with the activation of the aryl hydrocarbon receptor (AhR) and, consequently, the regulation of cytochrome P450.

However, it is important to note that the alkyl groups present in MOAH compounds might influence the biotransformation pathway. Therefore, bioactivation through substituted PAHs metabolism is still under investigation [62]. However, PAHs metabolism leads to the formation of epoxide groups, which in turn lead to the formation of electrophilic compounds able to bind to macromolecules such as proteins or nucleic acids [2,63]. Such covalent binding between the reactive electrophilic substances and the nucleophilic DNA and protein sites ends up in formation of adducts. The capacity of chemical to bind DNA, either metabolised or not, is considered to be evidence of their carcinogenic and mutagenic potential [64].

Recent studies, such as that by Wang et al. [65], highlight the importance of evaluating these carcinogenic and mutagenic characteristics in MOH. They found that the degradation products of alkylated polyaromatic hydrocarbons (PACs) can be more mutagenic than those of the parent compounds. Given that the MOAH fraction of MO primarily consists of PACs, assessing their toxicological potential is crucial especially knowing that polycyclic aromatic hydrocarbons (PAHs) have already been categorised as carcinogenic, mutagenic and teratogenic (causing developmental malformations) [66].

❖ *AhR*

The AhR is a ligand-dependent transcription factor that regulates toxicological and biological effects associated with exposure to various chemicals. This receptor has been shown to play a role in various disorders and illnesses, including cancer, inflammatory diseases, and endocrine disruption [67]. In its unbound state, AhR is part of a cytosolic multiprotein complex linked to a heat shock protein (HSP) and often also linked to a tyrosine kinase protein (c-Src) in several cell types. However, upon ligand binding, the complex dissociates, allowing AhR to translocate into the cell nucleus where it forms a heterodimer with the AhR nuclear translocator. This newly formed complex then binds to xenobiotic-responsive elements (XREs) located in the enhancer region of specific genes, recruiting necessary transcriptional machinery for gene expression [67,68]. One of the target genes regulated by AhR is the one regulating cytochrome P450, and the different reactions (mono-oxidation, hydroxylation) catalyzed by CYP-1 (family of xenobiotic-metabolizing enzymes) may result in the generation of oxidative stress, leading to harmful effects on tissues through DNA modifications [67,69]. Figure 8 depicts the upregulation of cytochrome P450 expression by PAHs through AhR activation.

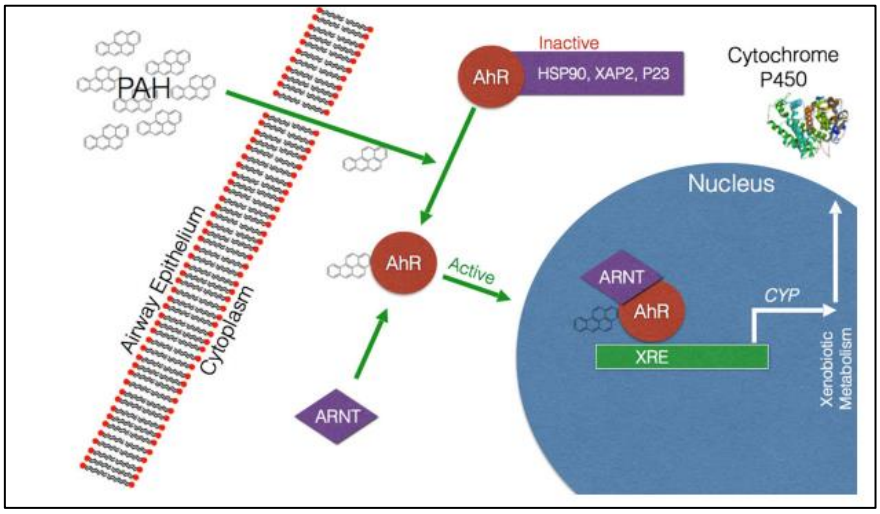

Figure 8: Upregulation of cytochrome P450 expression by PAHs. Reproduced from Klingbeil et al. [68].

❖ *P450 system*

Cytochromes P450 (CYP) are a superfamily of heme-containing enzymes primarily involved in xenobiotics metabolism in mammals. They are divided into families, subfamilies, and individual enzymes [70]. The metabolic oxidation system based on cytochrome P450 is primarily found in the liver, but also in the kidneys and lungs of humans and some other mammals. It processes various chemicals such as PAHs and aromatic amines, with the resulting metabolites potentially forming DNA-reactive compounds (electrophilic compounds) [51]. For certain PAHs like benzo[a]pyrene (BaP), metabolic transformations involving P450 enzymes produce dihydrodiol epoxides, which are of concern due to their potential to bind to DNA, leading to mutations and possibly cancer [62].

❖ *The bay region and alkylation effect*

The substitution of a methyl group on three or more polyaromatics hydrocarbons can generate a bay-region like structural motif (figure 9B). When in unsubstituted PACs, this region is oxidized, it results in the formation of mutagenic and extremely reactive epoxy-diol products [71]. Studies have shown that the methylation of phenanthrene in position 1 or 9 (figure 9B) lead to a positive Ames test result while methylation on position 2 and 3 lead to negative ones. What's more, the bioactivation of such methylated compounds was higher than the one associated to the parent compound and therefore increase the mutagenicity of these methylated compounds that create an additional bay-like region [62,65]. Figure 9A depicts a bay and a fjord region which are a 3 and 4 respectively fused ring conformations forming a concave structure.

The bay region is more susceptible to metabolic oxidation by exposing its angular benzene than fjord region as the latter possesses a higher steric stress around angular benzene, reducing its oxidation by P450 enzymes. The bay-region is more prone to be oxidised by monooxygenases CYP1 enzymes as the reactive surface of the angular benzene is increased and therefore a higher negative charge compared to the other rings is observed, favouring the oxidation reaction [72].

It is recognized that some PAHs, such as BaP and dibenzo[a,l]pyrene (DBalP), are carcinogenic and mutagenic compounds due to the oxidation of aromatic rings encountered during biotransformation in the human body [71,73]. However, the metabolization pathway of MOAH is less clear and requires further study. The wide and varied degree of alkylation in MOAH makes the biotransformation by the P450 enzymes more complex, as oxidation of the rings is shifted towards the alkyl chain, potentially reducing the hazardousness of the products [35,74]. Unfortunately, this is not always the case, and depending on the site of alkylation, the length of the alkyl chain, and the number of aromatic rings, oxidation of the rings may be more or less favoured [2,62,65]. However, even when compounds are highly alkylated and the metabolization process favours oxidation of the alkyl chains rather than the aromatic rings, carcinogenic properties are still associated with these chemicals [75].

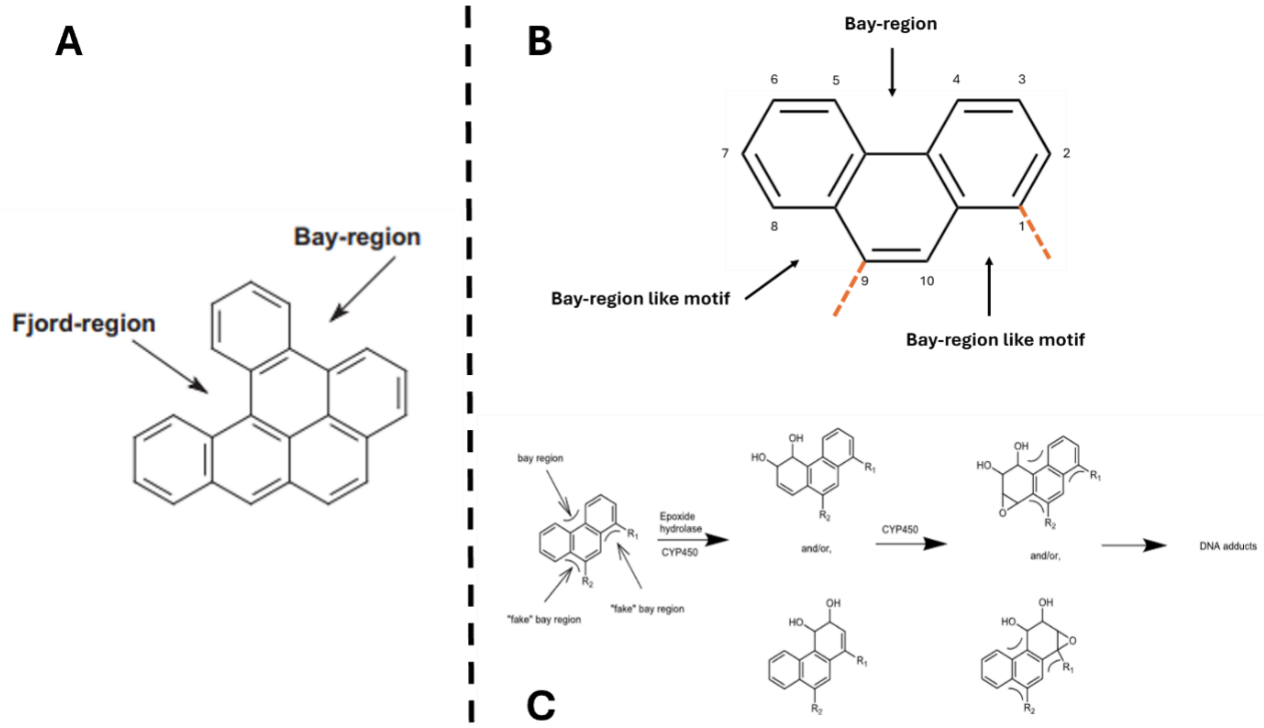

Figure 9: (A) Polycyclic aromatic hydrocarbon Fjord-region and Bay-region. Reproduced from Boogaard. (2011) [71]. (B) Phenanthrene bay-region and bay-region like motif when alkylated in position 1 and 9. Dashed orange line represents a methyl alkylation. (C) Bay region dihydrodiol-epoxide formation through possible metabolic pathway of 1-methyl and 9-mehtyl phenanthrene. Reproduced from Wang et al. (2022) [62].

In fact, in 2022, Wang et al [62,65] studied the effect of alkyl-substitution of phenanthrene and BaP on their associated biotransformation and mutagenicity. They illustrated that aromatic oxidation is indeed well shifted toward the alkyl chain except when the alkyl chain size reaches twelve carbons or more as in this case biotransformation is insignificant due to steric hindrance, preventing binding to the P450 enzyme active site [62,74]. It is also stated that the more the alkyl substitution is long the more oxidative metabolism is reduced with a threshold fixed at six carbon atoms from which even alkyl chain oxidation is significantly decreased [62,65]. What's more, when phenanthrene's alkyl-substituted chain length is superior to three carbon atoms, aromatic oxidation is not observed anymore [62]. The same biotransformation hampering phenomenon is observed with BaP but with an alkyl chain length equal and superior to 6 carbon atoms [65].

4.3.2.2. Accumulation

Regarding MOAH accumulation, it is believed that MOAH do not accumulate in the human body due to their metabolization. Such conclusions are drawn from studies conducted on humans where no MOAH were detected in the different tissues analysed, with limits of detection ranging between 0.5 and 5 mg/kg depending on the organ analysed [2,7].

5. Goal of the present research

The present work is part of a 4 years FNRS project (T.0187.23) that aims to better understand the toxicity of MO. The main goal of this project in the toxicological domain aims to verify the ability of MOSH to be activated in the liver and bioaccumulate in adipose tissues, clarify the metabolic and toxicological profiles of MOAH, determine the role of alkylation in the overall toxicological effect of MOAH and evaluate the suspected cocktail effects of MOAH. To reach these goals on the toxicological side, the support of a detailed analytical characterization of the complex mixture investigated is needed as well as the possibility to simplify them in sub-fractions to facilitate the understanding. The entire structure of the project is shown in the scheme below (figure 10).

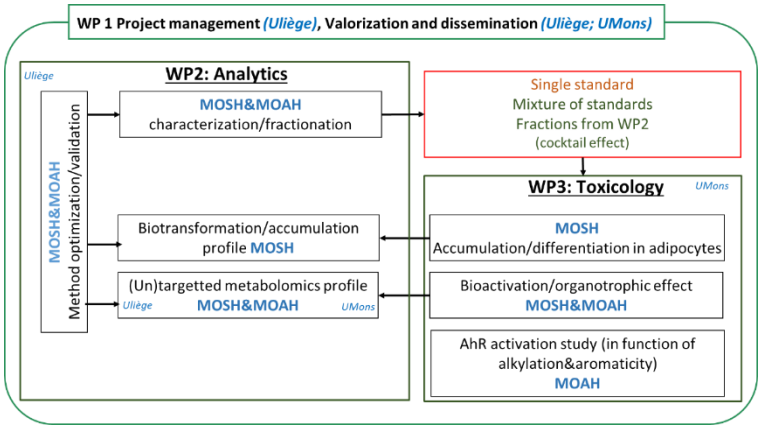

Figure 10 : Schematic representation of the FNRS (T.0187.23) project structure.

This thesis work aimed to develop the protocols necessary to start the project both from the analytical and toxicological viewpoint, with particular focus on the MOAH fraction.

The main goals during this thesis work have been to:

- Optimize a fractionation method to isolate MOSH and MOAH to study their effect separately.
- Optimize a fractionation method to isolate the sub-fraction of MOAH, notably 1-2 rings MOAH and MOAH with more than 3 rings.
- Characterise the isolated fractions.
- Set-up the protocols for the toxicological evaluation of these highly apolar fractions (solubility test, viability, Ames test and Micronucleus).

Material and methods

1. Solvents

Acetone, *n*-hexane, and iso-octane were purchased from Biosolve (Dieuze, France). n-Hexane was distilled before use to reach higher purity. Dicholormethane LiChrosolv was provided by Merck (Darmstadt, Germany). DMSO used was purchased from Sigma-Aldrich (Missouri, USA) and Fischer chemicals (New Jersey, USA).

2. Reagents and material and samples

Anhydrous sodium sulfate ≥ 99,0%, silver nitrate ≥ 99,0%, methoxyamine hydrochloride, silica gel (high purity grade, average pre size, 60 Å (52-73 Å), 70-230 mesh, 63-200 µm for column chromatography), crystal violet solution (HT901-8FOZ) and naphthalene were all purchased from Sigma-Aldrich (Missouri, USA). BSTFA, Triton X-100, Glutaraldehyde, crystal violet solution (2,3%), Dulbecco's Phosphate Buffered Saline (D-PBS), Eagle's Minimum Essential Medium (EMEM) M4655 and paraformaldehyde (PFA) were bought from Merck (Darmstadt, Germany). Fetal Bovine Serum (FBS) S181B was acquired from Biowest (Nuaillé, France).

Mineral oil samples were kindly provided by collaborators under different distillate extracts. These extracts originate from SN100 and SN500 mineral oil fractions and the 2 main fractions used were the "aromatic extract" and the "raffinate" ones. SN100 medicinal white oul has also been used. Moltox and Gravex samples were also provided by collaborators. Paraffin (*Paraffinum liquidum*) was purchased from Magis Pharma (Wilrijk, Belgium). 2,3,7,8-Tetrachlorodibenzo-p-dioxin was purchased from Cambridge Isotope Laboratories (Massachusetts, USA). The various lubricant samples used were found in private homes. Table 3 lists the various samples used for this work and their specifications.

Table 3 : Sample list and their characteristics used for all the tests carried out.

Sample name	Specification	MOAH content
SN 100 aromatic extract	Distillation fraction	70%
SN 100 raffinate	Distillation fraction	6%
SN100 white oil	Distillation fraction	0%
SN 500 aromatic extract	Distillation fraction	82%
SN 500 raffinate	Distillation fraction	16%
Sternel Motor Oil	Motor oil	48%
Retinax	Multi-purpose grease	49%
Dentax	Transmission oil	32%
Castrol classic	Motor oil	31%
Honda	Motor oil 15W40	28%
Gulf lub	Motor Oil	29%

Plastic material (plates, pipettes, cuvettes, …) for cell culture and toxicological tests were purchased from VWR (California, USA). Vectashield® Antifade mounting medium with DAPI (H-1200-10) has been purchased from Vector laboratories (California, USA). Ethanol used to degrease microscopic glass slides (CL00.1807.5000) was bought from Chem-lab (Zedelgem, Belgium)

3. Standards

MOSH MOAH internal standard (IS, Restek #31070), retention time standard (RTS, Restek #31076) and the 610 PAH calibration Mix A standard (Restek #31264) were kindly gifted by Restek company (Neukirchen-Vlun, Germany). The composition of the different standard is listed in the tables below (tables 4,5,6) and the roles of MOSH/MOAH standard compounds is described based on [12,76].

Table 4 – MOSH MOAH internal standard composition (Restek #31070).

Compound	Concentration (µg/mL)	Role
5-α-cholestane (Cho)	600	Establish the end of the MOSH elution in the LC column.
(C11) *n*-Undecane	300	Ensure no losses of the most volatile MOSH compounds (low molecular mass) occurred during the solvent evaporation in the retention gap by calculating the ratio CyCy:C_{11}, which should equal 1.
(C13) *n*-Tridecane	150	Ensure absence of co-eluting interferences by calculating the ratio CyCy:C_{13}, which should equal 2.
Bicyclohexyl (CyCy)	300	Internal standard for MOSH quantification.
n-Pentylbenzene (5B)	300	Ensure no loss from the low molecular mass MOAH
1-Methylnaphthalene (1MN)	300	Internal standard for MOAH quantification.
2-Methylnaphthalene (2MN)	300	Internal standard for MOAH quantification. Also ensure no co-eluting interferences with the quantification standard by calculating the ratio 2MN:1MN
1,3,5-Tri-tert-butylbenzene (TBB)	300	Establish the beginning of the MOAH elution in the LC column.
Perylene (Per)	600	Establish the end of the MOAH elution in the LC column

Table 5 - MOSH MOAH retention time standard composition (Restek #31076)

Alkane	Cas number	Concentration (µg/mL)
(C10) *n*-Decane	124-18-5	100
(C11) *n*-Undecane	1120-21-4	
(C13) *n*- Tridecane	629-50-5	
(C16) *n*-Hexadecane	544-76-3	
(C20) *n*-Eicosane	112-95-8	
(C24) *n*-Tetracosane	646-31-1	
(C25) *n*-Pentacosane	629-99-2	
(C35) *n*-Pentatriacontane	630-07-9	
(C40) *n*-Tetracontane	4181-95-7	
(C50) *n*-Pentacontane	6596-40-3	

Table 6 - 610 PAH Calibration Mix A composition (Restek #31264)

Compound	Cas number	Concentration (µg/mL)
Acenaphthene (Ac)	83-32-9	1000
Acenaphthylene (Ap)	208-96-8	1000
Anthracene (A)	120-12-7	1000
Benz[a]anthracene (BaA)	56-55-3	500
Benzo[a]pyrene (BaP)	50-32-8	500
Benzo[b]fluoranthene (BbF)	205-99-2	500
Benzo[k]fluoranthene (BkF)	207-08-9	500
Benzo[g,h,i]perylene (BghiP)	191-24-2	500
Chrysene (Ch)	218-01-9	500
Dibenz[a,h]anthracene (DBahA)	53-70-3	500
Fluoranthene (Fl)	206-44-0	500
Fluorene (F)	86-73-7	1000
Indeno[1,2,3-cd]pyrene (IP)	193-39-5	500
Naphthalene (Na)	91-20-3	1000
Phenanthrene (Pa)	85-01-8	500
Pyrene (P)	129-00-0	500

4. Sample preparation

All laboratory equipment used was made of glass (Pasteur pipette, Hamilton syringes, volumetric flasks, …) and were carefully washed with pure solvents (3× acetone and 3× hexane) before each use. Plastic material was avoided as much as possible to limit contaminations with hydrocarbons.

4.1. MOSH/MOAH separation on SPE column

Mineral oil samples were separated on 6 mL silver silica lab-packed glass cartridge (Macherey-Nagel, Chromabond, Düren, Germany; Ø= 14,4 mm, L= 80mm). Fiberglass bottom frit (Macherey-Nagel, Chromabond, REF= 730192, Düren, Germany) was placed in the bottom of each column which were placed on a vacuum manifold (*Sep-Pak*, Alltech, Maryland, USA). The silver silica was prepared according to Moret et al., (2012) protocol [77]. The silica quantity and the elution steps were adapted from Moret's article to the specific goals and analysed samples. The final conditions of the SPE are reported in table 7.

Table 7 - MOSH/MOAH SPE separation conditions

Solvent/sample	Volume (mL)	Step
Hexane	5	Bed soaking
Hexane	6	Column conditioning
Sample	0.200-0.250	Sample loading
Hexane	2	Dead volume removal
Hexane	5	MOSH collection
Hexane	1	Free fraction collection
Dichloromethane	14	MOAH collection

4.2. Ring class separation on SPE column

Separation of the samples according to their ring number was performed on 2g pure silica lab-packed glass column (Designed by filter service, 30mL internal volume).

Different samples (SN100 aromatic extract and Moltox) were separated into three different sub-fractions (1-2 rings, intermediate fraction, 3+ rings). The elution gradient and volume used was specific to each sample and are reported in table 8 and table 9. The different areas (1-2 rings MOAH and 3+ rings MOAH) were defined based on the elution pattern of a heavy vacuum gas oil (HVGO) sample, presenting an interesting distribution of aromatic compounds, carbon fractions and degrees of alkylation. The GC×GC-FID chromatogram of this sample can be found in Annex 1.

Table 8: SN100 sample gradient for ring separation

Solvent/sample	Volume (mL)	Step
Hexane (100%)	10	Bed soaking
Hexane (100%)	7	Column conditioning
Sample	0.200	Sample loading
Hexane (100%)	8	Dead volume removal
Hexane/DCM (98%/2%)	5	MOSH removal
Hexane/DCM (98%/2%)	5	1-2 rings collection
Hexane/DCM (95%/5%)	5 (x2)	Intermediate fraction collection
DCM (100%)	15	3+ rings collection

Table 9: MOLTOX sample gradient for ring separation

Solvent/sample	Volume (mL)	Step
Hexane (100%)	10	Bed soaking
Hexane (100%)	7	Column conditioning
Sample	0.200	Sample loading
Hexane (100%)	5	Dead volume removal
Hexane (100%)	5	MOSH removal
Hexane/DCM (98%/2%)	4	
Hexane/DCM (98%/2%)	5	1-2 rings collection
Hexane/DCM (98%/2%)	1	Intermediate fraction collection
Hexane/DCM (95%/5%)	5 (x2)	
DCM (100%)	15	3+ rings collection

5. LC/GC×(GC)-TOFMS/FID Analysis

The analyses were all performed on the LC/GC×GC-TOFMS/FID instrument either in 1D (LC/GC) or 2D (LC/GC×GC). The relative information of this systems is given in Annex 2.

6. UV European Pharmacopoeia test

The correlation test was performed on the following samples: SN100 aromatic fraction, SN100 raffinate fraction, SN500 raffinate fraction, *Paraffinum liquidum*, and lubricant samples taken in private home (table 3). The method applied for this test is the European Pharmacopoeia one [20] adapted to reduce the quantity of sample used. To perform this scale down, the amount of sample and solvent used were all divided by a factor 2. The data were acquired on a UV-1800 spectrophotometer (Shimadzu, Tokyo, Japan) and treated with the software Shimadzu

software UVProbe (version 2.31). The positivity of the test was assessed by the comparison of all the sample absorbance values taken in the spectrum between 260nm and 420nm and the absorbance value of a 7mg/L naphthalene solution at 275nm. If any of the absorbance values in the spectrum was higher than a third of the naphthalene solution absorbance, the test was deemed positive.

7. Toxicological tests

7.1. Cell Line and cellular culture

In vitro test was performed through the use of HepG2-Lucia^{TM} AhR cells bought from InvivoGen (Toulouse, France). The human hepatoma cell line (HepG2) has been transfected with the Lucia luciferase gene regulated under the control of a minimal promoter coupled with the human CYP1A1 gene entire regulatory sequence.

The cell culture process (cell line defrosting, passages, cell culture media changes) has kindly been performed by members of the human biology and toxicology department of the University of Mons.

7.2. Viability test

The solubility of MOAH sample SN100 in different solvents has been investigated to determine maximum concentration achievable in these solvents. Cell culture media employed was Dulbecco's Modified Eagle Medium (DMEM) + 10% fetal bovine serum (FBS). Cells were incubated at 37°C in a Memmert IN160 incubator (Büchenbach, Germany), maintaining a CO_2 level at 5% for 24h before being put in contact with the different samples. Cells were then incubated for a time period of 24h and their viability was thereafter assessed through the "crystal violet" method.

Briefly, cell culture media was removed from the 96 wells plate (VWR, California, USA) and cells were washed twice with a D-PBS solution. One hundred microliters of a 1% glutaraldehyde solution were added to each well and incubated at room temperature for 15 minutes. Glutaraldehyde is then removed, and the same volume of the crystal violet solution (0.1 %) is added and let at room temperature for 30 minutes. The plate is then properly washed twice with distilled water and dried at room temperature. One hundred microliters of tritonX100 0.2% is added to each well and the plate is left under agitation for 60 minutes before reading the absorbance at 570 nm (*VersaMax Tunable Microplate Reader*, Molecular Devices, California, USA). The software used is SoftMax Pro.

7.3. Ames test

The Ames test has been carried out according to the OECD guideline No 471 requirements [54]. The Moltox 31-300 kit (Ames FT TA98/TA100 mutagenicity Test kit 31-300) has been the one used to perform all the Ames test. The protocol used is the one delivered by Moltox for this specific test [78]. Absorbance of the cell culture was read at 600 nm on a Jenway 7200 spectrophotometer (Cole-Parmer, Stone, UK). Cells were incubated 90 minutes on shaking plate in an incubator set at 37°C (Memmert, Büchenbach, Germany). The 48h incubation was done in an INCU-Line incubator at 37°C (VWR, California, USA). Analysis of the results was made by visual observation of the well colors and the absorbance of the wells was also recorded at 420 nm and 590 nm on a BioTek Synergy H1 microplate reader (Agilent Technologies, Waldbronn, Germany). The absorbance values were processed by an algorithm created as part of this work and available in annex 3 of this document as well as the values that had to be set for the code to run properly. The positivity of the test was deemed if the A ratio was higher than a value of 2. The A ratio is calculated as such:

$$A_{ratio} = \frac{number\ of\ positive\ wells\ in\ the\ sample\ condition}{number\ of\ negative\ wells\ in\ the\ negative\ control}$$

7.4. Micronucleus test

The Micronucleus test has been performed as follows:

Sterile round glass coverslips were placed in the bottom of the wells of a 24-well plate and each well was seeded with 50 000 cells. Hepatocytes HEPG2 cells were cultured for 24h at 37°C and 5% of CO_2. After 24h of cell culture, the different samples were put in contact with the cells at a final concentration of 0.5 mg/mL in the well, except for the MOSH sample that had a concentration of 0.2 mg/mL (due to solubility limitations). Triplicates were performed for each sample. Cells were again cultivated for 24h after which the culture media was removed, and cells washed twice with D-PBS. Cell fixation was then performed using PFA at 4°C for 5 minutes followed by 5 minutes at room temperature, after which three washes of 5 minutes each with D-PBS were performed. The slides used were degreased with ethanol and a drop of Vectashield containing DAPI fluorochrome was added on each. The coverslips were then placed upside down on the Vectashield drop and were sealed with commercial transparent nail polish. The slides were then observed thanks to an optical microscope (Leitz Orthoplan) equipped with a Leica DFC 7000 T camera (Wetzlar, Germany). The micronucleus number was counted at 250X magnification by Denis Nonclercq, Professor of histology at the University of Mons and the number of total cells counted with ImageJ software (version 1.54f).

8. Statistical analyses:

Data were statistically treated using RStudio® to monitor the normality of populations and the homogeneity of variance. Microsoft® Excel was used to perform Student t-test and Welch test. The significance of the student t-test was settled as *, ** and *** if the p-value was respectively <0.05, <0.01, <0.001. Whenever the homogeneity of the variance was not respected, a Welch test was performed rather than a student t-test. When the normality of the population was not respected, no other statistical test was performed as these cases were not frequent and the implementation of another test would generate differences in the statistical test carried out within the same condition.

Results and discussion

The flowchart below (figure 11) outlines the tests and procedures performed in this master's thesis. MOH was separated into MOSH and MOAH, with further separation of MOAH based on aromatic content, necessary for subsequent toxicological testing. Various tests (Ames and micronucleus assays) were conducted on the MOSH and MOAH fractions, but not on the MOAH sub-fractions. These untested sub-fractions will be examined soon. Additionally, the solubility of the MOSH and MOAH fractions and their impact on cell viability were assessed before performing the toxicological tests. In parallel, the Ph. Eur. UV method was evaluated on lubricant samples to understand the relation of what is measured in this test with the effective MOAH composition of the samples analysed by GC×GC.

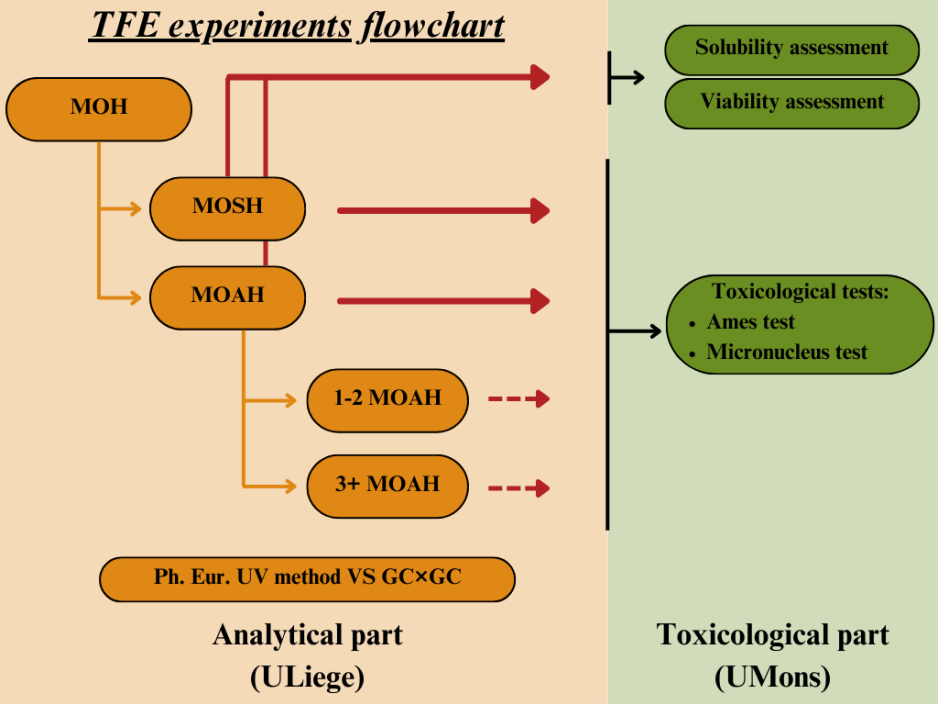

Figure 11 : Flowchart of the experiments performed in the frame of the master's thesis work. Orange and green backgrounds represent the analytical side and the toxicological part respectively. Orange lines depict fractionation steps. The red lines indicate the completion of the of the test to which they point. Red dashed lines indicate the non-completion of the tests to which they point but that were aimed to be done.

1. Preliminary method optimisation

1.1. Extraction of total MOAH from mineral oils

1.1.1. Optimization using SN100 aromatic extract

The toxicological assessments in this study focused on the MOAH fraction of MO, requiring pure MOAH samples. The MOSH and MOAH composition of different pure MO samples present in the lab was characterized particularly for different products from the SN100 and SN500 production lines, with these codes referring to the viscosity and compositional characteristics of the products (Table 10). However, even aromatic MO extracts contained some

MOSH (Figure 12). Thus, it was necessary to optimize a purification step to obtain the purest MOAH extract possible (free of MOSH).

Table 10 : Composition of the different mineral oils available in the laboratory.

SN100						
	AROMATIC EXTRACT	DISTILLATE	RAFFINATE	BASE OIL	TECHNICAL WHITE OIL	MEDICINAL WHITE OIL
%MOAH	70%	31%	6%	8%	5%	<0.2%
% <3AR	67%	70%	100%	99%	100%	94%
% >3AR	33%	30%	0%	1%	0%	6%

SN500						
	AROMATIC EXTRACT	DISTILLATE	RAFFINATE	BASE OIL	TECHNICAL WHITE OIL	MEDICINAL WHITE OIL
%MOAH	82%	37%	16%	19%	13%	<0.3%
% <3AR	52%	64%	97%	97%	98%	0%
% >3AR	48%	36%	3%	3%	2%	0%

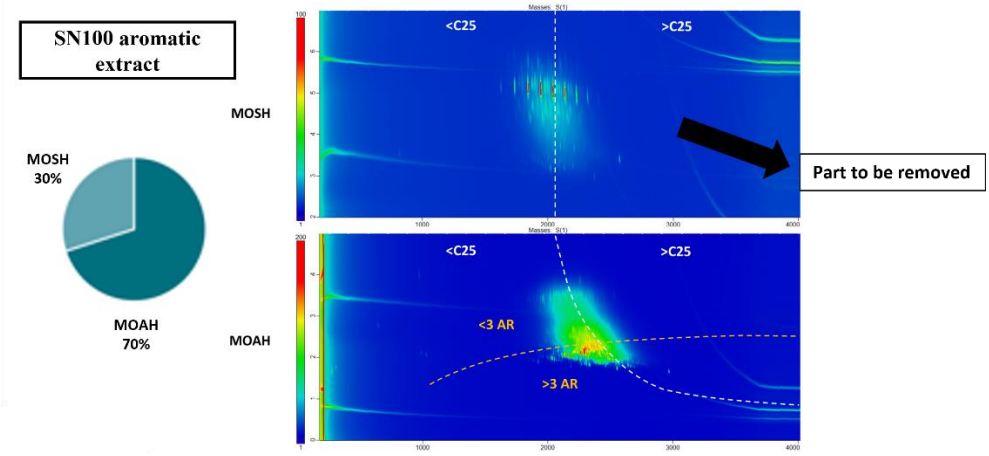

Figure 12 :MOSH and MOAH compositions of the SN100 aromatic extract and corresponding GC×GC-FID chromatograms. AR stands for aromatic ring, while <C25 and >C25 refer to compounds having a carbon number of less or more than 25, respectively.

The purification of MOSH from the MOAH fraction was performed by solid phase extraction (SPE) on silver silica using a procedure inspired by Moret et al. [77]. The latter being applied to samples containing ppm levels of MOSH and MOAH, such as cardboard and dry food extracts, it had to be adapted for pure MO samples.

This optimization was performed using the SN100 aromatic extract (AE), a pure mineral oil containing very high amounts of MOAH compared to other available samples in the laboratory (Table 10). SN500 AE had even a higher MOAH content, but it was not selected due to its very high viscosity, which makes manipulation challenging.

The starting point of the optimization process was very similar to the protocol by Moret et al. [77]. Briefly, the sample is loaded on a 1g silver silica column and thereafter eluted with 2.5 mL of pure C6 to remove MOSH followed by a 0.5 mL addition of 1:1 C6/DCM mixture. The subsequent 0.5 mL addition results in a fraction free of MOSH and MOAH, used to control the separation efficiency. Then, 7 mL of this same mixture are used to elute the MOAH fraction.

The original protocol also specifies that proper MOSH/MOAH separation is achieved by loading up to 50 mg of fat onto the column, meaning that between the eluting MOSH and MOAH fractions, the intermediate fraction is free from both types of compounds. Although MO and fat are two very different matrices, the optimization trials were started using the same mass.

Fifty milligrams of pure MO (dissolved in 300 µL of hexane) were therefore loaded onto the SPE column, and the original elution conditions were applied. Three fractions have been collected to control the elution process. The first one (called MOSH) should only contain MOSH while the second one (called free fraction) should be free of MOSH and MOAH. The last fraction collected (named MOAH) should only contain MOAH. The results of this first trial are shown in figure 13 (line 1).

As can be seen from the GC×GC chromatograms of the collected fractions (figure 13, line 1), the MOSH and MOAH fraction contains respectively only MOSH and only MOAH. This observation has also been confirmed by injecting separately in HPLC the MOSH and MOAH fraction to collect the respective MOSH and MOAH fraction of each SPE collected fraction (Annex 4). However, the free fraction, which should be free of MOSH and MOAH, shows the co-presence of them, highlighting the need to adapt the original separation protocol to this specific matrix.

In order to reduce MOAH breakthrough in the free fraction, another test (test 2) was conducted in which the amount of silver silica was increased (from 1g to 2g) to provide more interaction sites. The solvent quantities were doubled, also adjusted to account for changes in dead volume due to the increased silica quantity. As a result, the free fraction was free of MOAH but still contained a small amount of MOSH as shown in figure 13 (line 2).

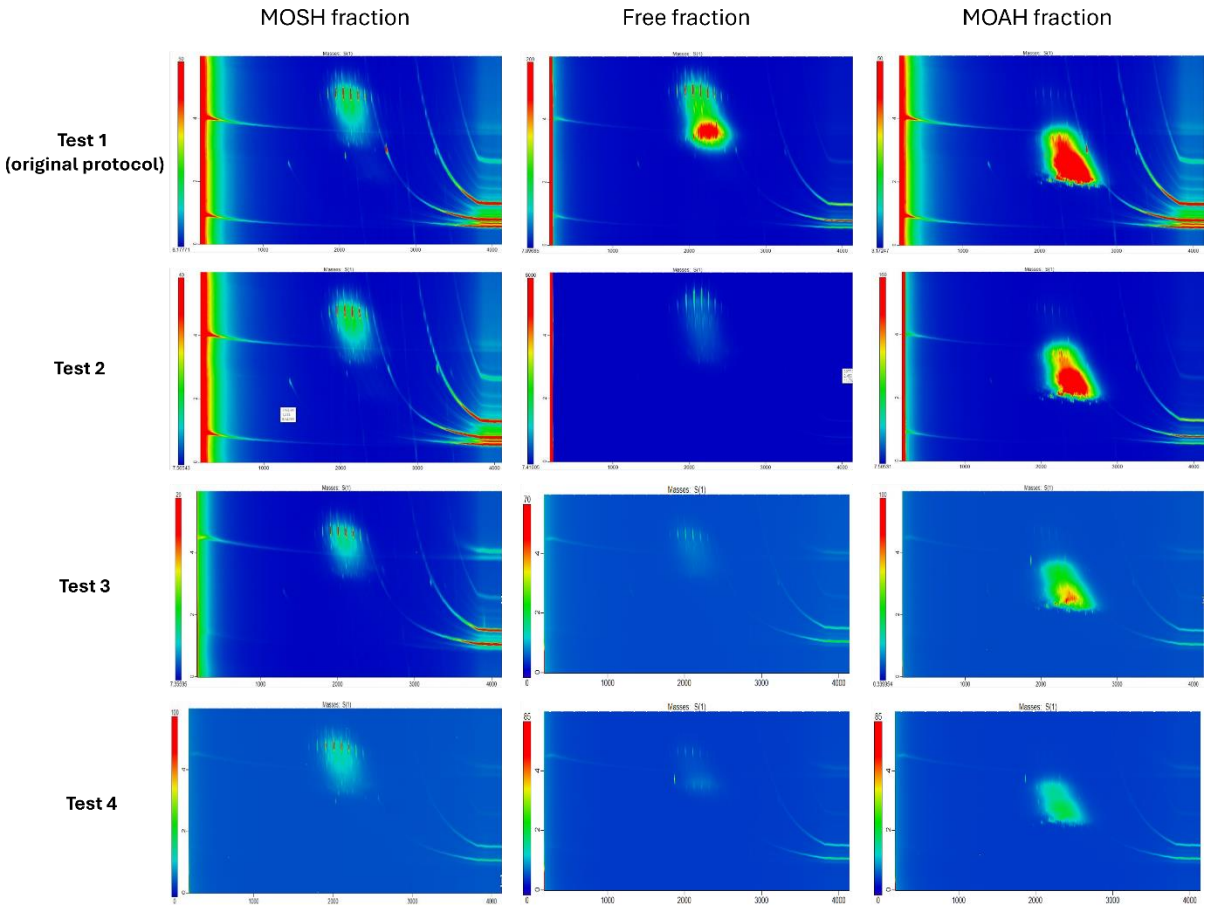

Figure 13 : GC×GC-FID chromatograms of the different fractions collected from SN100 AE sample. In the first line: first test performed with the same elution process as described by Moret et al. [77]. Second line, test 2 with quantity of silver silica and solvent doubled. Third line, test 3 with increased C6 quantity (4mL) for MOSH elution. Last line, test 4 with 5 mL for MOSH collection and free fraction collected with only C6 instead of 1:1 C6:DCM and MOAH fraction collected with DCM only instead of 1:1 C6:DCM mixture.

To try to eliminate the remaining MOSH, the next modification consisted in increasing the C6 volume used for MOSH collection. A 4 mL C6 volume was therefore used (instead of 3 mL previously), but a slight presence of MOSH was still detected at the beginning of the free fraction (figure 13, line 3).

In the fourth test, the used volume of C6 to elute MOSH was increased even further to 5 mL. Consequently, to prevent the too early elution of the least retained MOAH, 1 mL of only C6 was used to elute the free fraction, instead of 1 mL of a mixture of C6:DCM (1:1) (which would have had a too strong elution strength). Additionally, pure DCM was used to elute the MOAH fraction instead of the 1:1 C6:DCM mixture. The goal was to elute the entire MOAH fraction with the smallest possible volume. The results were satisfactory, with no MOAH observed in the free fraction, and only a trace amount of MOSH was detected (figure 13, line 4). Nevertheless, the successive collection and analysis of the eluting MOAH revealed that even after addition of 10 mL of DCM, some MOAH were still eluting from the column, highlighting the strong retention of these compounds on silver silica.

The final test aimed to increase the amount of DCM used to elute the MOAH fraction, but the results were similar to the fourth test, with some MOAH still retained after 14 mL of dichloromethane. Table 11 summarizes the conditions of each optimization test performed.

Table 11: Optimisation steps performed to properly separate SN100 aromatic extract by SPE into MOSH and MOAH fractions. The colour of the boxes and the symbol associated with each colour show the solvent used. Blue and sphere represent C6; green and square represent DCM; orange and triangle represent C6:DCM (1:1).

Test number	1 (Moret et al. conditions)	2	3	4	5
Silver silica quantity (g)	1	2	2	2	2
Sample mass loaded (mg)	52	52	52	57	62
Dead volume	• 1 mL	• 2 mL	• 2 mL	• 2 mL	• 2 mL
MOSH elution	• 1.5 mL	• 2 mL • 0.5 mL • 0.5 mL	• 3 mL • 0.5 mL • 0.5 mL	• 5 ml	• 5 mL
Free fraction elution	▲ 0.5 mL	▲ 0.5 mL ▲ 0.5 mL	▲ 0.5 mL ▲ 0.5 mL	• 1 mL	• 0.4 mL • 0.3 mL • 0.3 mL
MOAH elution	▲ 7 mL	▲ 7 mL ▲ 3 mL ▲ 3mL	▲ 13 mL	■ 4 mL ■ 2 mL ■ 1 mL ■ 1 mL ■ 2 mL	■ 10 mL ■ 1 mL ■ 1 mL ■ 1 mL ■ 1 mL

To obtain 523 mg of pure MOAH from the SN100 AE sample, 18 (3×6) parallel SPEs were performed, accounting for approximately 380 mL of hexane, 320 mL of DCM, and 80 mL of acetone (for glass rinsing), and 15h of work. Considering only the major costs (reagents, analysis, operator salary), about €262 are required to yield 523 mg of pure MOAH (starting from 921 mg of pure SN100 sample). Therefore, 1 g of purified MOAH fraction has an estimated cost of €500 (assuming the original sample contains 70% MOAH). This highlights the precious nature of these purified samples and partially explains why so few toxicological data are available in the literature regarding pure MOAH.

1.1.2. Application to other mineral oil samples

The previously optimised method was used to purify the MOAH fraction from other readily available MO samples (Moltox, SN500 AE, Gravex). These samples were selected to cover a broad diversity in MOAH composition, including variations in carbon range, number of aromatic rings, and degree of alkylation. The aim being to then use these different MOAH samples for subsequent toxicological assessments. The GC×GC profiles of the selected samples are presented in Figure 14.

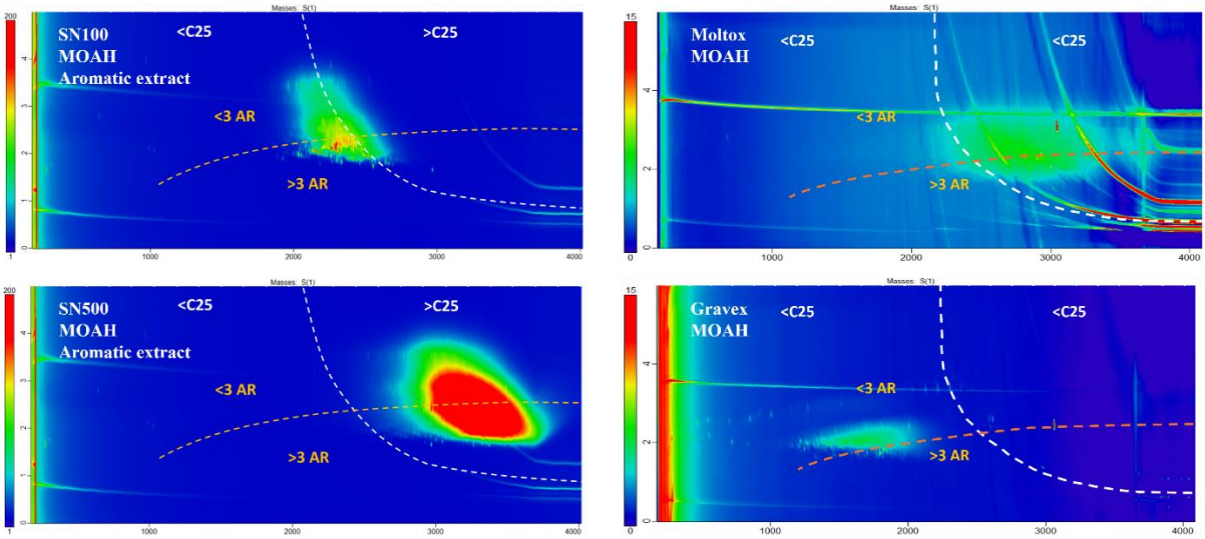

Figure 14: GC×GC-FID chromatograms of the MOAH fractions of the selected mineral oil samples for further toxicological studies on MOAH.

Table 12 shows the mass of MOAH extracted for each sample. The same SPE conditions were applied to Moltox and Gravex as to the SN100 AE (*i.e.*, the conditions reported in Table 11, test 4). The SN500 AE required a minor adjustment: an additional 4 mL of DCM was used to elute the MOAH fraction, ensuring maximum recovery of strongly retained MOAH. SN500 AE is more retained on the column due to its higher content of polar compounds, which increases interaction with the column.

Table 12 : MOAH extracted mass for all the selected samples and the number of SPE columns required to obtain that amount of MOAH.

Sample name	Number of SPE columns performed	MOSH/MOAH composition (%)	Pure MOAH amount available
SN 100 AE	18	30/70	523.2 mg
SN 500 AE	4	18/82	126.2 mg
MOLTOX	5	66/33	55.8 mg
Gravex	5	70/30	23.4 mg

The difference in the mass extracted is obviously correlated to the number of SPE performed. However, some sample such as Gravex and Moltox yield a lower extracted mass considering the same number of SPE columns. The low extracted mass of Gravex might be due to the evaporation step that led to the loss of the most volatile fraction. Indeed, as shown in figure 14, the Gravex composition comprise low carbon number compounds, confirming the hypothesis of volatile loss. Additionally, the MOSH/MOAH amount in Gravex and Moltox is not fully known and the presence of other components such as additives might create a shift in the elution. Moreover, some losses in the transfer from the collected tubes and flasks are inevitable as well as the loss related to the SPE column itself.

Therefore, the elution must be properly adapted case-by-case to maximize extraction. However, adapting the elution for each sample was not the objective of this work, and the quantities of pure MOAH obtained were sufficient for the planned experiments.

1.2. Separation of MOAH in sub-classes (ring class separation)

Already available toxicological literature related to MO mentions that MOAH with 3-7 rings possess carcinogenic properties, while those with 1-2 rings are not yet recognized as carcinogenic but should be handled with caution due to a lack of available toxicological data [4,79,80]. Therefore, to gather more detailed information, it is necessary to fractionate MOAH into distinct sub-fractions based on the number of aromatic rings [80].

Based on analytical scientific literature, sub-fractionation can be separated through amino bonded silica column relying on π-π interactions with the amino group but, the size exclusion effect in such silica limits the efficient separation of highly alkylated aromatics [81]. Donor acceptor complex chromatography (DACC) is another kind of column that allows sub-fractionation of MOAH based on the number of aromatic rings but still present the same drawbacks as the amino bonded silica. However, Koch et al. [79] stated a better separation by using a DACC column.

The observations reported in the literature are based on the use of chromatographic LC column, therefore characterized by a much higher efficiency of a column or SPE separation, but with the limitation of the amount that can be loaded in the column, which is way too low compared to the quantity needed for the toxicological tests (at least dozens of mg). Therefore, it was necessary to find an efficient way to scale up the separation to the collect the amount needed.

Firstly, amino-bonded silica SPE was tested, as already available in the lab. Nevertheless, the commonly commercially available SPE columns are made of plastic. Before optimizing any separation, the feasibility of using plastic SPE was tested for contamination of the sample. The contact of C6 and DCM with the cartridge plastic led to significant hydrocarbons contamination of the collected fractions, preventing their use (Figure 15).

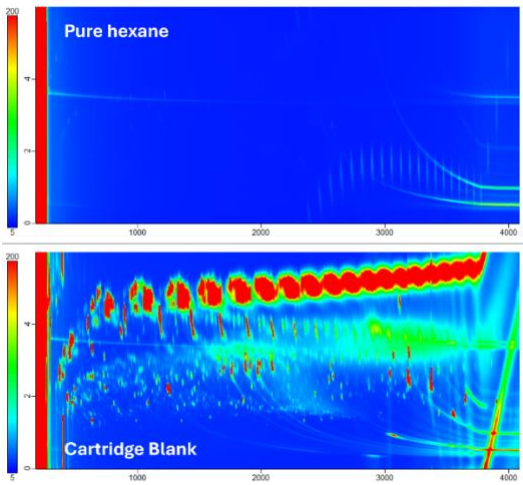

Figure 15 : GC×GC-FID chromatograms of the amino-bonded silica cartridge blank test aiming to determine the possible cartridge plastic's migration following solvents contact.

Therefore, separation by DACC or pure silica remained as options. DACC columns are not available for SPE and are only used in HPLC. Since a large quantity of products was needed for the toxicological tests, it was decided to use glass cartridge packed with pure silica.

The elution was optimized to separate MOAH sub-fractions using this support, with the elution conditions from the internal HPLC method adapted for SPE separation of MO. This internal elution conditions used for SPE separation of MO is reported as "original elution conditions" in table 13. The optimised elution condition for MOAH sub-fractionation is reported in table 13 as (optimised elution conditions). The comparison of the two gradients is shown in Table 13.

Table 13 : Gradient comparison used to separate MO in various MOAH sub-fractions. (Left) original elution conditions, not optimised for the separation. (Right) optimised elution conditions used to separate SN100 AE and MOLTOX samples.

Original elution conditions		
Volume used (mL)	**C6 %**	**DCM %**
8	100	0
2 × 5	98	2
2 × 5	95	5
2 × 6	50	50

Optimised elution conditions			
Volume used (mL)	**C6 %**	**DCM %**	**Fraction**
10	100	0	Wetting
7	100	0	Conditioning
0.2	\	\	Sample loading
5	100	0	Dead volume removal
5	100	0	MOSH collection
4	98	2	MOSH collection
5	98	2	MOAH 1-2 rings
1	98	2	Intermediate fraction
5	95	5	Intermediate fraction
5	95	5	Intermediate fraction
12	0	100	MOAH 3+ rings

SN100 AE and Moltox were separated using the same optimised elution conditions. A preliminary test on a single SPE cartridge was conducted to verify the separation of the sample based on the number of aromatic rings before collecting the final necessary quantity. However, the SN 500 AE sample exhibited poor sub-fractionation of aromatic rings, indicating the need for adjusted elution conditions for this specific sample. Consequently, SN 500 AE was not separated into subfractions. The resulting fractions were analysed by GCxGC to observe elution patterns, with those of Moltox and SN 500 AE shown in figure 16.

As observed on the GC×GC-FID chromatograms presented in figure 16, the optimised elution conditions presented in table 14 yield a good the Moltox separation in sub-classes. The 1-2 rings MOAH fraction is well eluted in the area of 1-2 rings compounds and the same observation with the 3+ rings area is made with the 3+ rings MOAH fraction. However, the observation of 1-2 rings MOAH fraction of the SN 500 AE sample indicates the presence of 3+ rings compounds in the 1-2 rings MOAH fraction. These 3+ ring compounds are likely the most alkylated because increased alkylation shifts the alkylated compounds elution due to reduced

interaction with the column as a result of size exclusion effects [9,79]. Therefore, more highly alkylated compounds elute earlier than less alkylated ones. Additionally, the assumption of alkylated 3+ MOAH compounds in the 1-2 rings MOAH fraction is supported by the fact that SN 500 AE has a very heavy carbon fraction (C-fraction) and has a lot of alkylation in the aromatic part as previously shown in Figure 14. What's more, the 3+ rings MOAH fraction still presents 1-2 rings MOAH compounds but also a lot of unknown peaks, highlighting a possible contamination. The solvent used to elute this 3+ rings MOAH fraction was pure DCM, which is more polar than C6 and therefore might have extracted more polar compounds present on the column. These contaminants could come from the silica itself or from the glass support or used material if not properly washed.

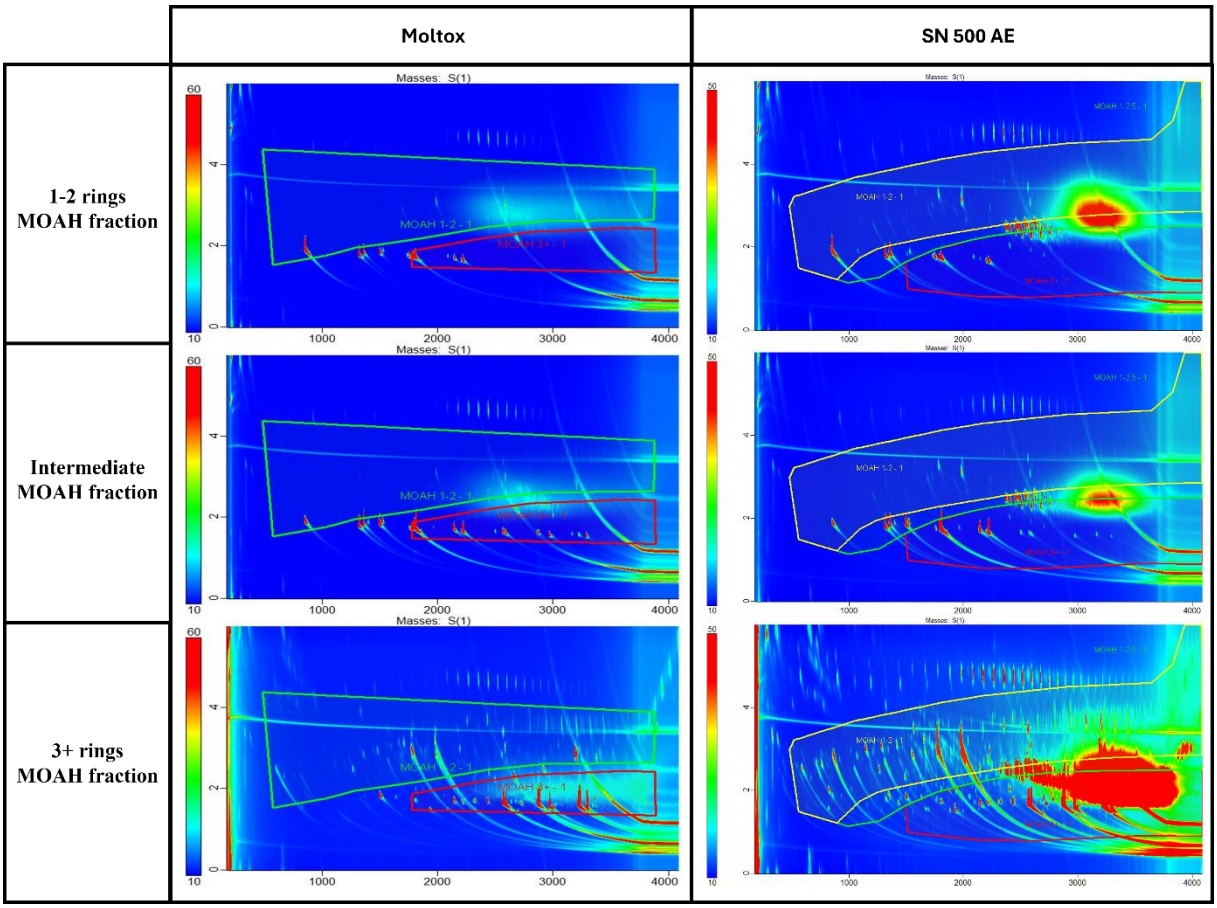

Figure 16 : GC×GC-FID chromatograms of the sub-fractionation preliminary test of Moltox and SN 500 AE with the optimised elution conditions presented in table 13. MOAH 1-2 mask represents the area where 1-2 rings MOAH are located. MOAH 3+ mask represents the area where 3+ rings MOAH are located.

Table 14 : Mass of MOAH extracted for each subfractions starting from SN100 AE and MOLTOX samples, and number of SPE columns required to obtain these different MOAH quantities.

Sample name	Number of SPE columns performed	MOSH/MOAH composition (%)	1-2 rings MOAH extracted (mg)	Intermediate fraction MOAH extracted (mg)	3+ rings MOAH extracted (mg)
SN 100 AE	5	30/70	48.1	56.7	37.7
Moltox	15	66/33	69.8	78.7	77.7

Table 14 provides information on the separation of SN100 and Moltox samples based on their number of aromatic rings. The number of SPE cartridges required to obtain the extracted mass is significant, especially for Moltox. The manipulation time to yield the SN 100 AE and Moltox fractions was approximately 7 hours and 15 hours, respectively. As performed for the SN 100 AE MOSH/MOAH separation, a rough cost estimation for this sub-fractionation was made. The cost to obtain the 3+ rings MOAH fraction is approximately €5160/g for SN100 AE and €5000/g for Moltox.

Figure 17 shows the different fractions obtained from the samples' separation into sub-fractions based on aromatic ring content, as well as the purified MOAH fractions separated from the original samples (called entire MOAH fraction).

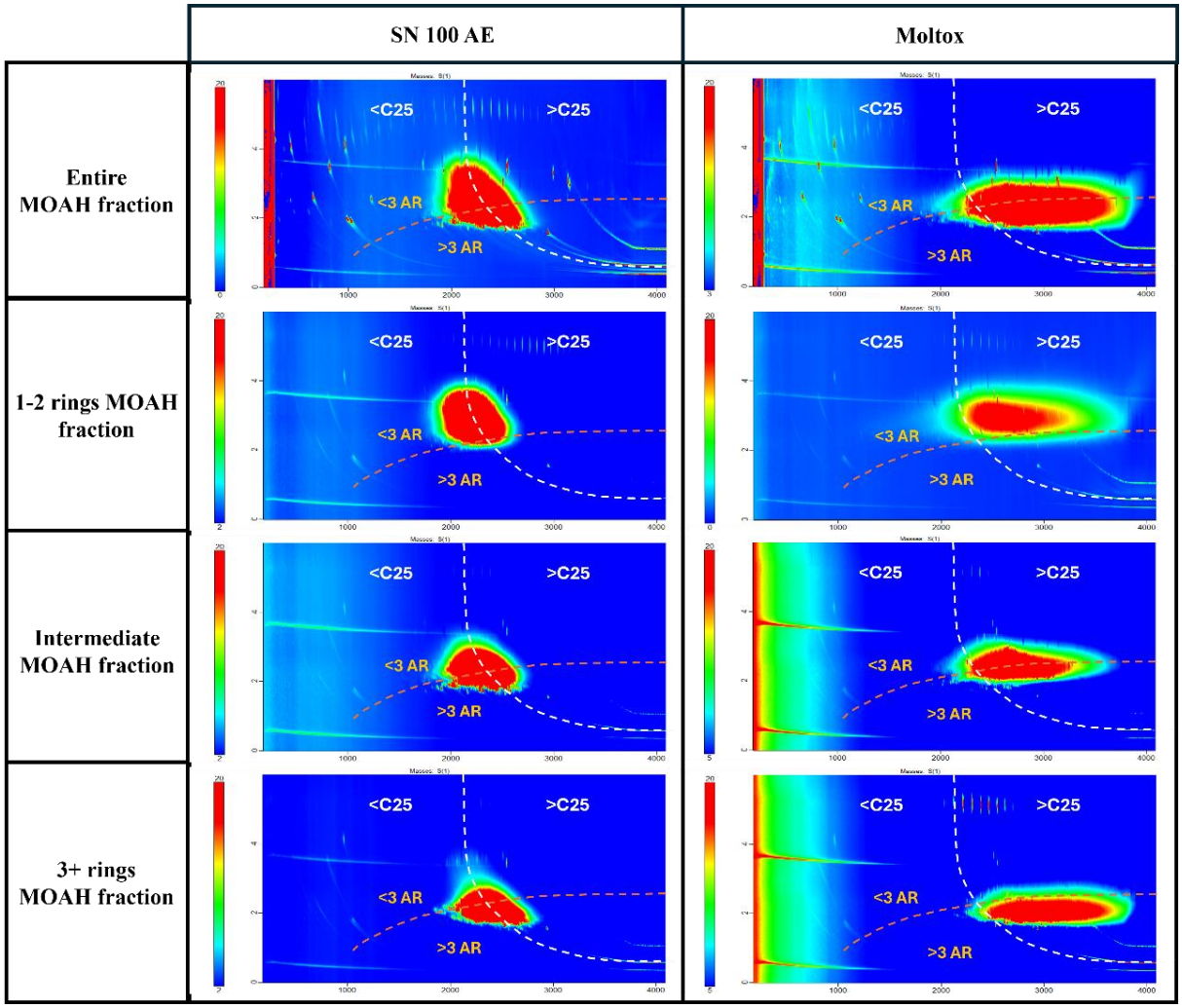

Figure 17 : Samples used or intended to be used in the toxicological Ames and micronucleus tests. All the represented samples are the SPE purified fraction and sub fractions in the case of SN100 AE and MOLTOX. From the top to the bottom and the left to the right: (line 1) SN100 AE MOAH, SN100 AE MOAH 1-2 rings fraction, SN100 AE MOAH intermediate fraction; (line 2) SN100 AE MOAH 3+ rings fraction, MOLTOX MOAH, MOLTOX MOAH 1-2 rings fraction; (line 3) MOLTOX MOAH intermediate fraction, MOLTOX MOAH 3+ rings fraction, Gravex MOAH; (line 4) SN500 AE MOAH, SN100 MOSH (medicinal white oil).

Figure 18 shows the measured aromatic ring (AR) and C-fraction ratios for each MOAH fraction and sub-fraction. The AR separation of SN100 AE and Moltox was successful, yielding fractions enriched in the desired AR ranges (Figure 18A). However, the separation is not perfect; for example, the SN 100 AE and Moltox 3+ ring fractions contain approximately 30% of 1-2 AR compounds. This observation of 1-2 ring MOAH in the 3+ ring fraction might be due to column overloading. It is unlikely that a significant amount of 1-2 ring MOAH is present in the 3+ ring fraction of Moltox, as the preliminary SPE column yielded a clean separation with a good elution profile (Figure 17). The high 1-2 ring MOAH content in the 3+ ring fraction of Moltox and SN 100 AE could also be due to the increased number of columns used, possibly leading to handling errors and an increased presence of 1-2 ring MOAH compounds in the 3+ ring fraction.

Figure 18B depicts the separation of each fraction according to the carbon range number to give a rough idea of the degree of alkylation. But it has to be taken into account that the MOAH with a higher number of rings elute in the later fraction in terms of carbon range. So, the carbon range more properly relates to the degree of alkylation within the same ting number. of 1-2 rings MOAH is not equivalent to the one of the MOAH with higher aromatic rings.

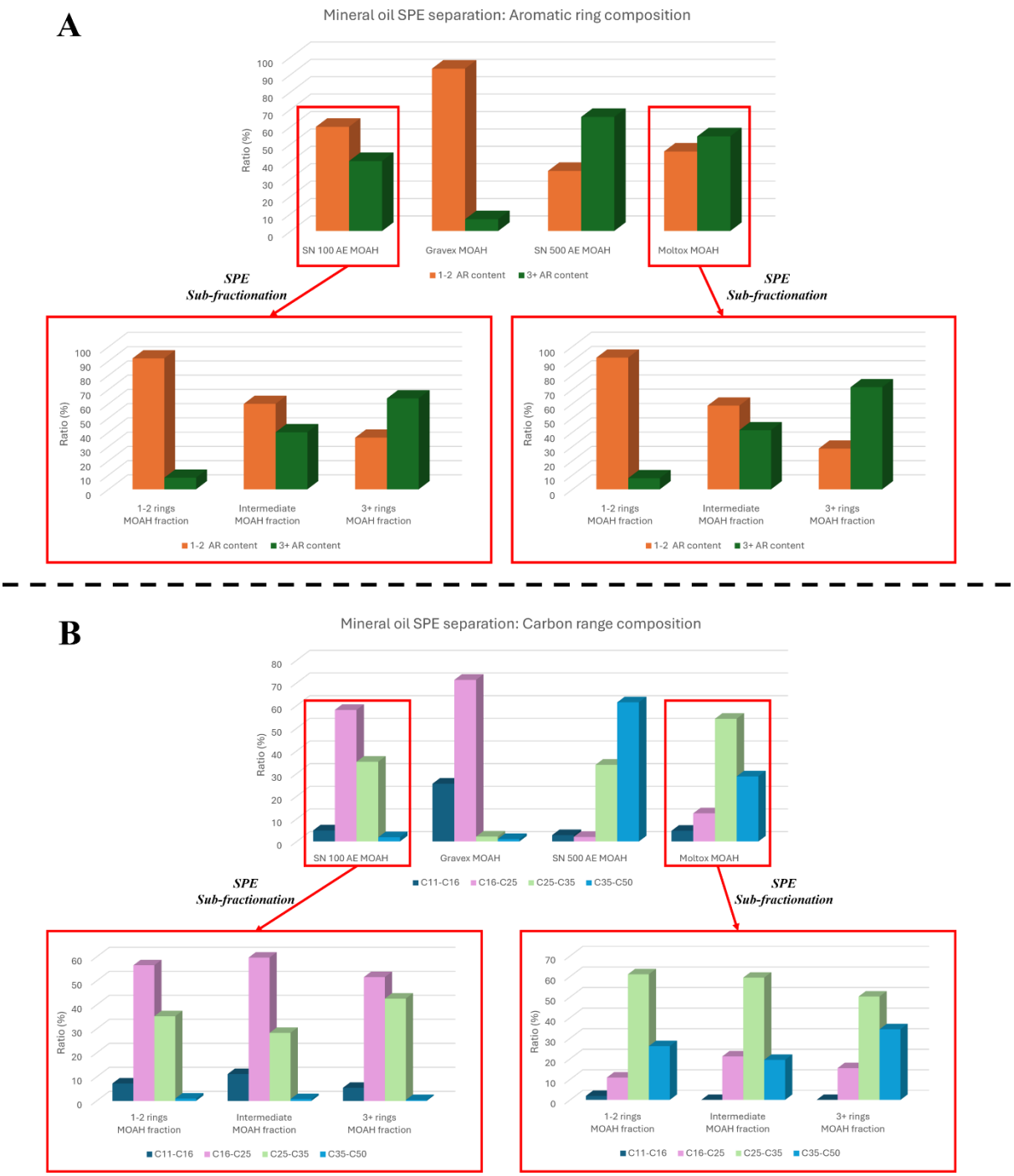

Figure 18: Sample composition ratios of the mineral oils SPE separated into MOSH and MOAH fractions and MOAH subfractions for SN100 AE and Moltox. (A) Represents the aromatic ring composition of each fraction and sub-fraction. (B) Represents the carbon range composition of each fraction and sub-fraction to give a rough idea of the alkylation degree of these fractions.

1.3. Evaluation of MOAH solubility in various solvents

The toxicological tests that were performed in the present work required the solubilisation of the chemical substances to be assessed (MOAH) in cell culture media. The latter being aqueous, while MOAH rather hydrophobic, a co-solvent of intermediate polarity needed to be used. However, not any solvent can be chosen and applied on the cells as some solvents can interfere with the cell viability and therefore, bias the results generated. Solvents were then selected based on OECD guidelines recommendations for Ames test assay [54],

which provide a reference article listing solvents suitable for solubilizing compounds and safe for cell contact [82]. And the 1% maximum solvent concentration was set according to the micronucleus assay requirements [46]. Three candidates were selected: DMSO, acetone, and methanol.

A preliminary test aiming to assess the solubility of MOSH and MOAH was conducted by a lab technician at the UMons toxicology department. The results of this test concluded that methanol was not an appropriate solvent four our research purposes, as only MOAH at 1% concentration in methanol showed a homogenous solution (table 15). However, acetone and DMSO showed encouraging solubility potential (Table 15). Therefore, these two solvents were chosen to assess the solubility of the SN100 MOSH and MOAH fractions.

Table 15 : Solubility potential of the selected solvents intended to dilute MOSH and MOAH fractions. Red cross account for no solubilisation of the sample by the observation of two distinct phases. Green checkmarks account for the observation of a one phase solution.

Compounds' concentration tested	Fraction	Acetone	Methanol	DMSO	Cell culture media
1%	MOSH	X	X	V	X
	MOAH	V	V	V	X
10%	MOSH	X	X	V	X
	MOAH	V	X	?	X
50%	MOSH	X	X	X	X
	MOAH	\	\	\	\

The MOSH and MOAH concentration presented in table 15 were percentages of MOSH and MOAH in volumes as the purified MOSH and MOAH fractions are liquid. However, these MOSH and MOAH fractions are viscous, and the density of the fraction were not known, making it impossible to know the exact mass of MOSH and MOAH present in each further used solution. Therefore, the density of the SN100 MOSH and SN 100 AE MOAH fractions were measured to have an idea of the mass quantity present in the further prepared solutions.

A significant difference in density was observed between the different MOAH fractions, purified from MOSH, sent to UMons. The first SN 100 AE MOAH purified fraction had a measured density of 0.4913 mg/µL, while the second had a density of 0.9979 mg/µL. This large difference might be due to a more effective evaporation step for the second purified fraction. Additionally, when assessing the density of the viscous MOAH fraction with a Hamilton syringe, significant loss on the syringe walls occurred, which could partly explain the density variation. To ensure data reliability in subsequent experiments, only the second fraction with a density of 0.9979 mg/µL was used.

Table 16 shows the maximum solubility levels of MOSH and MOAH in acetone and DMSO. These values were determined by dissolving measured masses of MOSH and MOAH in a 1mL or 2mL volumetric flask, followed by the observation of a single homogeneous phase.

Table 16 : Maximum measured solubility of MOSH and MOAH in acetone and DMSO.

	Acetone	DMSO
MOSH	45.0 mg/mL	4.00 mg/mL
MOAH	145 mg/mL	41.5 mg/mL

These results favour acetone over DMSO as a better candidate for future steps due to the higher solubility of both MOSH and MOAH in acetone. However, acetone has a lower boiling point and is much more volatile than DMSO. Therefore, during incubation with cells (at 37°C), part of the acetone would vaporise, potentially leaving some MOAH non solubilised and creating an uncontrollable bias. Consequently, DMSO was selected for the toxicological experiments, although acetone was still tested in the viability assay (discussed in section 1.4).

The concentrations shown in table 16 represent the maximum solubility of the fractions in the solvent. Unfortunately, the OECD guideline specific to the micronucleus test [46] sets the employed solvent maximum concentration at 1% in the culture media. This 1% limit is set to prevent any major effects, such a decrease in cell viability, of the solvent on the cells [82,83]. Indeed, DMSO has been proven to be non-cytotoxic up to a 2% concentration in HEPG2 cell lines [84]. Adding 1% DMSO at 40 mg/mL of MOAH in the viability test cell culture media (final concentration in MOAH of 0.4 mg/mL) resulted in a blurry effect, which was not observed with MOSH.

This effect could be due to incomplete solubilisation of the compounds, resulting in a suspension rather than a solution. Figure 19 illustrates the observed blurry effect. The blur was noticeable up to a concentration of 0.075 mg/mL but not below this level for MOAH. Therefore, a concentration of 0.05 mg/mL was chosen as the highest concentration of MOAH that produced a clear solution and could be used for further tests.

A study by led by Hochegger et al. [14] assessed the mutagenicity of MOSH and MOAH fractions at different MOAH concentrations and mixed MOAH with DMSO up to 80 mg/mL. Therefore, it is likely that Hochegger encountered a final MOAH concentration in the culture media higher than this 0.075 mg/mL value. As such, the compounds would have been suspended rather than fully dissolved. However, no mention of this phenomenon has been depicted by Hochegger, casting doubts on the state of the molecules during its test.

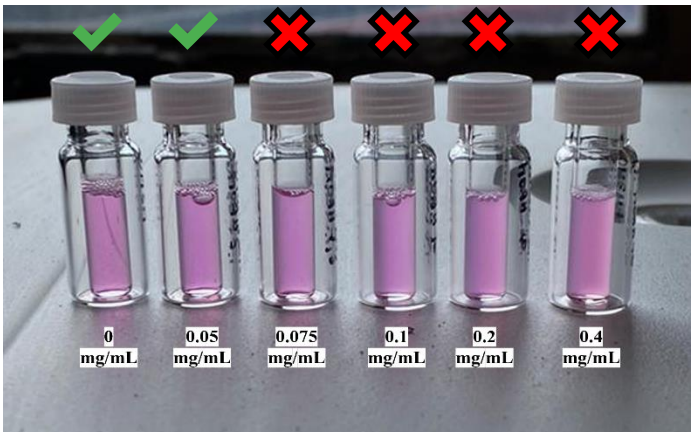

Figure 19 : Final concentrations of SN 100 AE MOAH in cell culture medium after 1% dilution of DMSO. The red crosses depict the observation of a blurry effect while the green checkmarks show no observation of blurry effect.

This undesired suspension phenomenon is important to consider, as cells do not absorb exogenous compounds similarly in soluble versus suspended forms [85,86]. Soluble compounds can enter cells via simple diffusion or carrier-mediated processes, while higher molecular weight compounds typically enter through other pathways, such as endocytosis [85,87]. Therefore, the way the compounds enter the cells might impact the following processes such as metabolization that they will encounter.

1.4. Evaluation of the viability of HEPG2 hepatocyte cells

The toxicological tests conducted in this work used the human hepatocyte cell line HEPG2. It was necessary to ensure that neither the solvent nor the concentration of the tested chemicals affected cell viability, such as increasing mortality. Crystal violet assays were performed to evaluate the impact of the compounds and solvent on the cells. This photometric test measures absorbance of crystal violet, which stains the DNA and proteins of living cells. After a washing step that removes dead cells, crystal violet stains only the viable adherent cells. Following cell lysis, the absorbance of the released crystal violet in the media is measured [88].

A preliminary viability test was conducted to assess the effects of the solvents on the cells. Each plate tested nine concentrations, with six replicates per concentration. Three plates were used for the experiment, and the concentrations tested were:

- **For DMSO**

  0.25%-0.5%-0.75%-1% (v/v)

- **For acetone**

  0.2%-0.4%-0.6%-0.8%-1% (v/v)

The results of this viability test, presented in Figure 20, show that neither solvent at any concentration has a significant negative effect on cell viability. Specifically, DMSO at 0.5%, 0.75%, and 1% as well as acetone at 0.2%, 0.4%, and 0.6% exhibit significant or highly

significant effects, with viability increasing. A same increase in cell viability has been described in the literature up to 0.8% DMSO however, it was related to a B lymphocyte cell line [89]. Since neither solvent decrease significantly cell viability, any of the tested concentrations can be used for further toxicological tests. To ensure that the highest concentration of MOSH and MOAH is tested in the Ames and the micronucleus test, the highest solvent concentration (1%) was chosen.

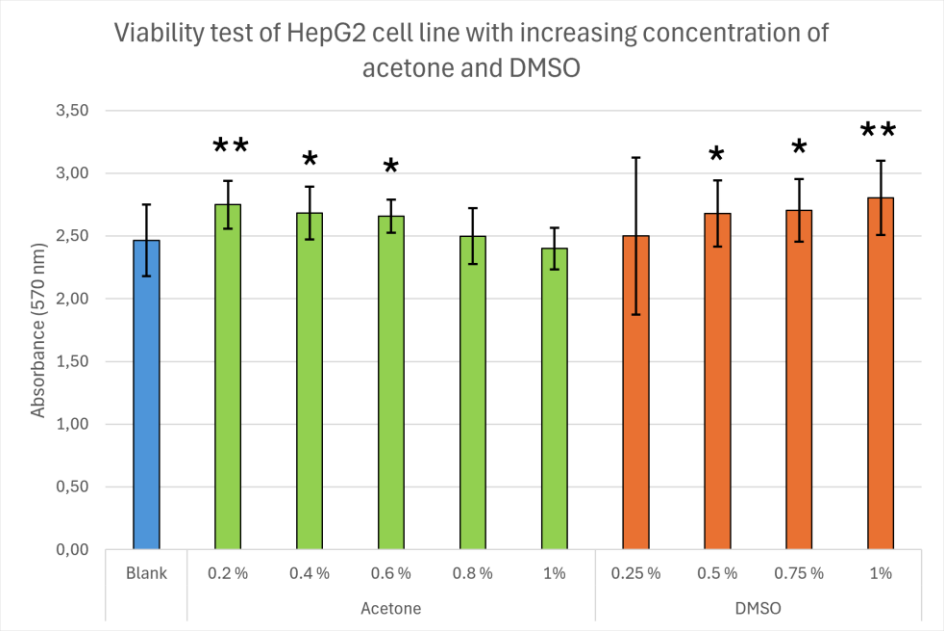

Figure 20 : Viability test results of the HEPG2 hepatocyte cells treated with different acetone (green) and DMSO (orange) concentrations. Blue represents the blank.

A second viability test was conducted to evaluate the effects of MOSH and MOAH on cell viability and to determine if any of the tested concentrations had a significant impact. The tested concentrations were determined by starting with the maximum solubility of MOSH and MOAH in acetone and DMSO, then sequentially halving it. These concentrations are listed in Table 17, and the results are presented in figure 21.

Table 17 : Final concentrations of MOSH and MOAH (in µg/mL) in contact with the cells according to different solvents used to perform the viability assay.

	Acetone		DMSO	
	MOSH	**MOAH**	**MOSH**	**MOAH**
Concentration µg/mL	406.00	48.30	41.10	50.40
	203.00	24.10	20.50	25.20
	102.00	12.10	10.30	12.60
	50.80	6.03	5.14	6.30
	25.40	3.02	2.57	3.15
	12.70	1.51	1.28	1.58

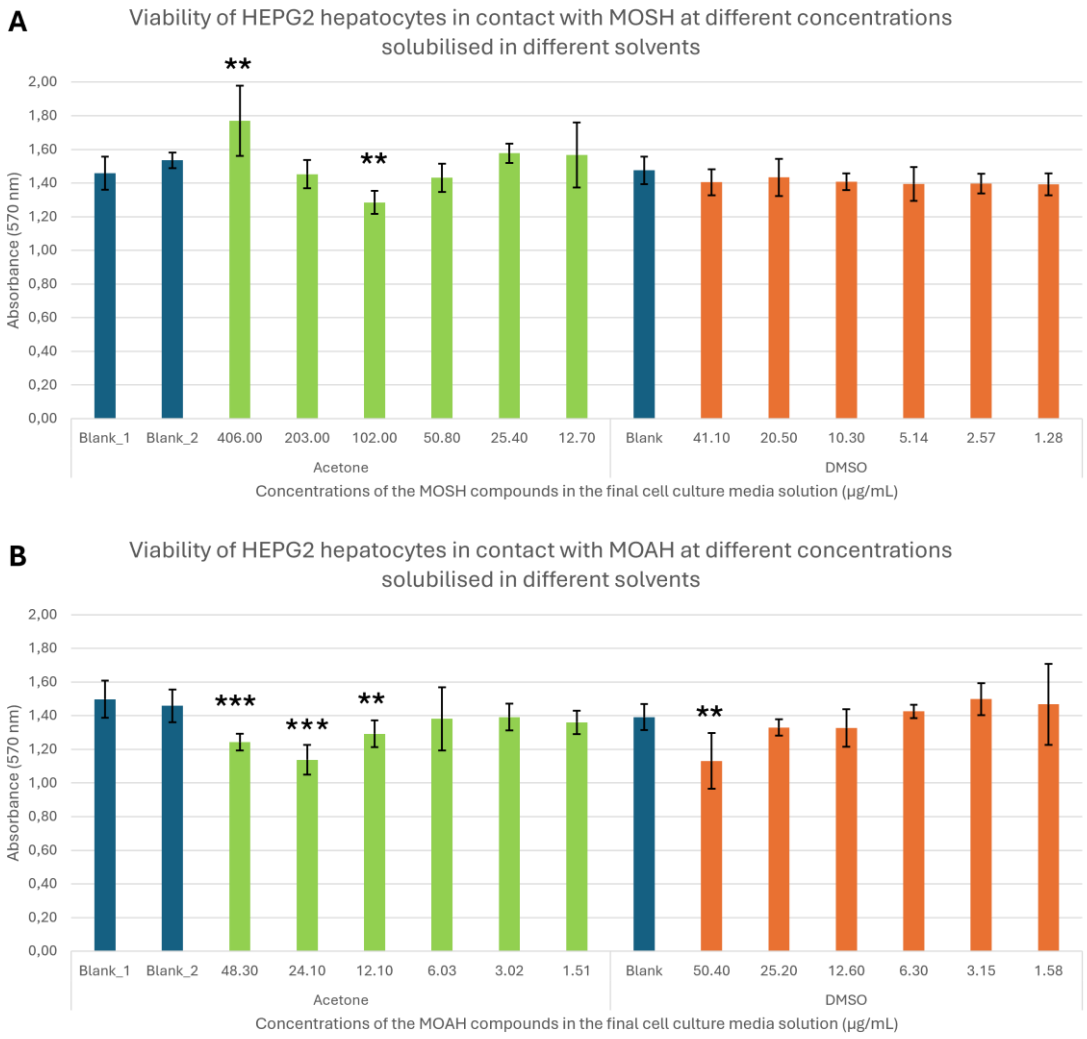

Figure 21 : Viability assay results. (A) Viability assay results of the MOSH fraction at different concentrations in DMSO and acetone. (B) Viability assay results of the MOAH fraction at different concentrations in DMSO and acetone. Blank_1 and Blank_2 represent the different blank wells in each plate, needed to compare the conditions displayed on the different plates. Blue bars represent the blanks, green bars represent acetone and orange bars represent DMSO.

Analysis of the test outcomes shows that MOSH did not negatively affect cell viability, except when diluted in acetone at a final concentration of 102 µg/mL. Both higher and lower concentrations did not show such effects, suggesting that this significant result might be an anomaly or due to issues during data collection or cell treatment. For instance, the use of tips during media removal or washing could potentially dislodge cells from the well bottom, reducing absorbance and leading to erroneous results.

Figure 21B clearly shows that MOAH at final concentrations in cell culture media ranging from 12.10 to 48.30 µg/mL with acetone as solvent and at 50.40 µg/mL with DMSO as solvent significantly decreased cell viability. Therefore, these "t-test positive" concentrations should be avoided in further toxicological tests to accurately assess the effects of the compounds. Since DMSO has been selected as the solvent for all toxicological tests, maximum concentrations of 25.20 µg/mL for MOAH and 41.10 µg/mL for MOSH should be used in the final solution.

2. Toxicological characterisation of mineral oil

2.1. Evaluation of the mutagenicity of MOAH using the Ames test

The Ames test is an assay used to detect the mutagenic potential of chemical compounds by evaluating their ability to induce mutations in specific strains of *Salmonella typhimurium*. In this study, the TA98 and TA100 strains were employed to assess both frameshift mutations and base-pair substitutions, respectively. Each test was conducted with and without a rat S9 metabolic activation system, allowing to differentiate between direct-acting mutagens and those requiring metabolic conversion to exhibit mutagenicity.

In total, four tests were performed for the TA98 strain, and two tests for the TA100 strain. Six types of MOSH or MOAH samples were selected for the assessment: SN100 medicinal white oil (pure MOSH), and MOAH purified extracts (as described in section 1.1) of SN100 AE, SN500 AE, Gravex, Moltox, as well as a DMSO extract of the latter following [90] procedure. Only one concentration of each sample was evaluated at this point, corresponding to the maximal MOAH SN 500 AE concentration soluble in DMSO. All the other MOAH fraction concentration were arbitrarily aligned with this concentration to facilitate comparison of the different fractions. The MOSH concentration was slightly over the highest concentration that yielded solubility in DMSO in the solubility test (described in section 1.3). The exact concentrations are presented in Table 18.

Table 18 : Concentrations of the sample solutions used for the Ames test. Step 1 and step 2 refers to the different steps where culture media is added to the wells. Step 1 yields a 25× dilution from the stock solutions and step 2 yields a 12× dilution from step 1 solutions.

Sample name	Stock solution concentration in DMSO (mg/mL)	Final concentration in the culture media after step 1 (mg/mL)	Final concentration in the culture media after step 2 (µg/mL)
MOAH SN 100 AE	12.5	0.5	41.6
MOAH SN 500 AE	12.5	0.5	41.6
MOAH Gravex	12.5	0.5	41.6
MOAH Moltox	12.5	0.5	41.6
MOSH SN 100 (medicinal white oil)	5.0	0.2	16.7

However, among all performed tests, only one experiment per strain yielded interpretable results. For the TA98 strain, three tests were discarded for the following reasons. In the first trial, the reagents used were expired, resulting in the test not functioning. In the second trial, all 384 wells from the S9 treated plates (metabolised compounds) showed positive results, including the negative control, rendering any conclusions unreliable. In the third trial, the wrong substance was added as a positive control in the unmetabolized plates (without S9 fraction), again making interpretation difficult. The fourth test was successful. Regarding the

TA100 strain, one of the two tests produced questionable results due to the absence of a positive response in the positive control wells. The second test was successful. Annex 6 presents a figure showing images of the failed tests and the segmentation pattern of the 384 well plates.

Focusing now on the two successful tests (one for TA98 and one for TA100), the gathered results are presented in Figure 22, which contains different plot giving the "A-ratio" in function of the type of MOSH and MOAH sample, the type of strain, and the presence or absence of rat S9 metabolic activation system. The A ratio is calculated as presented in material and method (section 277.3) and when its value is superior to 2, the evaluated compound is considered as mutagenic. Nevertheless, Given the variability in human color perception and the time required to visually assess each plate, an alternative approach was developed. Specifically, an automated algorithm was created to calculate the A ratio based on the absorbance values of each well. The ratio between absorbance at 430 nm and 590 nm is calculated for each well, and a threshold value is used to determine the positivity of each well. An Excel file is automatically generated, including the A ratio for each tested sample, with positive results highlighted.

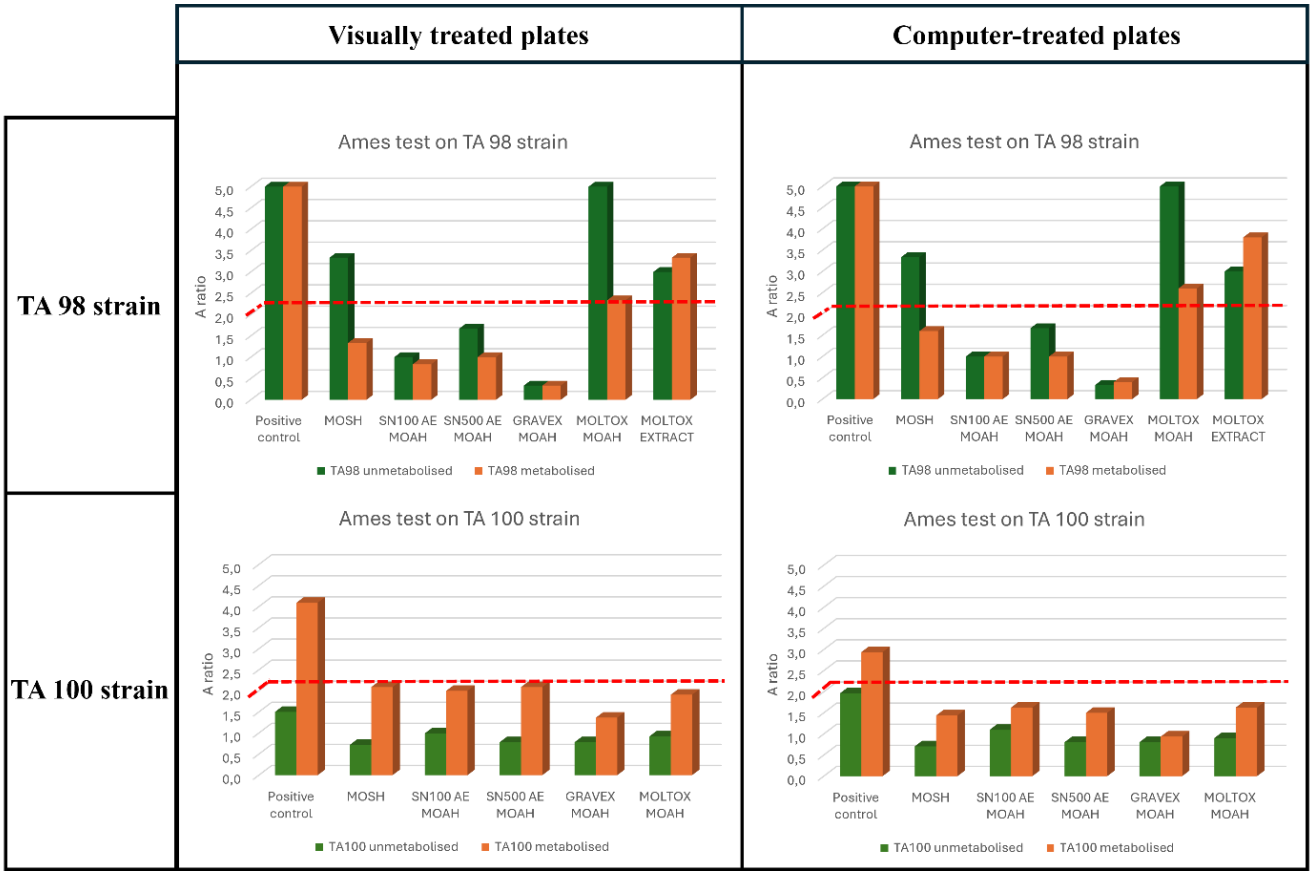

Figure 22 : Successful Ames test results of the TA98 and TA100 strain. Comparison between the visually treated plates and the computer treated plates. The red dashed line represents the threshold of positivity of the test. A-ratio value higher than 2 proves the mutagenicity of the sample.

The Ames test on TA100 strain, used to assess the induction of base-pair substitutions by the studied compounds, gave no clear positive results, apart the metabolised samples from the visually treated plates appearing slightly close to positivity. The computer-treated data of TA100 metabolised, in the opposite, show a negative test result for all the samples except the positive control. This negativity toward the base-pair substitution pathway has been reported in the literature, as the TA100 strain shows a lower sensitivity and specificity to the aromatic compounds than the TA98 [91]. Therefore, the results suggest that MOSH and MOAH do not exhibit base pair substitution mutagenic activity or that the sensitivity of the test provided by the use of rat S9 metabolic activity is not sufficiently high.

The TA98 strain results exhibited by the computer-analyzed and visually inspected plates are more or less similar. The positive control shows a high A ratio value in both the visual and computer-treated plates but, both of interpretation also show a high A-ratio value for the MOSH sample. Given that MOSH is certified medicinal white oil and used in regulated cosmetic and pharmaceutical products, it is unlikely to be mutagenic as previous studies must have confirmed that such oils do not exhibit toxicological effects at high doses, such as those used in medicinal products (several thousand mg for some products such as laxatives [18,35]).

However, a consistent trend is observed with both Moltox and Moltox extract in visually and computer-analysed plates. Both metabolised and non-metabolised fractions show positivity for Moltox and Moltox extract, suggesting that they can induce frameshift mutations in *Salmonella typhimurium* cells. However, the non-metabolised Moltox sample appears to induce mutations more frequently than its metabolised fraction. In contrast, for the Moltox DMSO extract, the metabolised fraction shows a higher A ratio, while the non-metabolised fraction shows a lower A ratio. Additional tests on this fraction are needed to confirm the observed trend.

Correlation between the Ames test and in vivo assay has already been demonstrated by correlating the positive results of the Ames test with carcinogenic potential in rodents [92]. However, this not perfect and it must be kept in mind that prokaryotes lack the complex mechanisms eukaryotic cells use to counteract toxicity. Molecular mechanisms in eukaryotes are generally more intricate than those in bacteria [93]. Therefore, mutations observed in *Salmonella typhimurium* strains may not be directly relevant to humans or may not induce similar effects in human cells.

The test results were generally as expected, except for the SN 100 AE fraction, which was anticipated to be positive in the Ames test with TA98 strain due to its internal composition depicted in figure 23. Examining the chromatograms of the tested samples provides additional context for interpreting these results.

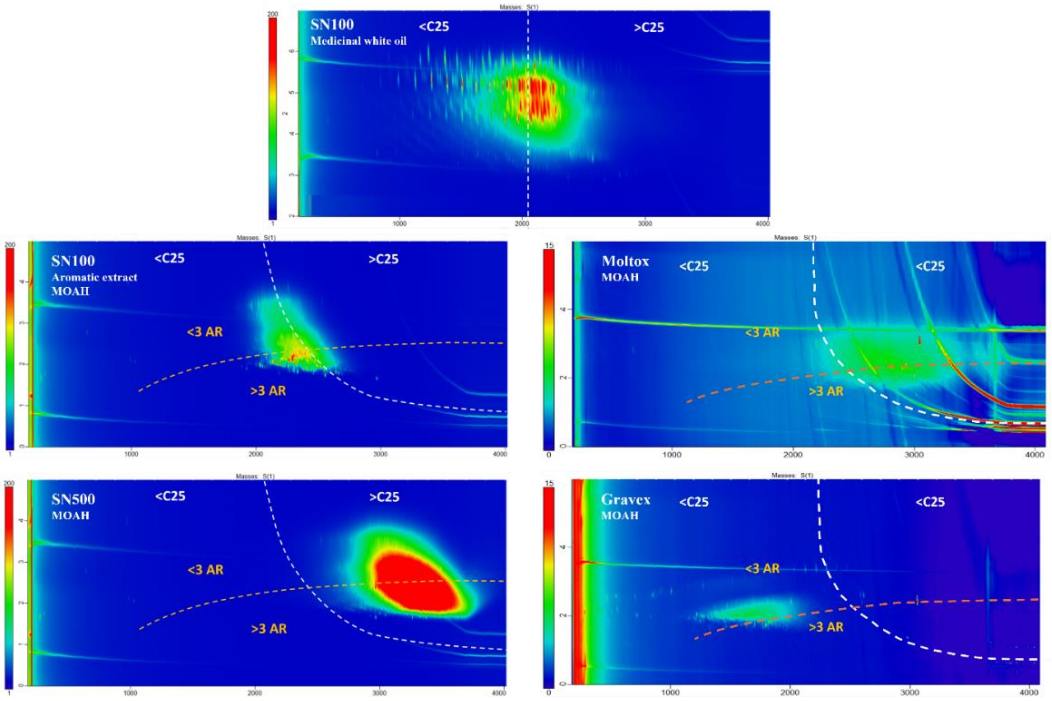

Figure 23 : 2D chromatograms of the used fractions samples in the Ames test. All samples are the MOAH fraction of the original sample except for SN100 medicinal white oil which is 100% MOSH.

Indeed, it was expected that the SN 100 AE MOAH internal composition, including both 1+2 and 3+ rings as well as <C25 and >C25 fractions, would yield a positive Ames test result. However, no such positivity was observed. One possible reason is the S9 fraction used in the test. The rat liver S9 fraction is less sensitive compared to the hamster liver S9 fraction, which is more commonly used for Ames tests on petroleum products [49,50,90]. Using the hamster S9 fraction could provide more conclusive evidence regarding the potential mutagenicity of the SN 100 AE.

Regarding the Moltox sample composition, it depicts a heavy C-fraction, but to a lesser extent compared to SN500, and it also contains a small amount of >3 AR. Its Ames test positivity, compared to other samples, may be due to the covering of a higher carbon range number (>C25) and less alkylation than SN500. Lower alkylation might lead to increased oxidation of aromatic rings, potentially forming more DNA-reactive species. Another possibility is that the Moltox sample might present an abnormally higher PAH composition to other samples, increasing its toxicological effects.

The SN500 sample, although presenting a significant >3+ aromatic ring composition, is highly alkylated and seems to provide results in adequacy with the hypothesis of Wang et al. [62,65] of aromatic ring oxidation delocalisation towards the alkyl chains.

The light C-fraction and aromatic composition of Gravex, led to the expectation of negative results for this sample. Such results were obtained following this test either metabolised or not. Therefore, even with a more sensitive test, it seems unlikely that these samples would yield a positive Ames test result.

- ***General overview of the test:***

Obtaining reliable and reproducible results proved to be more complicated than anticipated. Different types of Ames tests can yield varying responses, and result interpretation can be subjective, requiring skilled and experienced operator. Additionally, using different metabolic activation fractions can affect test sensitivity. While the S9 hamster liver fraction may provide more sensitive results, the S9 human liver fraction might offer better relevance to human toxicology.

2.2. Evaluation of the genotoxicity of MOAH using the micronucleus assay

The ability of MOSH and MOAH samples to induce chromosomal breakages was assessed using the micronucleus assay on HEPG2 hepatocyte cells. The same samples used in the Ames test were employed to further investigate their toxicological effects. TCDD was used as a positive control, as the HEPG2 cell line allows for sample metabolism through Ahr activation and P450 enzymes [94]. Although BaP was initially considered as a positive control, it was discarded due to its classification as a Group 1 carcinogen; TCDD was deemed more appropriate. The results of this test are presented in the tables and figures below, with Table 19 containing all the data generated

Table 19: Mined data from the micronucleus test. Circled area represents an outlier value that must be considered with care as not really representative of the reality." \" means that the average values could not be determined due to various possibilities.

	Mean nuclei number/image	Mean cell nucleus diameter (µm)	Average number of cell nuclei/ 1 micronucleus
Control	309	12,39	\
DMSO	228	12,88	177
TCDD	45	13,90	40
MOSH	84	13,13	24
Gravex	53	10,21	16
Moltox	57	14,31	15
SN100	35	12,78	\
SN500	59	20,87	36

Micronuclei were not observed in all conditions tested. For instance, in the case of SN100 (MOAH aromatic extract), excessive cytotoxicity led to cell death and DNA debris throughout the observed area (Figure 24). This lysis prevented any counting of micronuclei, even by experienced scientists. Micronuclei were also not detected in the negative control. While no micronuclei were observed in the analysed area, it is possible that micronuclei could have been present in other areas of the coverslips as they can naturally appear in cells [95]. Consequently, it can be stated that no micronuclei were observed among the 300 cells examined in the studied area.

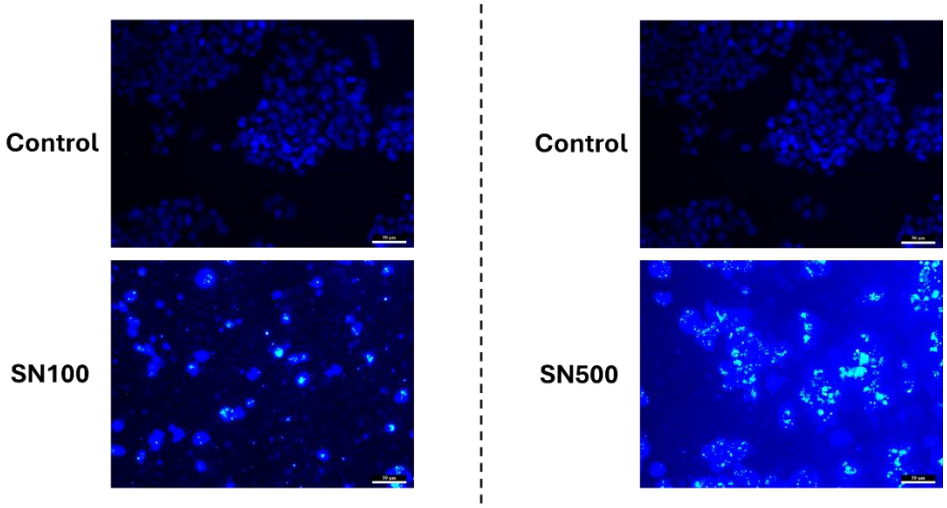

Figure 24 : (Left) DNA particle debris observed for the SN100 AE sample compared to the control sample. (Right) cellular aggregate of the SN500 sample compared to the control.

An unexpected effect was observed with the SN500 sample, which caused cell agglomerations and diffused DNA, making accurate cell counts and representative measurements of nuclear diameter difficult (Figure 24). Consequently, results from this sample should be interpreted with caution and not considered absolute. Funayama et al. [96] describe that senescent cell nuclei stained with DAPI (a fluorescent stain that binds strongly to DNA) exhibit spreading DAPI foci (i.e. areas of concentrated fluorescence), a phenomenon which seems to be observed with SN500 as shown in Figure 24.

Figure 25 shows the statistical significance, as measured by a Student's t-test, between the DMSO condition and the negative control. A significant difference is observed in the average number of cell nuclei, indicating a substantial reduction in cell count and, consequently, cell viability. This effect was not observed in the preliminary viability test, likely due to the higher DMSO concentration used in this micronucleus test. Specifically, a 25X dilution factor was applied, resulting in a DMSO concentration of up to 4%, compared to 1% in the viability test. Figure 26 compares the remaining samples to the DMSO condition, as all tested compounds were diluted in DMSO.

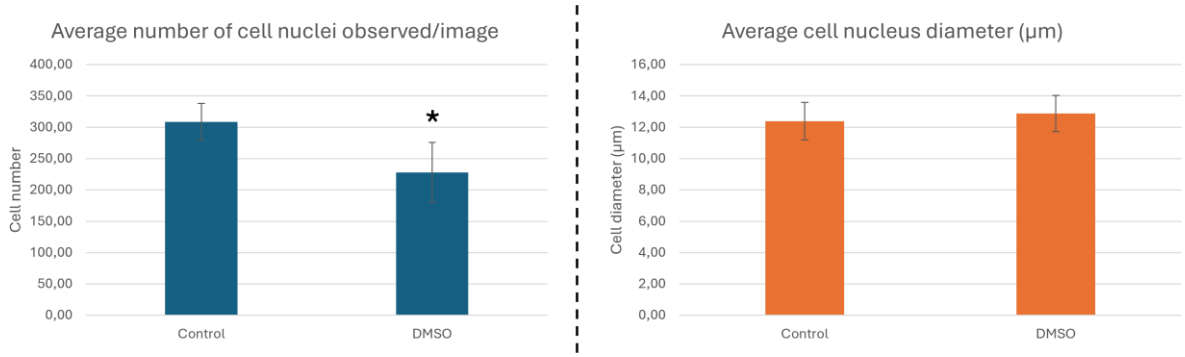

Figure 25 : Comparison of the control cells and the DMSO ones according to different parameters and emphasise on the student t test result. Three wells were seeded with cells for each condition.

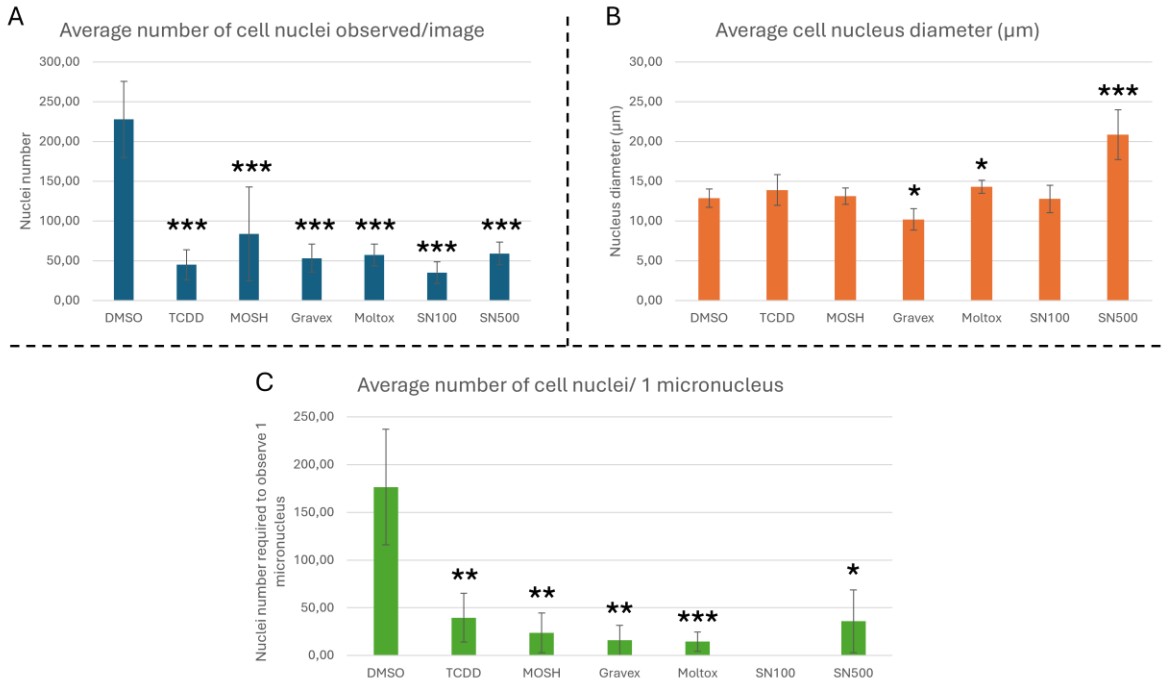

Figure 26 : Averaged data from the micronucleus test images and statistical significance of the sample comparison with the DMSO condition. Three wells have been seeded for each tested condition. (A) average number of cell nuclei observed/image. (B) Average cell nucleus diameter (µm). (C) Average number of cell nuclei/1 micronucleus.

Regarding the average number of cell nuclei observed per image, all conditions show a highly significant difference compared to the DMSO-treated cells, except for MOSH, which exhibits a significant difference. These differences indicate cell death, highlighting the substantial impact of all compounds on cell viability. A new viability test should be conducted with DMSO concentrations up to 4% and various concentrations of the SN100 sample to account for the increased DMSO concentration and assess its impact on viability and consolidate the already obtained results. But most importantly, the DMSO concentration of further micronucleus test should be maintained as low as 1% to avoid any cell cytotoxicity. The TCDD and SN500 data do not follow a normal distribution, invalidating the Student's t-test. Additionally, the variance among conditions is not homogeneous. Consequently, the Welch test was used for this parameter to address these issues.

In the remaining living cells, the nucleus diameter was measured. The average nucleus size is similar across half of the conditions. Gravex and Moltox samples show a significant difference from the DMSO control, but in opposite directions: Gravex decreases and Moltox increases nucleus size. This change in nucleus size (anisokaryosis) has been observed in rat hepatocytes following exposure to acridine (a nitrogen-containing anthracene analogue) and TCDD [97,98]. The SN500 sample shows a highly significant difference from the DMSO control, but this is due to cell agglomeration, which obscures individual nucleus measurement and reflects the diameter of cell clusters rather than single nuclei. Both the control and DMSO conditions yielded p-values below 0.05 in the Shapiro-Wilk test for normality, invalidating the t-test.

The number of micronuclei varied across the tested conditions, with Moltox samples showing a notably high number, surpassing even the TCDD sample. TCDD was not an ideal positive control as it does not directly damage DNA and may only be indirectly genotoxic through secondary mechanisms [99,100]. Figure 27 illustrates the micronuclei observed in cells treated with Moltox. SN500-treated cells showed a significantly higher number of micronuclei compared to the DMSO control. TCDD, MOSH, and Gravex also exhibited highly significant differences from the DMSO condition. Moltox generated the most micronuclei, showing a very highly significant difference from the DMSO condition. For SN500, results were difficult to interpret due to DNA diffusion in the images, likely caused by an excessively high sample concentration. The highly significant difference for MOSH was more surprising, given its certified safety for medicinal use, it might be attributed to the apoptotic state of the cells, which leads to DNA fragmentation and release of genetic material outside the nucleus [101]. Additionally, the MOSH data did not meet normality assumptions, invalidating the t-test results.

The Moltox condition was straightforward to interpret and showed no signs that would undermine the reliability of the results obtained. Both TCDD and MOSH did not follow a normal distribution, invalidating the t-test results. Gravex was also easy to interpret, but the limited number of images and insufficient data necessitate further testing to confirm the observed genotoxic effects, despite respecting normal distribution and variance homogeneity.

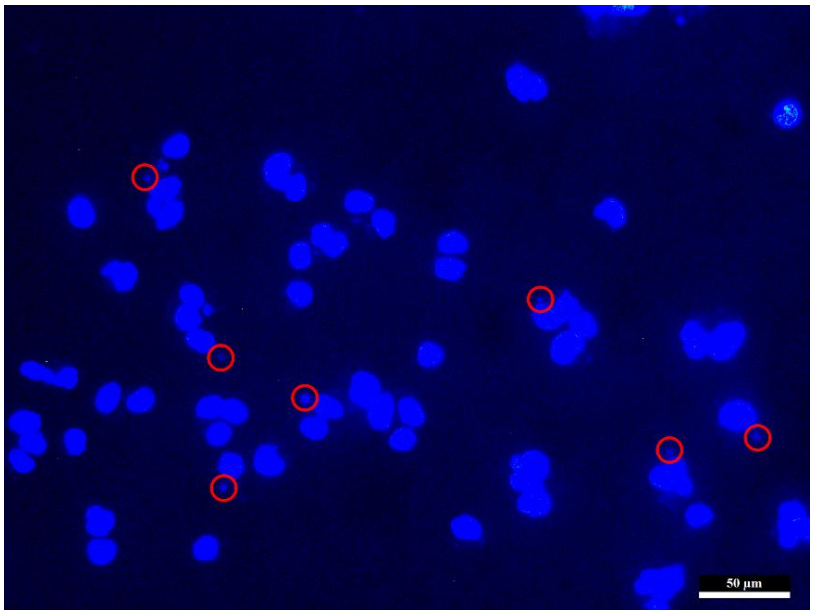

Figure 27 : Cells treated with the Moltox sample in the micronucleus assay. Each blue dot represents a cell nucleus. Red circles reveal the position of micronuclei. The scale bar represents a length of 50 µm.

- ***General overview of the test:***

The micronucleus test results suggest that the DMSO concentration used was too high, adversely affecting cell viability compared to the control. Additionally, the number of replicates for the various parameters may be insufficient to ensure a normal distribution and homogeneity of variances. To meet these requirements and enable a valid t-test comparison, additional images or replicates are needed. Among the tested samples, only Moltox provided reliable results, demonstrating its genotoxic effects. In contrast, SN100 AE and SN500 AE appear too aggressive for cells at the 0.5 mg/mL concentration, indicating a need to reduce the concentration and to perform dose-response for a more accurate assessment of potential genotoxic effects.

3. Evaluation of the DMSO extraction based methods with the GC×GC characterization

As mentioned briefly in the introduction, the carcinogenic potential of a lubricant base oil is assessed using the IP346 method. This gravimetric method is widely adopted in the industry to ensure product safety and has been shown to correlate with the mouse skin painting assay. The European Pharmacopoeia (Ph. Eur.) monograph outlines guidelines for ensuring the safe use of MO in medical and pharmaceutical applications. Similar to the IP346 method, which involves DMSO extraction followed by back extraction and gravimetric measurement, the Ph. Eur. method involves DMSO extraction of aromatic compounds and subsequent UV measurement. DMSO has a higher affinity for compounds with a high number of aromatic rings, while PACs with significant alkylation exhibit reduced affinity for DMSO due to steric hindrance [47]. Nevertheless, a more detailed characterization of the substances extracted in the DMSO phase, which are responsible for carcinogenic activity, has not yet been performed.

Therefore, to better understand the information provided by the method performed before marketing the products with the actual MOAH content and the toxic effects, a correlation study between the extracts generated by the Ph. Eur. method and their chemical characterization was performed.

Calibration curves plotting absorbance against MOAH concentration were generated using different MO samples with varying chemical compositions. Specifically, SN100 raffinate extract, Sternel motor oil (SMO), and LHM motor oil (LHM) were tested to represent a broad range of carbon numbers and aromatic compositions. SMO has a higher proportion of less volatile compounds, characterized by a composition centered above C25 and a high proportion of 3+ ring compounds. LHM contains only compounds with fewer than C25 and lacks 3+ ring compounds. The SN100 raffinate sample exhibits intermediate characteristics between the other two samples. These samples' characteristics are summarised in Table 20.

Table 20 : Samples selected to create the calibration curves composition.

Samples selected to create the calibration curves			
	SN100 raffinate	Sternel motor oil	LHM motor oil
% MOSH	94%	46%	97%
% MOAH	6%	54%	3%
% <3 AR	*100%*	*62%*	*100%*
% >3 AR	*0%*	*38%*	*0%*
% < C25	*55%*	*28%*	*99%*
% > C25	*45%*	*72%*	*1%*

It was expected that the SN100 raffinate sample would yield a negative result in the Ph. Eur. test due to its low MOAH content and the presence of only 1-2 aromatic rings. However, the results differed, as shown in Table 21. Subsequently, decreasing MOAH concentrations

were tested to determine the test's positivity threshold. *Paraffinum liquidum*, certified as negative for this test, was used as the solvent. Percentages in the table are expressed by mass rather than volume to account for the differing viscosities of *paraffinum liquidum*, SMO, and SN100, thereby avoiding significant biases from pipette wall losses when handling small MOAH quantities. The test's positivity threshold was defined as an absorbance value of 0.123, based on the mean of seven replicates, which corresponds to one-third of the absorbance at 275 nm of a 7 mg/L naphthalene solution (n=7). Only one measurement was obtained for the LHM sample before it was discarded due to the presence of pigments that were DMSO-extracted, skewing the absorbance measurements. No other available samples in the laboratory matched the composition pattern of LHM, making replacement impossible.

Table 21 : European Pharmacopoeia test result at varying MOAH concentrations for SN100 raffinate and SMO sample. Blue coloured lines represent the negative samples. "" represents the values out of range, just added as a rough indication of intensity.*

	MOAH % in the solution	Total MOAH µg/mL DMSO	1-2 rings MOAH µg/mL	3+ rings MOAH µg/mL	Absorbance (260 nm)	Ph. Eur. Outcomes
Naphthalene 7mg/mL					0.123 (at 275 nm)	
SN100	6.00	22.40	8.00	14.35	2.61*	+
SN100	2.00	7.50	2.70	4.78	1.50	+
SN100	0.80	3.00	1.10	1.91	0.71	+
SN100	0.50	1.90	0.70	1.20	0.47	+
SN100	0.15	0.60	0.20	0.36	0.27	+
SN100	0.10	0.40	0.10	0.24	0.19	+
SN100	0.03	0.11	0.040	0.072	0.13	+
SMO	0.50	47.70	13.39	46.73	2.41*	+
SMO	0.01	1.00	0.27	0.94	1.29	+
SMO	0.005	0.50	0.13	0.47	0.64	+
SMO	0.0025	0.24	0.07	0.23	0.35	+
SMO	0,001	0,10	0,027	0,0935	0.14	+
SMO	0.0005	0.05	0.01	0.05	0.12	-
SMO	0.0001	0.01	0.003	0.009	0.05	-
SMO	0.000001	0.00010	0.00003	0.0001	0.03	-

Two calibration curves were built after eliminating the values out of range. The correlation was built considering the total MOAH back extracted from the DMSO fraction where the UV measurements were done. The profile comparison between the original MOAH fraction and the back extracted fraction from DMSO is shown in Figure 28.

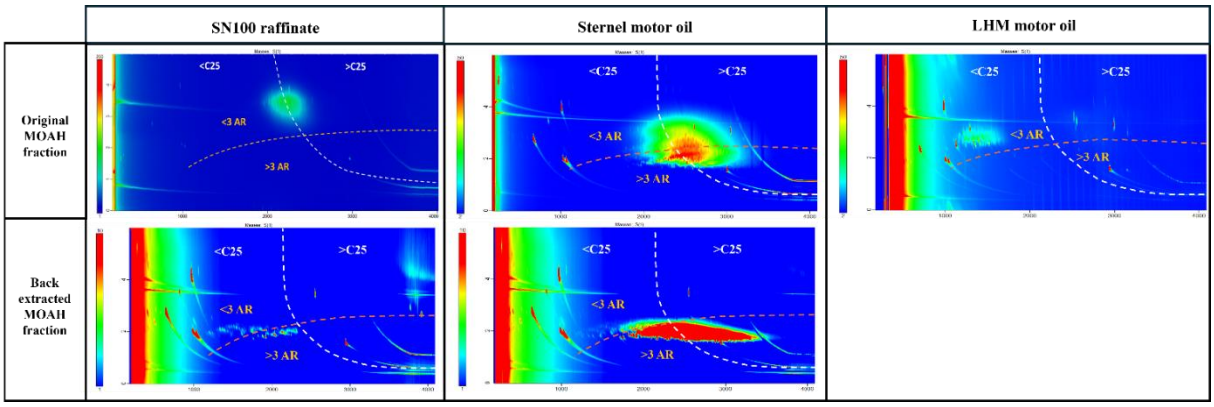

Figure 28 : MOAH original fractions and DMSO back extracted fractions of the selected samples intended to create the calibration curves.

As observed, the DMSO back extract concentrated the less alkylated fraction. In the SN100 sample, the profile seems strange, as compounds not present in the original sample seemed to be concentrated in the DMSO extract. This requires further verification, as the profile closely resembled that of SMO, suggesting possible cross-contamination. However, it could also be explained by the approximately 100-fold concentration factor of the DMSO back extract. This experiment will be repeated in future studies.

Nevertheless, assuming the data are correct, a strong correlation between the total MOAH back extracted from DMSO and the absorbance was observed in both SN100 and SMO samples. Interestingly, the limit of positivity, when looking at the MOAH DMSO concentration, appears to be consistent in both calibration curves (threshold value = 0.123).

Comparing these calibration curves reveals that the SMO sample concentrations required to fall within the linear range are much lower than those of the SN100 raffinate sample. This suggests that the method's sensitivity is higher for samples with a greater 3+ ring content and lower for those with a low 3+ ring ratio. However, it is challenging to correlate the observed absorbance with the degree of alkylation, as it may affect the measurement by shifting the absorbance maximum compared to the parent PAH or lower alkylated PAC, or by altering the absorbance intensity (either reducing, enhancing it or a combination of both) [102].

The correlation was confirmed when considering only the MOAH with 3 or more rings against absorbance (Figure 29), but the absorbance values differed significantly between SN100 and SMO at similar concentrations.

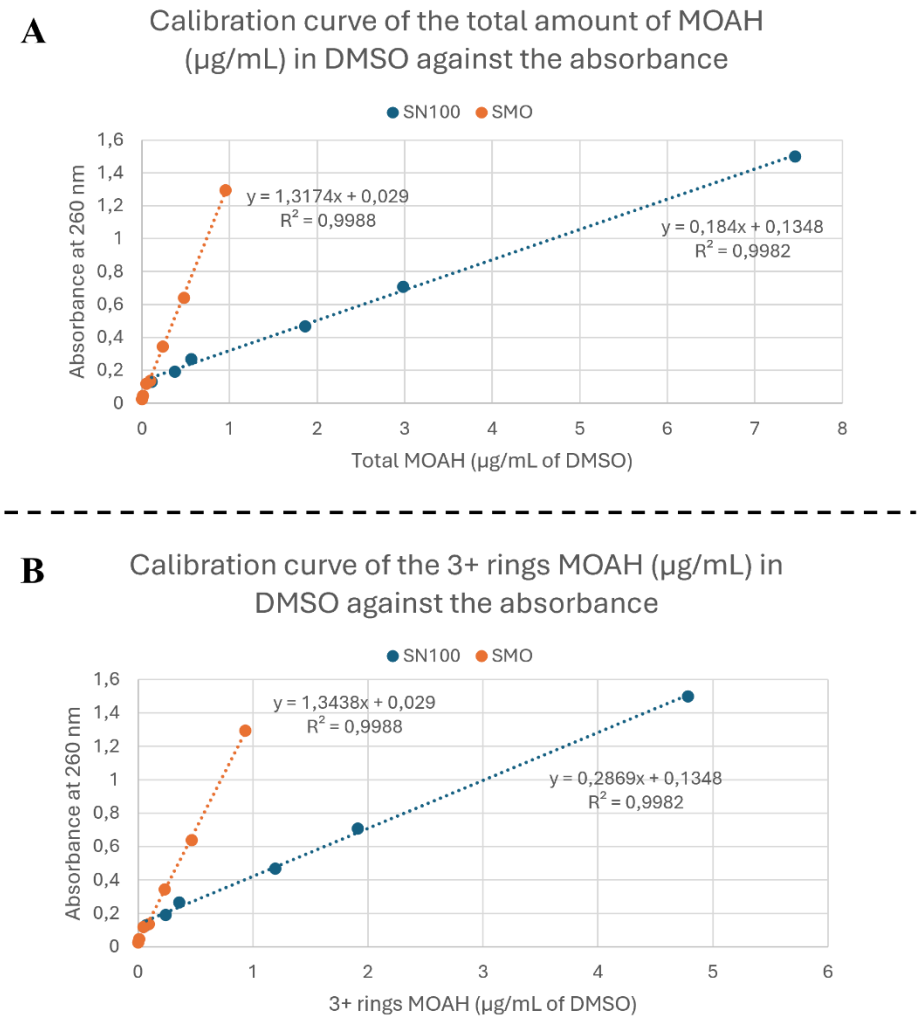

Figure 29 : Calibration curves of (A) the total amount of MOAH (µg/mL of DMSO) against the absorbance after DMSO back extraction and (B) the 3+ ring MOAH content (µg/mL of DMSO) against the absorbance after DMSO back extraction.

The calibration curves were performed only in single due to time and economic constraints, as well as limited sample availability. Further investigation is required to clarify the observed behavior. To further investigate the relationship between DMSO extraction and UV absorbance readings, several lubricant samples were tested using the same protocol. The hexane back-extract of their DMSO phase was injected into GC×GC-FID to gain deeper insights into their internal composition. Five samples were selected from an eleven-sample list to represent a wide range of compositions. The complete list of samples is available in the Annex 5, while the MOAH fractions and their DMSO back extracts of the five selected samples are shown in Figure 30. Only Retinax has a significant 3+ ring MOAH content, and all samples cover a specific carbon fraction range.

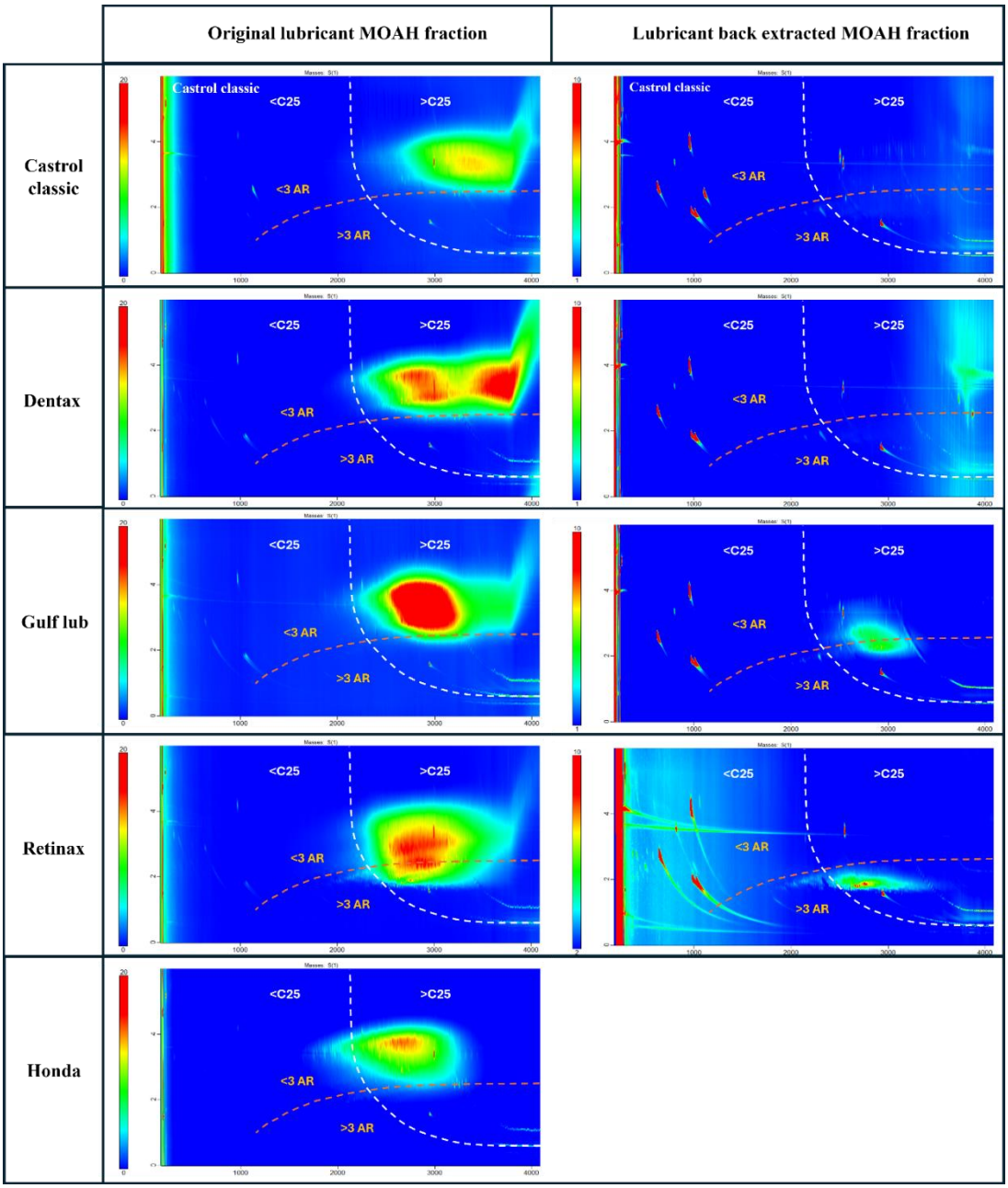

Figure 30 : MOAH fraction of the lubricants selected for the correlation test and their DMSO back-extracted fraction. The Honda sample does not have a back-extracted chromatogram due to issues encountered during handling, which led to the sample being discarded.

The Castrol classic and the Dentax DMSO back extracted fractions present strange chromatograms, leading to the conclusion that no MOAH is present in the DMSO back extract. This can be explained by a low MOAH 3+ rings initial composition and the dilution factor applied (175× for Dentax and 300× for Castrol classic) before injection. Therefore, it is likely that these samples concentration were below the limit of detection and thus yielded these "3+ rings MOAH free" chromatograms.

These samples were subjected to the Ph. Eur. test. It is important to note that the samples are primarily motor oil and lubricant oil. According to the Ph. Eur. monograph 7.0, this test is

intended for paraffin hard, light liquid, liquid, white soft, and yellow soft. Therefore, the lubricants used, although mainly composed of MOSH, are not suitable for this test. These motor oils are not pure and may contain substances such as emulsifiers and pigments, which can interfere with the test by creating emulsions that prevent the formation of two distinct phases, one of which is the DMSO to be analysed. To address this, the samples were centrifuged to break the emulsion and recover the DMSO phase. Despite these extra steps, the Honda sample could not be recovered and had to be discarded.

All samples tested positive after DMSO extract measurement. Their absorbance value reached 4, indicating that the sample composition saturated the detector. But the main goal was to evaluate the partition behaviour in the DMSO back extract.

Figure 31 presents the integration results of the original lubricants (Figure 31A) and the back extracts (Figure 31B) divided based on the number of ring and the C-range.

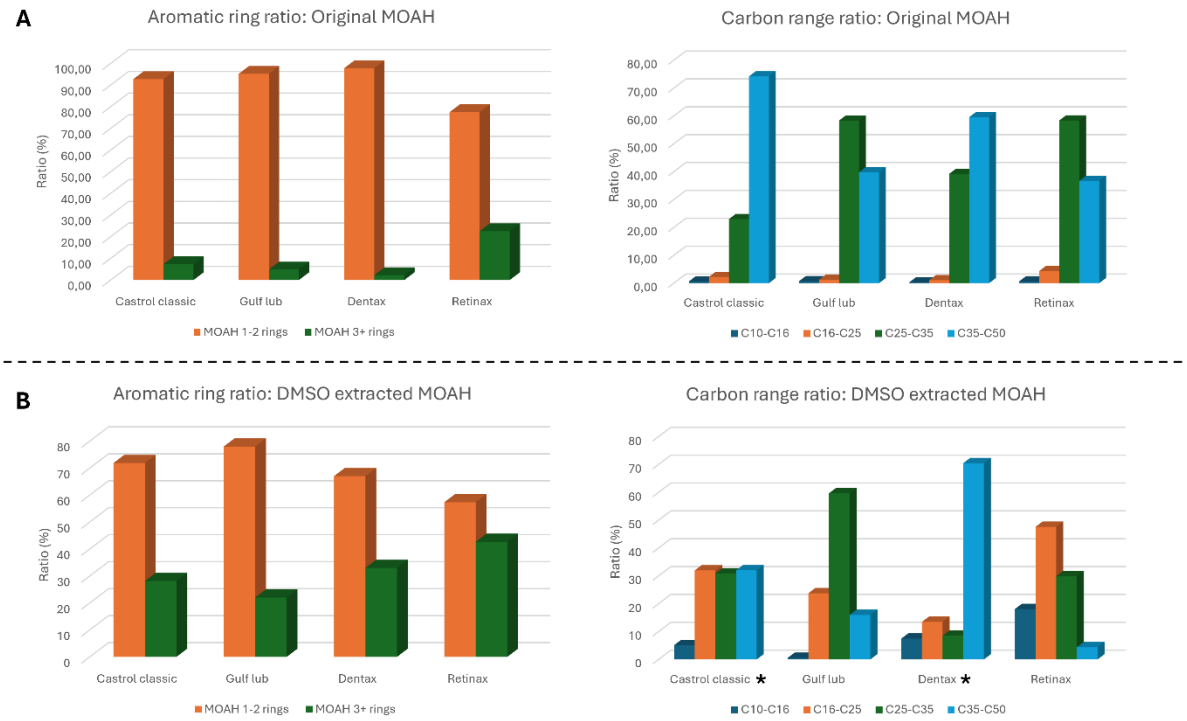

Figure 31 : Integration results of the internal composition of the correlation test samples. (A) Composition of the lubricants before Ph. Eur. method. (B) Composition of the lubricants after Ph. Eur. test and so after DMSO back extraction. "" represents non-reliable results.*

This comparison clearly shows that the applied method is more selective for 3+ aromatic rings, with their ratio increasing for all lubricants. Regarding the carbon range data, the samples were primarily composed of < C25 fractions before the Ph. Eur. test. However, after the test and back extraction, the ratios of the C10-C16 and C16-C25 fractions, which were low before the test, are now much higher, at the expense of higher carbon number fractions. This phenomenon confirmed that DMSO is not selective towards highly alkylated compounds and

has a greater affinity for less alkylated compounds [47]. The asterisk present in figure 31B highlights the sample from which the results are not reliable due to the absence of MOAH in the chromatograms. Therefore, the quantification led to unreal results which cannot be considered as the back extracted compounds from the initial sample.

To better understand the behaviour of MOAH in DMSO and what exactly the Ph.Eur. method (and consequently the IP346) is looking at, further experiments are needed. It is necessary to characterize in more details the MOAH fraction in terms of degree of alkylation and investigate the effect of alkylation on the absorbance values.

Conclusion and perspectives

In conclusion, generating valuable toxicological data on the MOAH fraction of MO is highly challenging but eagerly awaited by the scientific community and international health safety agencies. The initial difficulty lies in finding mineral oil samples with high MOAH content also covering various types of molecular structure and purifying these samples, which requires significant time, money, and expertise. Conducting various toxicological tests, such as the Ames and micronucleus tests, on these purified fractions is also demanding and requires special attention to produce valid, high-quality results. Indeed, the hydrophobic nature of these compounds make them more difficult to handle for biological assays. Correlating these toxicological results with the detailed composition of the samples is also essential to fully understand the health impacts of MOAH composition.

The findings from the preliminary steps highlight the necessity to optimise the separation of pure MO into MOSH and MOAH, as it can be critical and affected by major changes in the sample composition. This is even more critical in the sub-fraction separation. The sample composition is also impacting the solubility of it in solvents suitable for the toxicological tests. The viability of cells, such as hepatocytes, needs to be carefully assessed to account for the effects of both the samples and the solvents. DMSO concentrations up to 1% do not significantly decrease cell viability, nor do MOAH concentrations up to 25.2 µg/mL in contact with the cells.

The toxicological test findings suggest that the various MOAH samples tested do not induce base pair substitution mutations in hepatocyte cells. However, Moltox was the only sample to yield positive results with the *Salmonella typhimurium* TA98 strain, indicating its mutagenicity through frameshift mutations. Genotoxicity assessment revealed a significant effect of Moltox, as indicated by a high quantity of micronuclei, revealing DNA damage in hepatocytes. Similar conclusions could not be drawn for the other samples due to apoptosis

phenomena and a low number of replicates, which compromised the statistical validity of the test conditions. The test was also hampered by excessively high DMSO concentrations, which biased the findings.

The investigation on how the Ph. Eur. method correlated with the composition of the samples concluded that samples with a higher content of compounds with more than three aromatic rings increase the test's sensitivity. The DMSO showed a clear higher affinity toward the MOAH with more than 3 rings and low degree of alkylation.

This project is just at the beginning and several adjustments and additional tests have been highlighted as essential aspects for its future:

- Viability assessment should be performed more thoroughly to evaluate the maximum solvent concentration that can be used without harming the cells.
- Mutagenicity assessment should be studied further by repeating the existing tests and by testing other modified Salmonella strains to better understand the mutation pathways. The hamster liver metabolic S9 fraction should be used instead of the rat one to assess its effect on test sensitivity. A miniaturized Ames test could also be considered to address sample quantity issues and reduce the solvent needed to purify samples.
- The micronucleus test should be better designed, and alternative positive controls to TCDD should be used. Lower DMSO concentrations should be employed to avoid affecting cell viability, and sample concentrations should be lowered to ensure compounds are in solution, not suspension.
- The composition of the DMSO extract assessed in rapid tests as the Ph. Eur. Method and the IP346 should be better investigated to evaluate the analytical and compositional basis of the measurement performed. The effect of alkylation on the UV absorbance should be studied in depth as well as the partition into the DMSO of the different MOAH compounds.

Bibliography

[1] 'Contaminants - European Commission'. https://food.ec.europa.eu/safety/chemical-safety/contaminants_en (accessed May 07, 2024).

[2] EFSA Panel on Contaminants in the Food Chain (CONTAM) *et al.*, 'Update of the risk assessment of mineral oil hydrocarbons in food', *EFS2*, vol. 21, no. 9, Sep. 2023, doi: 10.2903/j.efsa.2023.8215.

[3] EFSA Panel on Contaminants in the Food Chain (CONTAM), 'Scientific Opinion on Mineral Oil Hydrocarbons in Food', *EFS2*, vol. 10, no. 6, juin 2012, doi: 10.2903/j.efsa.2012.2704.

[4] G. Bauwens, A. Gorska, and G. Purcaro, 'The role of comprehensive two-dimensional gas chromatography in mineral oil determination', *Anal Bioanal Chem*, vol. 415, no. 21, pp. 5067–5082, Sep. 2023, doi: 10.1007/s00216-023-04718-3.

[5] S. Moret, K. Grob, and L. S. Conte, 'Mineral oil polyaromatic hydrocarbons in foods, e.g. from jute bags, by on-line LC-solvent evaporation (SE)-LC-GC-FID', *Zeitschrift f□r Lebensmitteluntersuchung und -Forschung A*, vol. 204, no. 3, pp. 241–246, Mar. 1997, doi: 10.1007/s002170050071.

[6] European Commission. Joint Research Centre., *Guidance on sampling, analysis and data reporting for the monitoring of mineral oil hydrocarbons in food and food contact materials.* LU: Publications Office, 2019. Accessed: Feb. 19, 2024. [Online]. Available: https://data.europa.eu/doi/10.2760/208879

[7] A. Hochegger *et al.*, 'Mineral oil risk assessment: Knowledge gaps and roadmap. Outcome of a multi-stakeholders workshop', *Trends in Food Science & Technology*, vol. 113, pp. 151–166, Jul. 2021, doi: 10.1016/j.tifs.2021.03.021.

[8] L. Menegoz Ursol, C. Conchione, A. Srbinovska, and S. Moret, 'Optimization and validation of microwave assisted saponification (MAS) followed by epoxidation for high-sensitivity determination of mineral oil aromatic hydrocarbons (MOAH) in extra virgin olive oil', *Food Chemistry*, vol. 370, p. 130966, Feb. 2022, doi: 10.1016/j.foodchem.2021.130966.

[9] M. Biedermann, C. Munoz, and K. Grob, 'Update of on-line coupled liquid chromatography – gas chromatography for the analysis of mineral oil hydrocarbons in foods and cosmetics', *Journal of Chromatography A*, vol. 1521, pp. 140–149, Oct. 2017, doi: 10.1016/j.chroma.2017.09.028.

[10] G. Purcaro, 'Classical and comprehensive 2D LC-GC', in *Hyphenations of Capillary Chromatography with Mass Spectrometry*, Elsevier, 2020, pp. 227–275. doi: 10.1016/B978-0-12-809638-3.00006-5.

[11] M. Biedermann and K. Grob, 'On-line coupled high performance liquid chromatography–gas chromatography for the analysis of contamination by mineral oil. Part 1: Method of analysis', *Journal of Chromatography A*, vol. 1255, pp. 56–75, Sep. 2012, doi: 10.1016/j.chroma.2012.05.095.

[12] N. Sdrigotti, G. Bauwens, and G. Purcaro, 'A Review of MOSH and MOAH Analysis in Food', 2021.

[13] 'ISO 20122:2024', *ISO*. https://www.iso.org/standard/86091.html (accessed May 12, 2024).

[14] A. Hochegger, R. Wagenhofer, S. Savić, E. Mayrhofer, M. Washüttl, and E. Leitner, 'Combination of Multidimensional Instrumental Analysis and the Ames Test for the Toxicological Evaluation of Mineral Oil Aromatic Hydrocarbons', *J. Agric. Food Chem.*, vol. 70, no. 51, pp. 16401–16409, Dec. 2022, doi: 10.1021/acs.jafc.2c05970.

[15] M. Biedermann and K. Grob, 'Comprehensive two-dimensional gas chromatography for characterizing mineral oils in foods and distinguishing them from synthetic hydrocarbons',

Journal of Chromatography A, vol. 1375, pp. 146–153, Jan. 2015, doi: 10.1016/j.chroma.2014.11.064.

[16] M. Biedermann and K. Grob, 'Comprehensive two-dimensional GC after HPLC preseparation for the characterization of aromatic hydrocarbons of mineral oil origin in contaminated sunflower oil', *J of Separation Science*, vol. 32, no. 21, pp. 3726–3737, Nov. 2009, doi: 10.1002/jssc.200900366.

[17] A. Hedelin, 'Mineral oil – Origin, production and composition', 2013.

[18] Concawe, 'Mineral Oils Are Safe For Human Health ?', 2017. https://www.concawe.eu/wp-content/uploads/mineral-oils-are-safe-for-human-health.pdf (accessed May 14, 2024).

[19] C. R. Mackerer, L. C. Griffis, J. S. Grabowski, and F. A. Reitman, 'Petroleum Mineral Oil Refining and Evaluation of Cancer Hazard', *Applied Occupational and Environmental Hygiene*, vol. 18, no. 11, pp. 890–901, Nov. 2003, doi: 10.1080/10473220390237467.

[20] EDQM Council of Europe, *European pharmacopoeia*, 7th ed. Strasbourg: Council Of Europe : European Directorate for the Quality of Medicines and Healthcare, 2010.

[21] U.S. Food and Drug Administration, *21CFR178.3620. TITLE 21--FOOD AND DRUGS CHAPTER I--FOOD AND DRUG ADMINISTRATION DEPARTMENT OF HEALTH AND HUMAN SERVICES SUBCHAPTER B - FOOD FOR HUMAN CONSUMPTION (CONTINUED) PART 178 -- INDIRECT FOOD ADDITIVES: ADJUVANTS, PRODUCTION AIDS, AND SANITIZERS Subpart D - Certain Adjuvants and Production Aids*. 2024. Accessed: Jul. 08, 2024. [Online]. Available: https://www.accessdata.fda.gov/scripts/cdrh/cfdocs/cfcfr/CFRSearch.cfm?fr=178.3620

[22] K. Grob, M. Biedermann, A. Artho, and J. Egli, 'Food contamination by hydrocarbons from packaging materials determined by coupled LC-GC', *Z Lebensm Unters Forch*, vol. 193, no. 3, pp. 213–219, Sep. 1991, doi: 10.1007/BF01199968.

[23] M. Biedermann, K. Grob, and W. Meier, 'Partially concurrent eluent evaporation with an early vapor exit; detection of food irradiation through coupled LC-GC analysis of the fat', *J. High Resol. Chromatogr.*, vol. 12, no. 9, pp. 591–598, Sep. 1989, doi: 10.1002/jhrc.1240120904.

[24] M. J. Dennis, R. C. Massey, and D. J. McWeeny, 'A Method of Analysis for Paraffinic Waxes on Ducks', *International Journal of Environmental Analytical Chemistry*, vol. 30, no. 1–2, pp. 29–35, Jun. 1987, doi: 10.1080/03067318708075453.

[25] European Food Safety Authority (EFSA), D. Arcella, K. Baert, and M. Binaglia, 'Rapid risk assessment on the possible risk for public health due to the contamination of infant formula and follow-on formula by mineral oil aromatic hydrocarbons (MOAH)', *EFS3*, vol. 16, no. 11, Nov. 2019, doi: 10.2903/sp.efsa.2019.EN-1741.

[26] 'Catalogue - European Commission'. https://food.ec.europa.eu/safety/chemical-safety/contaminants/catalogue_en (accessed May 06, 2024).

[27] Foodwatch, 'Project_report_baby_milk.pdf', Oct. 24, 2019. https://www.foodwatch.org/fileadmin/-INT/mineral_oil/documents/2019-10-24_Projectreport_babymilk_FINAL.pdf (accessed May 06, 2024).

[28] Bundesinstitut Für Risikobewertung, 'Highly refined mineral oils in cosmetics: Health risks are not to be expected according to current knowledge: BfR Opinion No 008/2018 of 27 February 2018', *BfR-Stellungnahmen*, vol. 2018, no. no. 008, Feb. 2018, doi: 10.17590/20180702-124741-0.

[29] B. Chuberre, E. Araviiskaia, T. Bieber, and A. Barbaud, 'Mineral oils and waxes in cosmetics: an overview mainly based on the current European regulations and the safety profile of these compounds', *Acad Dermatol Venereol*, vol. 33, no. S7, pp. 5–14, Nov. 2019, doi: 10.1111/jdv.15946.

[30] H.-P. Neukom, K. Grob, M. Biedermann, and A. Noti, 'Food contamination by C20–C50 mineral paraffins from the atmosphere', *Atmospheric Environment*, vol. 36, no. 30, pp. 4839–4847, Oct. 2002, doi: 10.1016/S1352-2310(02)00358-8.

[31] K. Grob, A. Artho, M. Biedermann, and J. Egli, 'Food contamination by hydrocarbons from lubricating oils and release agents: Determination by coupled LC-GC', *Food Additives and Contaminants*, vol. 8, no. 4, pp. 437–446, Jul. 1991, doi: 10.1080/02652039109373993.

[32] A. Vollmer *et al.*, 'Migration of mineral oil from printed paperboard into dry foods: survey of the German market', *Eur Food Res Technol*, vol. 232, no. 1, pp. 175–182, Jan. 2011, doi: 10.1007/s00217-010-1376-6.

[33] M. Biedermann and K. Grob, 'Is recycled newspaper suitable for food contact materials? Technical grade mineral oils from printing inks', *Eur Food Res Technol*, vol. 230, no. 5, pp. 785–796, Mar. 2010, doi: 10.1007/s00217-010-1223-9.

[34] K. Grob, M. Huber, U. Boderius, and M. Bronz, 'Mineral oil material in canned foods', *Food Additives and Contaminants*, vol. 14, no. 1, pp. 83–88, Jan. 1997, doi: 10.1080/02652039709374500.

[35] R. Pirow *et al.*, 'Mineral oil in food, cosmetic products, and in products regulated by other legislations', *Critical Reviews in Toxicology*, vol. 49, no. 9, pp. 742–789, Oct. 2019, doi: 10.1080/10408444.2019.1694862.

[36] 'Standing Committee on Plants, Animals, Food and Feed Section Novel Food and Toxicological Safety of the Food Chain', Oct. 19, 2022. https://food.ec.europa.eu/document/download/d77a6725-2ccd-41a7-8a88-9d76f93fe972_en?filename=reg-com_toxic_20221019_sum.pdf (accessed Jul. 03, 2024).

[37] *Commission Regulation (EU) No 10/2011 of 14 January 2011 on plastic materials and articles intended to come into contact with food (Text with EEA relevance)Text with EEA relevance*. 2023. Accessed: Mar. 29, 2024. [Online]. Available: http://data.europa.eu/eli/reg/2011/10/2023-08-31/eng

[38] *Commission Regulation (EC) No 889/2008 of 5 September 2008 laying down detailed rules for the implementation of Council Regulation (EC) No 834/2007 on organic production and labelling of organic products with regard to organic production, labelling and control*, vol. 250. 2008. Accessed: Mar. 28, 2024. [Online]. Available: http://data.europa.eu/eli/reg/2008/889/oj/eng

[39] *Commission Implementing Regulation (EU) 2021/1165 of 15 July 2021 authorising certain products and substances for use in organic production and establishing their lists (Text with EEA relevance)Text with EEA relevance*. 2023. Accessed: Mar. 28, 2024. [Online]. Available: http://data.europa.eu/eli/reg_impl/2021/1165/2023-11-15/eng

[40] *Regulation (EC) No 1223/2009 of the European Parliament and of the Council of 30 November 2009 on cosmetic products (recast) (Text with EEA relevance)*, vol. 342. 2009. Accessed: Mar. 29, 2024. [Online]. Available: http://data.europa.eu/eli/reg/2009/1223/oj/eng

[41] SCHER/SCCP/SCENIHR, 'Scientific opinion on the risk assessment methodologies and approaches for genotoxic and carcinogenic substances', Jan. 2009, Accessed: Jun. 30, 2024. [Online]. Available: https://ec.europa.eu/health/ph_risk/committees/04_scher/docs/scher_o_113.pdf

[42] S. Adler *et al.*, 'Alternative (non-animal) methods for cosmetics testing: current status and future prospects—2010', *Arch Toxicol*, vol. 85, no. 5, pp. 367–485, May 2011, doi: 10.1007/s00204-011-0693-2.

[43] ‘Carcinogenicity - European Commission’. https://joint-research-centre.ec.europa.eu/eu-reference-laboratory-alternatives-animal-testing-eurl-ecvam/alternative-methods-toxicity-testing/validated-test-methods-health-effects/carcinogenicity_en (accessed Jun. 30, 2024).
[44] OECD, *Overview on genetic toxicology TGs*. OECD, 2017. doi: 10.1787/9789264274761-en.
[45] Subcommittee on the Classification of carcinogenic substances, ‘Guideline for the classification of carcinogenic substances’, Jun. 2023.
[46] OECD, *Test No. 487: In Vitro Mammalian Cell Micronucleus Test*. OECD Publishing, 2014. doi: 10.1787/9789264224438-en.
[47] J.-C. Carrillo, A. Van Der Wiel, D. Danneels, O. Kral, and P. J. Boogaard, ‘The selective determination of potentially carcinogenic polycyclic aromatic compounds in lubricant base oils by the DMSO extraction method IP346 and its correlation to mouse skin painting carcinogenicity assays’, *Regulatory Toxicology and Pharmacology*, vol. 106, pp. 316–333, Aug. 2019, doi: 10.1016/j.yrtph.2019.05.012.
[48] R. J. Ellison, O. C. E. O. for Environmental, and H. P. H. M. Group, *The Use of the Dimethyl Sulphoxide (DMSO) Extract by the IP 346 Method as an Indicator of the Carcinogenicity of Lubricant Base Oils and Distillate Aromatic Extracts: This Report is Based on a Paper Given on Behalf of the CONCAWE Health Management Group to the Workshop on the Carcinogenicity of Coal and Petroleum Derived Substances Held at the EC Joint Research Centre at Ispra, Italy, May 25-26, 1992*. CONCAWE, 1994. [Online]. Available: https://books.google.be/books?id=kyfWPgAACAAJ
[49] G. R. Blackburn, R. A. Deitch, C. A. Schreiner, M. A. Mehlman, and C. R. Mackerer, ‘Estimation of the dermal carcinogenic activity of petroleum fractions using a modified Ames assay’, *Cell Biol Toxicol*, vol. 1, no. 1, pp. 67–80, Oct. 1984, doi: 10.1007/BF00125566.
[50] G. R. Blackburn, R. A. Deitch, C. A. Schreiner, and C. R. Mackerer, ‘Predicting carcinogenicity of petroleum distillation fractions using a modified Salmonella mutagenicity assay’, *Cell Biol Toxicol*, vol. 2, no. 1, pp. 63–84, Mar. 1986, doi: 10.1007/BF00117708.
[51] K. Mortelmans and E. Zeiger, ‘The Ames Salmonella/microsome mutagenicity assay’, *Mutation Research/Fundamental and Molecular Mechanisms of Mutagenesis*, vol. 455, no. 1–2, pp. 29–60, Nov. 2000, doi: 10.1016/S0027-5107(00)00064-6.
[52] E. Zeiger, ‘The test that changed the world: The Ames test and the regulation of chemicals’, *Mutation Research/Genetic Toxicology and Environmental Mutagenesis*, vol. 841, pp. 43–48, May 2019, doi: 10.1016/j.mrgentox.2019.05.007.
[53] D. N. Large, N. A. Van Doorn, and S. C. Timmons, ‘Cancer and chemicals: A research-inspired laboratory exercise based on the Ames test for mutagenicity’, *Biochem Molecular Bio Educ*, vol. 51, no. 1, pp. 103–113, Jan. 2023, doi: 10.1002/bmb.21674.
[54] OECD, *Test No. 471: Bacterial Reverse Mutation Test*. OECD, 2020. doi: 10.1787/9789264071247-en.
[55] M. H. Kung *et al.*, ‘Critical review of the relationship between IP346 and dermal carcinogenic activity’, pp. 1–16, Apr. 2016.
[56] IARC Working Group on the Evaluation of Carcinogenic Risks to Humans, ‘Chemical agents and related occupations’, *IARC Monogr Eval Carcinog Risks Hum*, vol. 100, no. Pt F, pp. 9–562, 2012.
[57] S. Harayama, H. Kishira, Y. Kasai, and K. Shutsubo, ‘Petroleum biodegradation in marine environments’, *J Mol Microbiol Biotechnol*, vol. 1, no. 1, pp. 63–70, Aug. 1999.
[58] R. Pirow, N. Concin, and K. Grob, ‘Evidence for an accumulation of mineral oil saturated hydrocarbons (MOSH) in human tissues: a re-evaluation of biopsy and autopsy data’, *J Consum Prot Food Saf*, Sep. 2023, doi: 10.1007/s00003-023-01458-5.

[59] L. Barp *et al.*, 'Mineral oil in human tissues, Part I: Concentrations and molecular mass distributions', *Food and Chemical Toxicology*, vol. 72, pp. 312–321, Oct. 2014, doi: 10.1016/j.fct.2014.04.029.
[60] L. Barp *et al.*, 'Accumulation of mineral oil saturated hydrocarbons (MOSH) in female Fischer 344 rats: Comparison with human data and consequences for risk assessment', *Science of The Total Environment*, vol. 575, pp. 1263–1278, Jan. 2017, doi: 10.1016/j.scitotenv.2016.09.203.
[61] J.-C. Carrillo, D. Danneels, and J. Woldhuis, 'Relevance of animal studies in the toxicological assessment of oil and wax hydrocarbons. Solving the puzzle for a new outlook in risk assessment', *Critical Reviews in Toxicology*, vol. 51, no. 5, pp. 418–455, May 2021, doi: 10.1080/10408444.2021.1944056.
[62] D. Wang *et al.*, 'The effect of alkyl substitution on the oxidative metabolism and mutagenicity of phenanthrene', *Arch Toxicol*, vol. 96, no. 4, pp. 1109–1131, Apr. 2022, doi: 10.1007/s00204-022-03239-9.
[63] 'Polycyclic Aromatic Hydrocarbons in Food - Scientific Opinion of the Panel on Contaminants in the Food Chain', *EFSA Journal*, no. EFSA Journal, doi: 10.2903/j.efsa.2008.724.
[64] B. Ewa and M.-Š. Danuta, 'Polycyclic aromatic hydrocarbons and PAH-related DNA adducts', *J Appl Genetics*, vol. 58, no. 3, pp. 321–330, Aug. 2017, doi: 10.1007/s13353-016-0380-3.
[65] D. Wang *et al.*, 'The influence of alkyl substitution on the in vitro metabolism and mutagenicity of benzo[a]pyrene', *Chemico-Biological Interactions*, vol. 363, p. 110007, Aug. 2022, doi: 10.1016/j.cbi.2022.110007.
[66] A. B. Patel, S. Shaikh, K. R. Jain, C. Desai, and D. Madamwar, 'Polycyclic Aromatic Hydrocarbons: Sources, Toxicity, and Remediation Approaches', *Front. Microbiol.*, vol. 11, p. 562813, Nov. 2020, doi: 10.3389/fmicb.2020.562813.
[67] N. C. Sondermann *et al.*, 'Functions of the aryl hydrocarbon receptor (AHR) beyond the canonical AHR/ARNT signaling pathway', *Biochemical Pharmacology*, vol. 208, p. 115371, Feb. 2023, doi: 10.1016/j.bcp.2022.115371.
[68] E. C. Klingbeil, K. M. Hew, U. C. Nygaard, and K. C. Nadeau, 'Polycyclic aromatic hydrocarbons, tobacco smoke, and epigenetic remodeling in asthma', *Immunol Res*, vol. 58, no. 2–3, pp. 369–373, May 2014, doi: 10.1007/s12026-014-8508-1.
[69] F. Li, W. Zhu, and F. J. Gonzalez, 'Potential role of CYP1B1 in the development and treatment of metabolic diseases', *Pharmacology & Therapeutics*, vol. 178, pp. 18–30, Oct. 2017, doi: 10.1016/j.pharmthera.2017.03.007.
[70] *Cytochromes P450: Drug Metabolism, Bioactivation and Biodiversity 2.0*. MDPI, 2021. doi: 10.3390/books978-3-0365-0257-1.
[71] P. J. Boogaard, 'Chapter 3F. Biomonitoring of Exposure to Polycyclic Aromatic Hydrocarbons', in *Issues in Toxicology*, vol. 1, L. Knudsen and D. F. Merlo, Eds. Cambridge: Royal Society of Chemistry, 2011, pp. 338–359. doi: 10.1039/9781849733373-00338.
[72] S. Manzetti, 'Ecotoxicity of polycyclic aromatic hydrocarbons, aromatic amines, and nitroarenes through molecular properties', *Environ Chem Lett*, vol. 10, no. 4, pp. 349–361, Dec. 2012, doi: 10.1007/s10311-012-0368-0.
[73] V. J. Melendez-Colon, A. Luch, A. Seidel, and W. M. Baird, 'Formation of Stable DNA Adducts and Apurinic Sites upon Metabolic Activation of Bay and Fjord Region Polycyclic Aromatic Hydrocarbons in Human Cell Cultures', *Chem. Res. Toxicol.*, vol. 13, no. 1, pp. 10–17, Jan. 2000, doi: 10.1021/tx9802724.
[74] D. Wang, B. Bruyneel, L. Kamelia, S. Wesseling, I. M. C. M. Rietjens, and P. J. Boogaard, 'In vitro metabolism of naphthalene and its alkylated congeners by human and rat liver microsomes via

alkyl side chain or aromatic oxidation', *Chemico-Biological Interactions*, vol. 315, p. 108905, Jan. 2020, doi: 10.1016/j.cbi.2019.108905.

[75] K. Grob, 'Toxicological Assessment of Mineral Hydrocarbons in Foods: State of Present Discussions', *J. Agric. Food Chem.*, vol. 66, no. 27, pp. 6968–6974, Jul. 2018, doi: 10.1021/acs.jafc.8b02225.

[76] J. L. H. Ruiz, J. A. Liébanas, J. L. M. Vidal, A. Garrido Frenich, and R. R. González, 'Offline Solid-Phase Extraction and Separation of Mineral Oil Saturated Hydrocarbons and Mineral Oil Aromatic Hydrocarbons in Edible Oils, and Analysis via GC with a Flame Ionization Detector', *Foods*, vol. 10, no. 9, p. 2026, Aug. 2021, doi: 10.3390/foods10092026.

[77] S. Moret, L. Barp, G. Purcaro, and L. S. Conte, 'Rapid and sensitive solid phase extraction-large volume injection-gas chromatography for the analysis of mineral oil saturated and aromatic hydrocarbons in cardboard and dried foods', *Journal of Chromatography A*, vol. 1243, pp. 1–5, Jun. 2012, doi: 10.1016/j.chroma.2012.04.040.

[78] MOLTOX, 'Ames FT TA98 TA100 Instruction Manual 31-300', 2021. https://moltox.com/docs/manuals/Ames%20FT%20TA98%20TA100%20Instruction%20Manual%2031-300%202021%20Version.pdf (accessed May 17, 2024).

[79] M. Koch, E. Becker, M. Päch, S. Kühn, and E. Kirchhoff, 'Separation of the mineral oil aromatic hydrocarbons of three and more aromatic rings from those of one or two aromatic rings', *J of Separation Science*, vol. 43, no. 6, pp. 1089–1099, Mar. 2020, doi: 10.1002/jssc.201900833.

[80] M. Lommatzsch, M. Eckardt, J. Holzapfel, S. Säger, and T. J. Simat, 'Advanced separation of mineral oil aromatic hydrocarbons by number of aromatic rings using donor-acceptor-complex chromatography to extend on-line coupled liquid chromatography-gas chromatography', *Journal of Chromatography A*, vol. 1715, p. 464600, Jan. 2024, doi: 10.1016/j.chroma.2023.464600.

[81] S. K. Panda, N. A. Alawani, T. A. Al-Qunaysi, M. Elanany, and H. Muller, 'Alkyl carbon number limits the ring-number separation of polycyclic aromatic compounds in petroleum analysis', *Fuel*, vol. 284, p. 118937, Jan. 2021, doi: 10.1016/j.fuel.2020.118937.

[82] D. Maron, J. Katzenellenbogen, and B. N. Ames, 'Compatibility of organic solvents with the Salmonella/microsome test', *Mutation Research/Genetic Toxicology*, vol. 88, no. 4, pp. 343–350, Apr. 1981, doi: 10.1016/0165-1218(81)90025-2.

[83] D. Li *et al.*, 'Effect of Regular Organic Solvents on Cytochrome P450-Mediated Metabolic Activities in Rat Liver Microsomes: Fig. 1.', *Drug Metab Dispos*, vol. 38, no. 11, pp. 1922–1925, Nov. 2010, doi: 10.1124/dmd.110.033894.

[84] K. Sumida *et al.*, 'Effects of DMSO on gene expression in human and rat hepatocytes', *Hum Exp Toxicol*, vol. 30, no. 10, pp. 1701–1709, Oct. 2011, doi: 10.1177/0960327111399325.

[85] J. Huwyler, H. Kettiger, A. Schipanski, and P. Wick, 'Engineered nanomaterial uptake and tissue distribution: from cell to organism', *IJN*, p. 3255, Aug. 2013, doi: 10.2147/IJN.S49770.

[86] S. Ahn, E. Seo, K. Kim, and S. J. Lee, 'Controlled cellular uptake and drug efficacy of nanotherapeutics', *Sci Rep*, vol. 3, no. 1, p. 1997, Jun. 2013, doi: 10.1038/srep01997.

[87] E. Bertram-Ralph and M. Amare, 'Factors affecting drug absorption and distribution', *Anaesthesia & Intensive Care Medicine*, vol. 24, no. 4, pp. 221–227, Apr. 2023, doi: 10.1016/j.mpaic.2022.12.023.

[88] M. Feoktistova, P. Geserick, and M. Leverkus, 'Crystal Violet Assay for Determining Viability of Cultured Cells', *Cold Spring Harb Protoc*, vol. 2016, no. 4, p. pdb.prot087379, Apr. 2016, doi: 10.1101/pdb.prot087379.

[89] J. Wen, Y. Tong, and Y. Zu, 'Low Concentration DMSO Stimulates Cell Growth and In vitro Transformation of Human Multiple Myeloma Cells', *BJMMR*, vol. 5, no. 1, pp. 65–74, Jan. 2015, doi: 10.9734/BJMMR/2015/5276.

[90] E34 Committee, 'Test Method for Determining Carcinogenic Potential of Virgin Base Oils in Metalworking Fluids'. ASTM International. doi: 10.1520/E1687-19.

[91] M. Hermann, O. Chaudé, N. Weill, H. Bedouelle, and M. Hofnung, 'Adaptation of the Salmonella/mammalian microsome test to the determination of the mutagenic properties of mineral oils', *Mutation Research/Genetic Toxicology*, vol. 77, no. 4, pp. 327–339, Apr. 1980, doi: 10.1016/0165-1218(80)90004-X.

[92] D. Kirkland *et al.*, 'Can in vitro mammalian cell genotoxicity test results be used to complement positive results in the Ames test and help predict carcinogenic or in vivo genotoxic activity? I. Reports of individual databases presented at an EURL ECVAM Workshop', *Mutation Research/Genetic Toxicology and Environmental Mutagenesis*, vol. 775–776, pp. 55–68, Dec. 2014, doi: 10.1016/j.mrgentox.2014.10.005.

[93] R. Morita *et al.*, 'Molecular Mechanisms of the Whole DNA Repair System: A Comparison of Bacterial and Eukaryotic Systems', *Journal of Nucleic Acids*, vol. 2010, no. 1, p. 179594, Jan. 2010, doi: 10.4061/2010/179594.

[94] C. Genies, A. Maître, E. Lefèbvre, A. Jullien, M. Chopard-Lallier, and T. Douki, 'The Extreme Variety of Genotoxic Response to Benzo[a]pyrene in Three Different Human Cell Lines from Three Different Organs', *PLoS ONE*, vol. 8, no. 11, p. e78356, Nov. 2013, doi: 10.1371/journal.pone.0078356.

[95] K. Krupina, A. Goginashvili, and D. W. Cleveland, 'Causes and consequences of micronuclei', *Current Opinion in Cell Biology*, vol. 70, pp. 91–99, Jun. 2021, doi: 10.1016/j.ceb.2021.01.004.

[96] R. Funayama and F. Ishikawa, 'Cellular senescence and chromatin structure', *Chromosoma*, vol. 116, no. 5, pp. 431–440, Oct. 2007, doi: 10.1007/s00412-007-0115-7.

[97] D. Moir *et al.*, 'The subchronic toxicity of acridine in the rat', *Journal of Environmental Science and Health, Part B*, vol. 32, no. 4, pp. 545–564, Jul. 1997, doi: 10.1080/03601239709373102.

[98] E. G. Besteman, K. L. Zimmerman, W. R. Huckle, M. R. Prater, R. M. Gogal, and S. D. Holladay, '2,3,7,8-Tetrachlorodibenzo- *P* -Dioxin (TCDD) or Diethylstilbestrol (DES) Cause Similar Hematopoietic Hypocellularity and Hepatocellular Changes in Murine Fetal Liver, but Differentially Affect Gene Expression', *Toxicol Pathol*, vol. 35, no. 6, pp. 786–792, Oct. 2007, doi: 10.1080/01926230701584155.

[99] International Agency for Research on Cancer, Ed., *Polychlorinated Dibenzo-para-dioxins and polychlorinated dibenzofurans: this publication represents the views and expert opinions of an IARC Working Group on the evaluation of carcinogenic risks to humans, which met in Lyon, 4-11 February 1997*. Lyon: IARC, 1997.

[100] Agency for Toxic Substances and Disease Registry (ATSDR)., 'Toxicological profile for Chlorinated Dibenzo-p-dioxins (CDDs)', 1998. https://www.atsdr.cdc.gov/toxprofiles/tp104.pdf (accessed Aug. 06, 2024).

[101] J. Suzuki and S. Nagata, 'Phospholipid Scrambling on the Plasma Membrane', in *Methods in Enzymology*, vol. 544, Elsevier, 2014, pp. 381–393. doi: 10.1016/B978-0-12-417158-9.00015-7.

[102] H.-H. Perkampus, *UV-VIS Spectroscopy and Its Applications*. Berlin, Heidelberg: Springer Berlin Heidelberg, 1992. doi: 10.1007/978-3-642-77477-5.

[103] LECO Corporation, 'ChromaTOF® Brand Software Instruction Manual Version 5.56'. Jan. 2024.

Annex

Annex 1

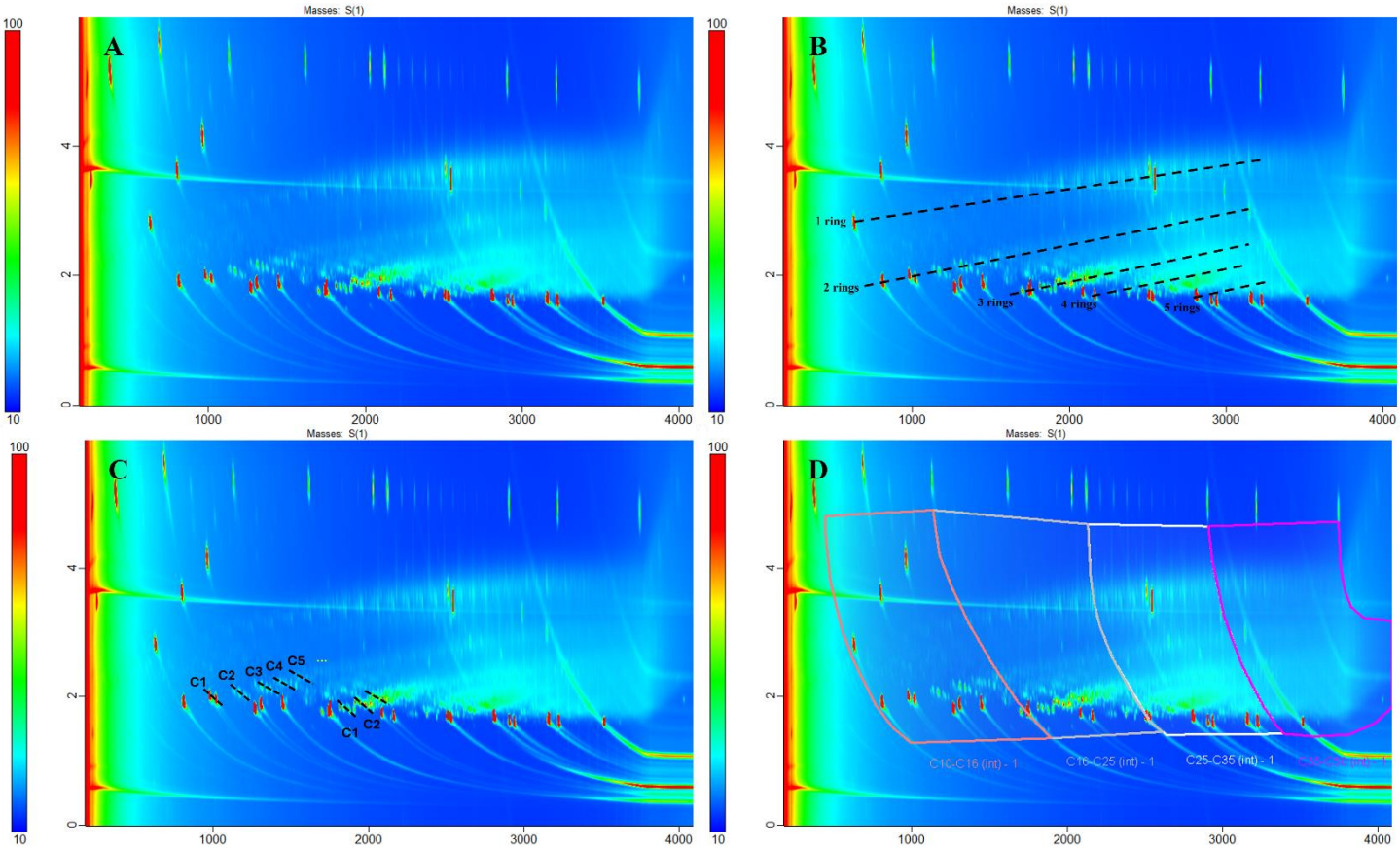

Annex 1 : GC×GC-FID chromatograms of a heavy vacuum gas oil (HVGO) sample. (A) HVGO sample. (B) HVGO sample with black dashed lines depicting the separation based on the number of aromatic rings. (C) Mask representing the separation according to the number of alkylation degree in the HVGO. The marks C1,C2,… states for the carbon number (representing the alkylation degree in this case). (D) Separation of the HVGO sample according to the carbon range. The different masks represent the C10-C16, C16-C25, C25-C35 and C35-C50 elution area.

Annex 2

The LC/GC×GC-TOFMS/FID instrument either operated in 1D (LC/GC) or 2D (LC/GC×GC) is schematised below.

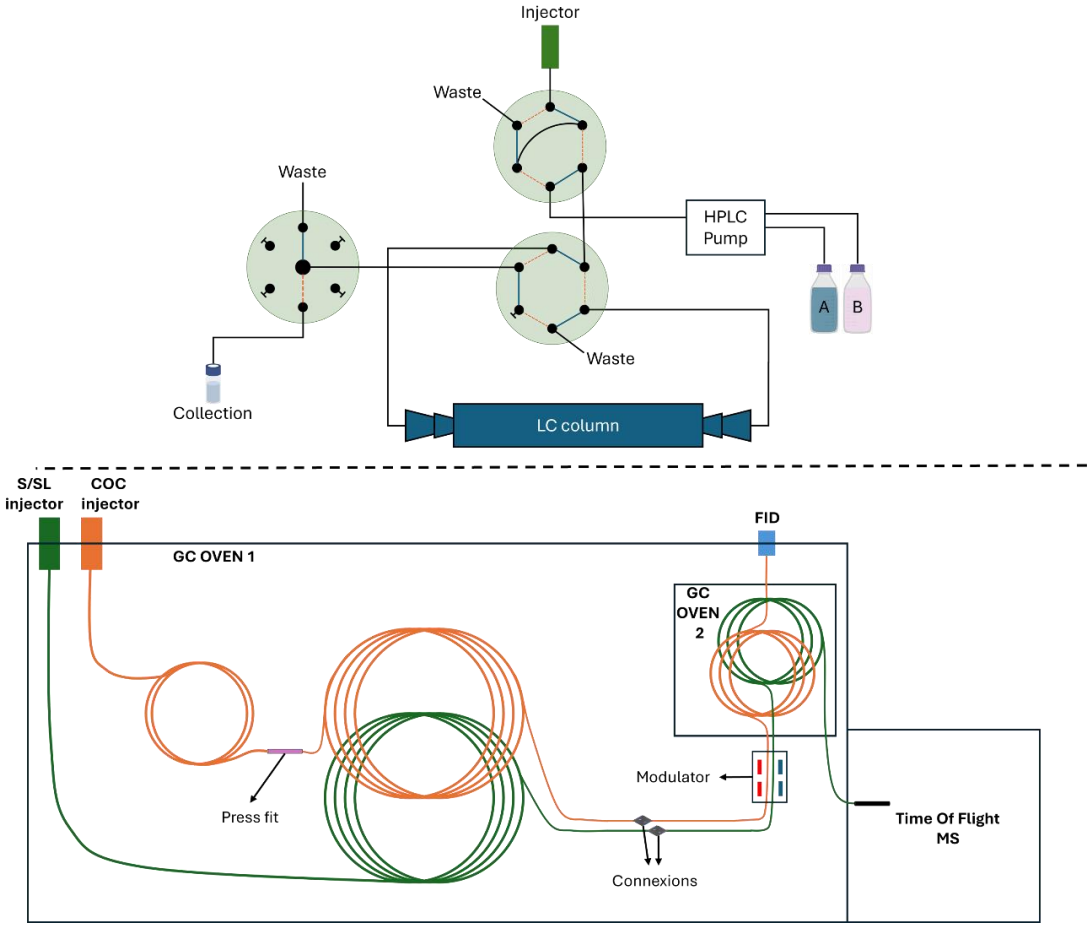

Annex 2 : Representation of the LC/GC×GC-TOFMS/FID instrument setup used for the MOSH/MOAH analysis in this work. S/SL stands for split/splitless and COC for cold on column. On the top is a representation of the LC system. The blue pathway represents the non-collection mode. The orange dashed lines represent the collection mode

MOSH and MOAH were separated in the LC column according to their elution windows described in table 22. The HPLC column used is an Allure silica column (Restek, Germany), 250 mm × 2.1mm i.d. × 5 µm d_p installed on an Agilent 1260 Infinity II LC system. A G7112B binary pump and a variable wavelength detector set at 230 nm (Agilent Technologies, Waldbronn, Germany) are also part of the equipment. Slight modifications have been implemented to the pump by Axel-Semrau for dead volume minimizations.

The collected fractions are reconcentrated to a volume of around 100µL with vacuum concentration (Eppendorf *Concentrator Plus*, Hamburg, Germany).

Table 22 - LC elution gradient used for MOSH MOAH fractionation

Time (min)	Phase	n-Hexane (%)	Dichloromethane (%)	Flow (mL/min)
0	Sample elution	100	0	0.3
1.5		65	35	0.3
2	MOSH collection	65	35	0.3
3.5				
4.4	MOAH collection	65	35	0.3
5.9				
6	Backflush start	65	35	0.3
6.10	Backflush	0	100	0.5
15.10	Re-equilibration	100	0	0.5
25.10				0.3
30	Ready for next analysis			

The LC reconcentrated fraction is then injected into two parallel GC columns connected either to FID or TOFMS. The FID line is equipped with an on-column injector and relies on the use of a retention gap (Rxi Guard Column, 4m × 0.53 mm i.d., #10073, Restek) interface working under solvent flooding mode [10]. The MS line features a split/splitless injector configured in splitless mode and thus do not have a retention gap at the injector level.

The GC×GC system used is a Pegasus BT 4D GC×GC TOF MS (LECO, Michigan, USA) device. It is made of an Agilent 7890A gas chromatograph including a secondary oven, a quad-jet dual-stage thermal modulator and a TOFMS as well as an FID. GC columns used were the same for both lines and consisted of Rxi-17SilMS (15m × 0.25mm i.d. × 0.25µm, #14120, Restek) for the first dimension and Rxi-1MS HT (0.8m × 0.15mm i.d. × 0.15µm, #578239, Restek) for the second dimension. The MS line possesses a retention gap after the secondary column (GC Guard column IP deactivation, 0.550 m × 0.15 mm i.d., #10042, Restek).

Table 23 displays the oven temperature program as well as the other parameters used for the analyses. All the data were acquired using the LECO software “ChromaTOF Version 5 for MOSH/MOAH”.

Table 23 - Parameters for 1 dimension (GC) and 2 dimensions (GC×GC) sample analysis

		MS line	FID line
Inlet	Inlet mode/type	Splitless	On-column
	Flow (mL/min)	1.3	1.5
	Septum purge (mL/min)	3	\
	Inlet purge flow (mL/min)	50	\
	Inlet purge time (s)	60	\
Oven temperature program	Initial temperature (°C)	59	
	Hold time (min)	5	
	Temperature ramp	1D → 20°C/min; 2D → 5°C/min	
	Final temperature (°C)	350	
	Hold time (min)	5	
	Secondary oven temperature (°C)	+5 °C from the primary oven temperature	
Modulator (only for 2D)	Modulation time (s)	6	
	Hot pulse (s)	1.8	
	Cool time (s)	1.2	
	Chiller temperature (°C)	-80	
Detector	Detector temperature (°C)	\	360
	Ion source temperature (°C)	250	\
	Transfer line temperature (°C)	330	\
	Carrier gas	Helium	Helium
	Make up gas flow (mL/min)	\	30
	Hydrogen fuel flow (mL/min)	\	40
	Air flow (mL/min)	\	400
	Data collection rate	\	100
	Acquisition delay (s)	\	180
	Data acquisition frequency (Hz)	1D → 20; 2D → 200	
	Ionisation mode	Electron ionization	\
	Voltage (eV)	70	

The different samples used in this work have been treated following the same procedure. A blank subtraction and a smoothing factor were applied to each chromatogram. This smoothing factor aims to remove the riding peaks on the top of the hump and allow better quantification [103]. A mask based on a HVGO sample injected during each sequence has been created and applied to all chromatograms. After the integration of the internal standard peak and the MOAH hump, the MOAH mass fraction has been calculated as such:

$$C_{MOAH} = \frac{A_{MOAH} * m_{2MN}}{A_{2MN} * V_{inj}}$$

Where C_{MOAH} represents the concentration of the MOAH hump in µg/mL, A_{MOAH} is the area corresponding to the MOAH hump after the blank subtraction, m_{2MN} and A_{2MN} are the mass of 2MN injected (ng) and the peak area of the 2MN internal standard compound respectively. V_{inj} corresponds to the injected volume in gas chromatography (µL).

Annex 3

The algorithm developed to automatically treat the Ames plates absorbance measurements at 430 nm and 590 nm is hosted on a document linked below.

https://docs.google.com/document/d/1eDmeCF3jx47h1mBKQCpwbloC1f1Ug-F14L0sxc65zAY/edit?usp=sharing

The absorbance of each well was measured at 430 nm and 590 nm to account for variations in absorbance depending on the colour of the culture medium. Cells that have mutated (whether due to the action of a mutagenic compound or not) will acidify the medium, causing the colour indicator to turn yellow. A wavelength of 430 nm, in the blue region of the visible spectrum, is therefore suitable for measuring the absorbance of these wells. However, wells with no cell growth remain purplish. In this case, 430 nm is not suitable, as the light is only weakly absorbed. In this case, a wavelength of 590 nm would be more appropriate.

The ratio between the absorbance of the well at 430nm and 590 nm is performed to yield a new value for each well. The mean value as well as the standard deviation of the absorbances ratio of visually observed negative wells has been determined (based on 845 negative wells). This mean value added by 3.6× the standard deviation is the first threshold value from which the algorithm is determining if a well is positive or negative in the positive control area. After these positive wells number counting in the positive control area, the algorithm sets a new threshold value based on the mean absorbance ratio added by 3.6× its standard deviation of the negative wells in this control positive area. This new threshold value is used to compare each well from the plate and if the observed value is higher than this new threshold, the well is

considered positive. Otherwise, the well is considered negative. Then the algorithms automatically sum the number of positive wells in each specified area and the sum of negative wells. Two excel file are generated containing the data generated by the algorithm. One of the excel file includes the A-ratio measurements and highlight the sample that gets out positive of this analysis. The other one contains a virtual reconstitution of the different plates to allow comparison with the real plates and see if the automatic algorithm ran properly.

	1	2	3	4	5	6	7	8	9	10	11	12	13	14	15	16	17	18	19	20	21	22	23	24
A	1	0	1	0	0	0	0	1	0	0	1	1	1	0	0	1	0	0	0	0	1	0	1	0
B	0	0	1	1	0	0	0	0	0	1	0	0	1	0	1	0	0	0	1	0	0	0	1	0
C	0	0	0	0	0	0	0	0	0	0	0	0	0	0	0	0	0	1	0	0	0	1	1	0
D	0	0	1	0	0	0	0	0	0	1	0	1	1	1	0	0	1	1	1	0	1	0	0	0
E	0	0	0	0	0	0	0	0	1	0	1	0	0	0	0	0	0	0	1	0	0	0	1	0
F	0	0	0	0	0	0	0	0	1	0	0	0	0	0	0	0	1	0	1	0	1	1	0	0
G	0	0	1	0	0	0	0	0	0	0	1	1	0	0	0	1	0	0	0	0	1	0	0	0
H	0	0	0	0	0	0	0	0	0	0	1	1	0	0	0	0	0	0	1	0	0	0	0	1
I	0	1	1	0	0	0	1	1	0	0	1	0	0	0	0	0	0	0	0	0	0	0	0	0
J	0	0	0	0	0	0	1	0	0	0	1	0	0	0	0	0	0	0	1	1	0	0	0	0
K	1	0	0	0	0	0	0	0	0	0	0	0	0	0	0	0	0	0	0	0	0	0	0	0
L	0	1	0	0	0	0	1	0	1	0	1	1	0	0	0	0	0	0	0	0	0	0	0	0
M	0	1	0	0	0	0	0	1	0	1	1	0												
N	0	0	0	1	0	0	1	0	0	0	1	0												
O	0	0	0	0	0	0	0	0	0	0	0	0												
P	0	0	0	0	0	0	0	0	0	0	0	0												

Annex 3 : Representation of the reconstructed Ames plate after data processing by the algorithm.

Annex 4

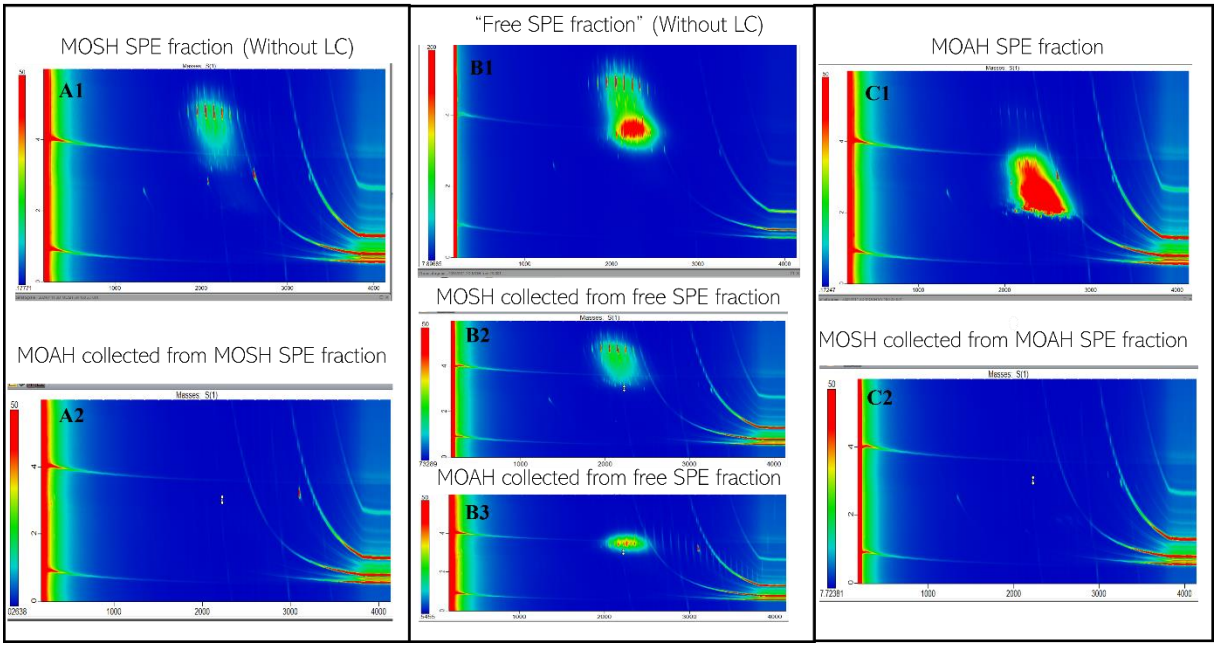

Annex 4 : GC×GC-FID chromatograms of the collected SPE fractions in the first test (original protocol) aiming to evaluate the MOSH/MOAH separation performances of unoptimized protocol. (A1) MOSH SPE fraction collected. (A2) MOAH HPLC collected fraction from the SPE collected MOSH fraction. (B1) Free fraction collected from the SPE separation. (B2) MOSH HPLC collected fraction from the free fraction collected in SPE. (B3) MOAH HPLC collected fraction from the free fraction collected in SPE. (C1) MOAH SPE fraction collected. (C2) MOSH HPLC collected fraction from MOAH SPE collected fraction.

Annex 5

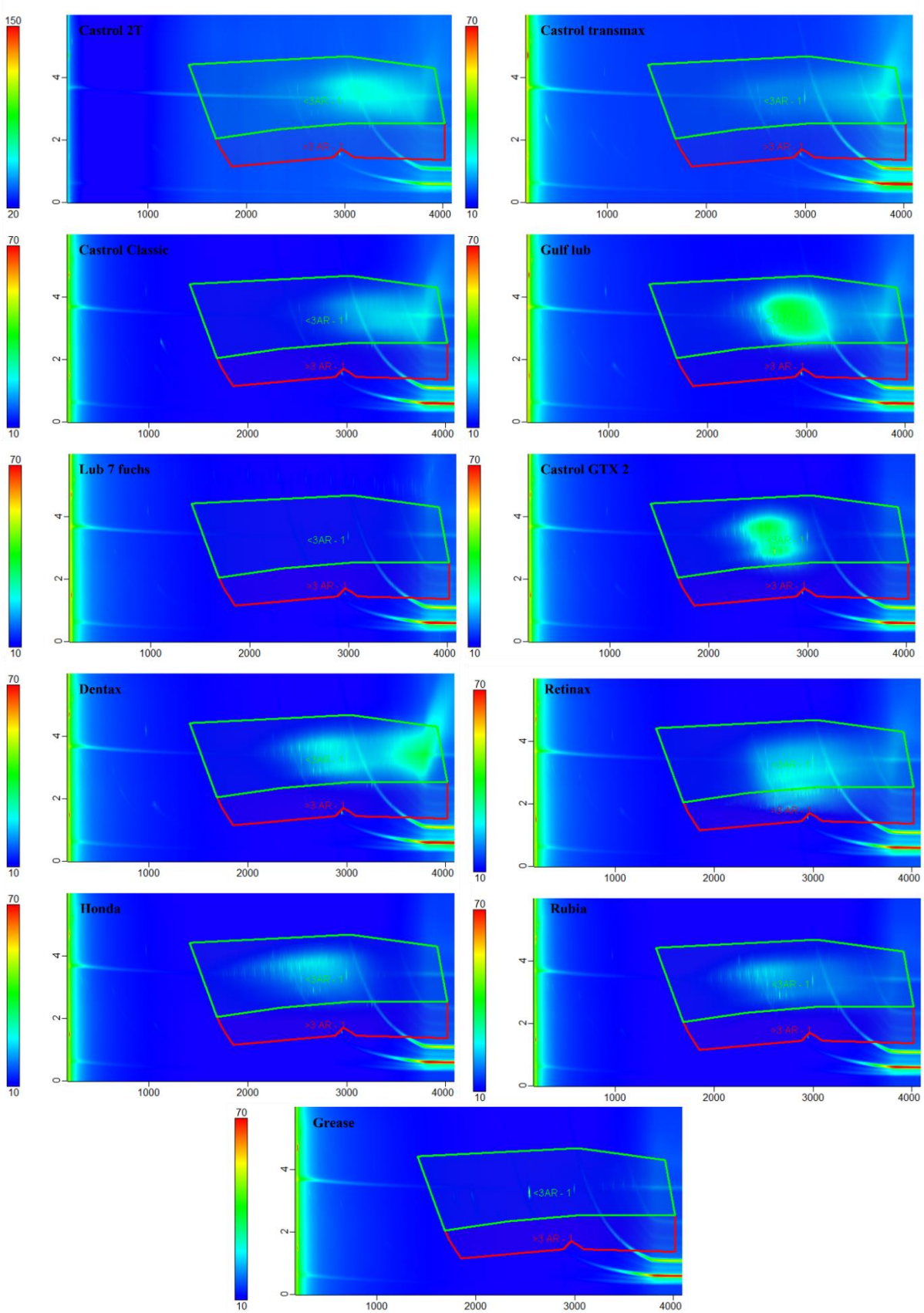

Annex 5 : GC×GC-FID chromatograms of the MOAH fraction of different lubricant oil available in the laboratory.

Annex 6

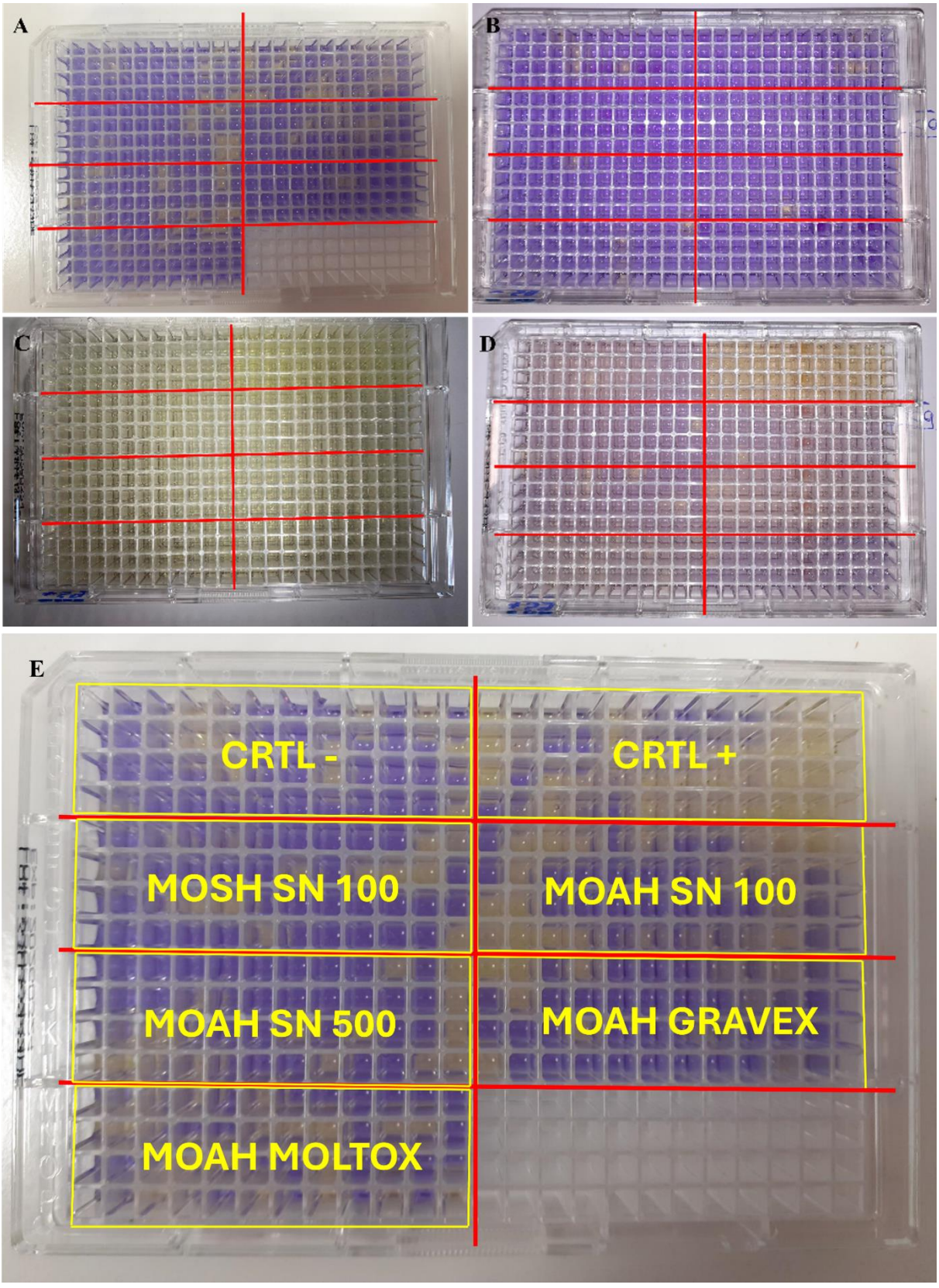

Annex 6 : Unfortunate events occurred during the multiple performed Ames test and plate segmentation pattern. (A) Normal succeeded test. (B) Positive control (top right quadrat) exhibiting almost only negative wells. (C) Contaminated plate exhibiting only positive wells. (D) Positive control (top right quadrat) shows 100% positive wells and negative wells (top left quadrat) being in between violet and yellow colour, preventing easy interpretation. (E) Ames plate segmentation pattern realised in the frame of this work.